Granular retrosplenial cortex layer 2/3 generates high-frequency oscillation events coupled with hippocampal sharp-wave ripples and Str. LM high gamma.

Kaiser C. Arndt

Dissertation submitted to the faculty of the Virginia Polytechnic Institute and State University in partial fulfillment of the requirements for the degree of

Doctor of Philosophy
In
Neuroscience

Daniel Fine English (Committee Chair)
Sam McKenzie
Timothy Jarome
Adrien Peyrache
Sujith Vijayan
Alexei Morozov

April 26th 2024
Blacksburg, VA

Keywords: Retrosplenial cortex, Hippocampus, Subiculum, medial entorhinal cortex, Sharp wave-ripples, High frequency oscillations, theta, gamma, power spectral density, current source density, independent component analysis, power-power comodulation, optogenetics

Granular retrosplenial cortex layer 2/3 generates high-frequency oscillation events coupled with hippocampal sharp-wave ripples and Str. LM high gamma.

Kaiser C. Arndt

ACADEMIC ABSTRACT

Encoding and consolidation of memories are two processes within the hippocampus, and connected cortical networks, that recruit different circuit level dynamics to effectively process and pass information from brain region to brain region. In the hippocampal CA1 pyramidal layer local field potential (LFP), these processes take the form of theta and sharp wave ripples (SPW-Rs) for encoding and consolidation, respectively. As an animal runs through an environment, neurons become active at specific locations in the environment (place cells) increasing their firing rate, functionally representing these specific locations. These firing rate increases are organized within the local theta oscillations and sequential activation of many place cells creates a map of the environment. Once the animal stops moving and begins consummatory behaviors, such as eating, drinking, or grooming, theta activity diminishes, and large irregular activity (LIA) begins to dominate the LFP. Spontaneously, with the LIA, the place cells active during the experience are replayed during SPW-Rs in the same spatial order they were encountered in the environment. Both theta and SPW-R oscillations and their associated neuronal firing are necessary for effective place recognition as well as

learning and memory. As such, interruption or termination of SPW-R events results in decreased learning performance over days. During exploration, the associated theta and sequential place cell activity is thought to encode the experience. During quiet restfulness or slow wave sleep (SWS), SPW-R events, that replay experience specific place sequences, are thought to be the signal by which systems consolidation progresses and the hippocampus guides cortical synaptic reorganization.

The granular retrosplenial cortex (gRSC) is an associational area that exhibits high frequency oscillations (HFOs) during both hippocampal theta and SPW-Rs, and is potentially a period when the gRSC interprets incoming content from the hippocampus during encoding and systems consolidation. However, the precise laminar organization of synaptic currents supporting HFOs, whether the local gRSC circuitry can support HFOs without patterned input, and the precise coupling of hippocmapla oscillations to gRSC HFOs across brain states remains unknown. We aimed to answer these questions using *in vivo,* awake electrophysiological recordings in head-fixed mice that were trained to run for water rewards in a 1D virtual environment. We show that gRSC synaptic currents supporting HFOs, across all awake brain states, are exclusively localized to layer 2/3 (L2/3), even when events are detected within layer 5 (L5). Using focal optogenetics, both L2/3 and L5 can generate induced HFOs given a strong enough broad stimulation. Spontaneous gRSC HFOs occurring outside of SPW-Rs are highly comodulated with medial entorhinal cortex (MEC) generated high gamma in hippocampal stratum lacunosum moleculare. gRSC HFOs may serve a necessary role in communication between the hippocampus during SPW-Rs states and between the

hippocampus, gRSC, and MEC during theta states to support memory consolidation and memory encoding, respectively.

Granular retrosplenial cortex layer 2/3 generates high-frequency oscillation events coupled with hippocampal sharp-wave ripples and Str. LM high gamma.

Kaiser C. Arndt

GENERAL AUDIENCE ABSTRACT

As an animal moves through an environment, individual neurons in the hippocampus, known as place cells, increase and decrease their firing rate as the animal enters and exits specific locations in the environment. Within an environment, multiple neurons become active in different locations, this cooperation of spiking in various locations creates a place map of the environment. Now let's say when the animal moved from one corner of the environment to another, place cells 'A', 'C', 'B', 'E', and 'D' became active in that order. This means, at any given point in the environment, the animal is standing in a venn-diagram-esque overlap of place fields, or locations individual place cells represent. A key question that entranced researchers for many years was how do these neurons know when to be active to not impinge on their neighbor's locations? The answer to this question rested with population electrical activity, known as the local field potential (LFP), that place cell activity is paced to. During active navigation through an environment, place cells activity is coupled to the phase of a slow ~8 hertz (Hz) theta oscillation. Within one theta cycle, or peak to peak, multiple place cells are active, representing the venn diagram of location the animal is in. Importantly,

this theta activity and encoding of place cell activity is largely seen during active running or rapid eye movement (REM) sleep.

During slow wave sleep (SWS), after an animal has experienced a specific environment and has created a place map, place cells are reactivated in the same order the animal experienced them in. From our previous example, the content of this reactivation would be the place cells 'A', 'C', 'B', 'E', and 'D' which all would be reactivated in that same order. These reactivations or replays occur during highly synchronous and fast LFP oscillations known as sharp wave-ripples (SPW-Rs). SPW-Rs are thought to be a key LFP event that drives memory consolidation and the eventual conversion of short-term memory into long-term memory. However, for consolidation to occur, connected cortical regions need to be able to receive and interpret the information within SPW-Rs. The granular retrosplenial cortex (gRSC) is one proposed region that serves this role. During SPW-Rs the superficial gRSC has been shown to exhibit high frequency oscillations (HFOs), which potentially serve the purpose for interpreting SPW-R content. However, HFOs have been reported during hippocampal theta, suggesting HFOs serve multiple purposes in interregional communication across different states. In this study, we found that naturally occurring gRSC HFOs occur exclusively in layer 2/3 across all awake brain states. Using focal optogenetic excitation we were able to evoke HFOs in both layer 2/3 and 5. Spontaneous gRSC HFOs occurring without SPW-Rs were highly comodulated with medial entorhinal cortex (MEC) generated high gamma in hippocampal stratum lacunosum moleculare. gRSC HFOs may serve a general role in

supporting hippocampo-cortical dialogue during SPW-R and theta brain states to support memory consolidation and encoding, respectively.

DEDICATION

To my parents and my sisters.

I wouldn't have gotten here without your endless love and support.

ACKNOWLEDGEMENTS

I would like to start by thanking my advisor, Dan. Coming from a microbiology and genetics bachelors, I had no classical neuroscience education, much less electrophysiology experience. Thank you for taking a leap of faith on me 6 years ago. You've taught me everything I know and I wouldn't have gotten this far without your support.

Thank you to my committee members Dr. Sam McKenzie, Dr. Adrien Peyrache, Dr. Alexei Morozov, Dr. Sujith Vijayan, and Dr. Tim Jarome. Thank you all for the hours spent listening to my project and the helpful support you have given me over the years. To Dr. McKenzie, thank you for the detailed critiques and guidance of every step of this project. Your keen attention to detail, both analytically and literarily, has deepened my understanding of every aspect of our field, thank you. To Dr. Jarome, in writing this it is difficult to find the right words to describe my sincere gratitude for your support over the years. Thank you for always making time for a spontaneous meeting and for giving insight on the intricacies or difficulties of academia that few ever talk about. You will forever have my utmost respect and highest regards as a scientist and an amazing human.

Thank you to my fellow English Lab members, Lianne Klaver, Earl Gilbert, Chelsea Buhler, and Alana Hutchinson as well as our collaborators, Jason Kim and Hengji Huang. Working with each of you has been one of my greatest pleasures. I am extremely grateful to have worked with such a caring, excited, and motivated group of people. To Lianne, thank you

for your understanding and willingness to answer all of those MATLAB questions in the beginning. I appreciate everything you have done for me over the years, you have become one of my closest friends and I hope that continues long into the future, wherever our lives take us. To Jason, your depth of knowledge on signal processing is truly remarkable and the hours of whiteboard talks will never be forgotten. Your impact on my education is immeasurable and I have enjoyed every moment with you, both in and outside the lab. See you on the rift. To Earl, of everyone I have worked with you have had the greatest impact on my life. The hundreds of hours of conversations we shared have opened my eyes to so many different perspectives and have helped me grow as a person more than I ever expected. Working and studying with you over these years has been an immense privilege of mine. You are an amazing scientist but even more, an amazing person. Thank you for everything.

To my best friends, Charlie Bootsmiller, Robbie Blythe, and Macon McInnis. Growing up with each of you, seeing where we started and watching where we've gone thus far has been an amazing journey. Each of you have become amazing men who I look up to and aspire to be like on daily basis. To Charlie, I hope I have made this clear over the years of our friendship, but you have been the bedrock of my support structure. Someone I knew you would always be there to listen, through the struggles of life and this process of getting my PhD. The "useless" debates we have had over the years have filled me with so much joy.

To my partner (Shannon Kincaid), the love I have for you is immeasurable, like a lot. Thank you for your patience, for showing me the world from your eyes, and for showing me what true faith is. Thank you for believing in me and supporting me every day and in every way, even when I doubted everything about myself. Thank you for building a life with me, your strength and perseverance continues to fill me with awe. You have made my life more enjoyable and more fulfilled in every way possible. You are the most amazing woman I have ever met, and it is my greatest privilege to call you my partner. I can't express how excited I am to grow with you in the future, both in life and work. I love you more than you will ever know.

To my sisters (Sabrina and Jordan Bleile), I love each of you so much and am immensely proud to be your brother. Thank you for your support over the years helping me move from place to place. Your willingness to listen to me vent or talk about work will always be appreciated. You are amazing women, thank you for your endless love and support.

To my stepparents (Scott Bleile and Denise Lindsay), thank you for coming into my life when you did and becoming irreplaceable support structures and for being people I can go to for anything. I wouldn't be the man I am today without your input, support and guidance through life. Unequivocally, you have made an irreplaceable impact on who I am. I am the luckiest man alive to have been raised by each of you. To Denise Lindsay, thank you teaching me your past isn't your future, that people can change, and everyone deserves the chance to

experience life with the excitement you express every day. I have never had a bad day with you around, you have always been a shining ray of optimism through whatever life throws at you, you are truly wonderful. I love you. To Scott Bleile, thank you for having the patience to teach a hyperactive kid like me everything you could (for as long as I could listen). Every day, without fail, I recall some memory of helping you repair or build something around the house. You have given me skills to take through the rest of my life, and that means more to me than anything I could accomplish academically. Everything you have given me is priceless. I love you.

To my dad (Kyle Arndt), we've come a long way, and I wouldn't change anything about the path. I am the man I am today because of you. You have shown me how to be strong, to pave my own path, to trust my choices, and to regularly throw some jokes into life. You have taught me the value of patience, humility, extreme ownership, and how to hold myself high in the face of adversity. You have taught me the value and beauty of life. Every moment with you is a blessing that I will never take for granted. You are my hero.

To my mom (Barb Bleile), I will never be able to give the adequate words to describe how much you mean to me, and to be honest this is the hardest part of this entire document for me to write. You have always been here for me, and I can't think of a memory that you aren't a part of in some way. The care and guidance you have shown me all my life has never gone unnoticed, even when I may not have shown it. You may not have known it at the time,

but you taught me the core lessons of a scientist from childhood. You taught me to question everything, to try to view situations from every angle or perspective, and that it's ok to be wrong. Everything you taught me outside of science is so much more valuable. You taught me what it means to be a true gentleman, to hold my head high in every situation, to treat everyone with respect, and always help others. Everything I have done up to this point and everything I will do in the future is because of you. As always, you are last.

To everyone, Memories are what tie us together.

Table of Contents

MAIN FIGURES

ABBREVIATIONS

BOLD	Blood oxygen level dependent signal
CA	Cornu amonis
ChR2	Channel rhodopsin
CSD	Current source density
EC	Entorhinal cortex
HFO	High frequency oscillation
HIR	High frequency oscillation during SPW-Rs
HOR	High frequency oscillation outside of SPW-Rs
HPC	Hippocampus
ICA	Independent component analysis
LFP	Local field potential
LR cell	Low rheobase cell
MEC	Medial entorhinal cortex
MS-DBB	Medial septum-dorsal band of brocca
PSD	Power spectral density
REM sleep	Rapid eye movement sleep
RSC	Retrosplenial cortex
dRSC	Dysgranular retrosplenial cortex
gRSC	Granular retrosplenial cortex
SPW-R	Sharp wave-ripple
SWS	Slow wave sleep
Str. LM	Stratum lacunosum moleculare
Str. Pyr	Stratum pyramidale
Str. Rad	Stratum radiatum

CHAPTER ONE: LITERATURE REVIEW

Abstract

Animals require functional learning and memory for survival. During active navigation, CA1 place cell sequences become active during hippocampal (HPC) theta and nested gamma allowing for the encoding of the present experience. Granular retrosplenial cortex (gRSC) high frequency oscillations (HFOs) are locked to the peak of gRSC and HPC theta. It is possible these HFOs are signatures of active computation within the gRSC to encode the present experience co-occurring with hippocampal theta and nested gamma. The theory of systems consolidation is supported by decades of work and describes the evolution of memory from a short-term hippocampal dependent form into a long-term hippocampal independent form. One proposed mechanism by which the hippocampus guides reorganization of cortical networks for the effective evolution of memories is through the sharp wave-ripple (SPW-R). SPW-R replay reactivates place cells in the same order they were active in a recent experience and is necessary for learning and memory consolidation. The spiking content within the SPW-R must be decoded by the cortex to allow systems consolidation to occur. gRSC HFOs have also been identified occurring with hippocampal SPW-Rs potentially serving as the local field potential signature of gRSC activity decoding SPW-R content. The gRSC is optimally positioned to undertake this role and relay both hippocampal SPW-R and theta associated information to distributed downstream cortical

regions. A promising mechanism by which the gRSC supports this information processing is through HFOs found in superficial gRSC.

Introduction

An animal's ability to reliably replicate behaviors or choices that they previously found to be beneficial is vital for their survival and thriving. What is deemed beneficial changes on an individual-by-individual basis, however, remembering the correct actions to achieve this outcome is nonetheless a necessity. Effective memory formation, throughout the life of an animal, shapes their behavior in every waking moment. Take us humans for example, at any given moment we are accessing some piece of information from a memory to respond to our surroundings. In a conversation with someone, you are accessing emotional memories about previous conversations that then inform how you behave with that person in the moment. You are also accessing episodic and/or semantic memories about the topic at hand, as well as the correct words required to effectively communicate your point without being misunderstood. In the same interaction, your brain is also accessing spatial memories about the present environment, where the walls of the room are, where other objects are in the room, and where you are located and facing relative to the entire space.

Over decades of studies, similar memory abilities have been found in numerous animal species. Birds need to remember vocalizations to attract mates, mark territory, or more generally communicate with neighboring birds (Bailey et al., 2009; Reiss & McCowan, 1993). Porpoises, such as dolphins, have been shown to learn and use vocalizations that are linked to

natural behaviors (Reiss & McCowan, 1993) as well as taught new sounds they learn to associate with novel objects. Foraging animals need to remember reliable locations of food or water, and in some cases where they have created caches to come back to later (Payne et al., 2021). A growing body of work is demonstrating the neural circuit activity supporting spatial memory is evolutionarily conserved across many animal species (Bailey et al., 2009; Blanco et al., 2024; Bragin et al., 1999; Buzsáki et al., 2013; Kanamori, 1985; Nokia et al., 2010; Payne et al., 2021; Reiss & McCowan, 1993; Shein-Idelson et al., 2016; Skaggs et al., 2007; Ulanovsky & Moss, 2007). Multiple animal models including mice, rats, rabbits, as well as humans have been shown to exhibit spatial dependent hippocampal activity across multiple brain states, in the form of place cells, theta sequences and sharp-wave ripples (SPW-Rs) (Ekstrom et al., 2003; Mou et al., 2018; Niediek & Bain, 2014; Nokia et al., 2020; O'Keefe, 1976; Payne et al., 2021).

However, hippocampal encoding of space doesn't exist in a vacuum, and learning and memory requires effective communication between the hippocampus and distributed cortical networks (Ben-Yakov et al., 2013; Ben-Yakov & Dudai, 2011; Dahal et al., 2023; Kitamura et al., 2017; Staresina et al., 2013; Tambini et al., 2010; Tomé et al., 2022) such as the granular retrosplenial cortex (gRSC). This communication likely depends upon, and changes with, specific brain states that promote different computationally advantageous regimes to most effectively encode and allow for systems consolidation of memories (Diekelmann & Born, 2010; Squire et al., 2015). Briefly, an example of this is the opposing nature of hippocampal theta activity during active navigation and REM sleep, and the SPW-Rs present during quiet

restfulness and SWS sleep (described in more detail below). Here we aim to outline the importance of hippocampal activity in these brain states, the gRSC's role in hippocampo-cortical communication, and how that communication may support encoding and eventual systems consolidation of memory.

Hippocampal Theta, gamma, and SPW-Rs

Hippocampal circuits organize their firing patterns at different time scales and frequencies that specifically occur during different brain states. As an animal runs or moves from one point in a room to another, individual neuron firing rates increase and decrease as the animal enters and exits arbitrary locations in the environment. These locations, where a neuron's firing rate increases, are known as place fields, and the excitatory cells that fire in specific locations of an environment are known as place cells (O'Keefe, 1976; O'Keefe & Dostrovsky, 1971). The excitatory synaptic currents of local place cells coordinate with inhibitory synaptic currents to create a larger, rhythmic, LFP (local field potential) oscillation within the hippocampus at about 8 Hz. This oscillation is known as theta. Hippocampal theta generation is thought to be the cause of 3 sources (Buzsáki, 2002). First, medial septum-dorsal band of brocca (MS-DBB) input to the HPC CA1 in 2 forms. Projections from cholinergic neurons slowly depolarizing pyramidal cells and interneurons in the hippocampus (Buzsáki et al., 1983), and 'pacemaker' GABAergic projections targeting interneurons create local rhythmic hyperpolarization in hippocampal networks (M. G. Lee et al., 1994). Second,

Excitatory input into CA1 stratum lacunosum moleculare (Str. LM) from entorhinal cortex layer 3 (L3) driving the theta current sink within this CA1 sublayer (Amaral & Witter, 1989; Kamondi et al., 1998). Third, CA3 recurrent network input to CA1 stratum radiatum (Str. Rad) (Amaral & Witter, 1989; Bragin et al., 1995). These sources aid in pacing and controlling spike timing to the theta oscillation at different times and brain states (Buzsáki, 2002). Individual place cell and interneuron firing is coordinated within each cycle of the theta oscillation by a faster, nested gamma oscillation (described in more detail below). As an animal enters a place field, the corresponding place cell starts firing at the peak of the theta oscillation and precesses to the trough as the animal moves to the center of the place field, and then back to the peak of theta as the animal nears the end of the place field (Dragoi, 2013; Dragoi & Buzsáki, 2006; Schmidt et al., 2009; Skaggs et al., 1996). Phase precession dynamics of individual place cells appear to be modulated by the interference of the faster active cell assembly excitatory and inhibitory conductance oscillations, and the slower global theta oscillation (O'Keefe & Recce, 1993; Valero et al., 2022). Every environment contains numerous place fields that often overlap to some extent (J. S. Lee et al., 2020). At any given moment, the animal is positioned in a venn-diagram-esque overlap of multiple fields, and the spatial information of the overlapping fields is encoded by an increased firing rate at specific phases of the theta cycle. This experientially dependent, sequential activation of place cells are termed theta sequences (Dragoi, 2013; Skaggs et al., 1996). Theta sequences provide a neural representation of the place field the animal is leaving (ascending theta phase), the place field the animal is centered in

(trough of theta phase), and the place field the animal is starting to enter (the peak of theta phase); functionally giving a view of past, present, and future locations.

Within each theta cycle a faster frequency, known as nested gamma, is present on top of the theta oscillation. These gamma oscillations (30-100 Hz) further refine single unit activity within the theta cycle using a balance between excitation and inhibition to effectively organize the theta sequences (Buzśaki & Wang, 2012; Fernandez-Ruiz et al., 2023). Across the sub layers of hippocampal CA1 there are 3 identified gamma generators. 1) The slow gamma (30-60 Hz) generator is present in the stratum radiatum (Str. Rad) and originates from hippocampal CA3 (Colgin et al., 2009; Schomburg et al., 2014). As an animal reaches the end of a place field, both place cell spike-LFP coupling and LFP gamma power increase. Additionally, the synchrony between place field spiking and slow gamma is increased during later trials of a task (Fernández-Ruiz et al., 2017). For memory retrieval, both CA3 activation and the consequent CA1 Str. Rad slow gamma are necessary (Colgin, 2016; Colgin et al., 2009; Dvorak et al., 2018; Etter et al., 2023; Hasselmo & Stern, 2014). 2) The mid gamma (60-100 Hz) generator is localized to the stratum lacunosum moleculare (Str. LM) and originates from entorhinal cortex (EC) layer 3 (Colgin et al., 2009). In the CA1 pyramidal layer, these oscillations have the strongest power and spike-LFP coupling at the start of a place field and during early, compared to late, trials (Fernández-Ruiz et al., 2017). This gamma band has also been reported to be important for conveying EC signals during memory encoding (Colgin, 2015a, 2015b; Colgin et al., 2009; Etter et al., 2023). Though, there remains some contention about the validity of these first two gamma sub bands being generated by external input coming from CA3 and EC inputs

(Zhou et al., 2019, 2022). For low gamma, it is possible a large part of the frequency range is derived from theta harmonics up to 48 Hz. For mid gamma, bicoherence analysis, which is a method that considers more precise frequency ranges, shows no significant cross-frequency coupling between Str. LM and EC layer 3 mid gamma bands. The evidence put forward by Zhou et al, point toward theta being the main coordinator of interregional circuit communication. Theta coordination thus allows for simultaneous local gamma frequency computation within each region. However, this is still an open discussion that requires much more work to understand the intricacies of the gamma cross frequency coupling between CA1 sublayers and CA3 or EC. 3) the fast gamma oscillation (100-150 Hz) is generated in stratum pyramidale (Str. Pyr) by local recurrent connections between excitatory pyramidal cells and fast spiking interneurons (Brunel & Wang, 2003; Buzśaki & Wang, 2012; Fernandez-Ruiz et al., 2023; Tiesinga & Sejnowski, 2009; X. J. Wang & Buzsáki, 1996; Whittington et al., 1995). Over 90% of place cell spiking within their fields are phase modulated to this frequency (Fernández-Ruiz et al., 2017). This phase modulation is due to the local CA1 neurons balancing excitatory inputs from CA3 and EC with recurrent inhibition from local fast-spiking interneurons. It is well known that hippocampal gamma is dependent on GABAa inhibitory currents which paces the frequency of the oscillation as well as gates which pyramidal cells become active (Buzśaki & Wang, 2012).

While each of these gamma bands contribute to the refinement of place cell activity during different stages of memory, the functional import is not the frequency itself, but the information conveyed within the generating neural circuit (Fernandez-Ruiz et al., 2023).

Excitable dendrites have been shown to be low pass filterers of electrical input. During theta and associated gamma patterned input to dendrites, the corresponding soma voltage responds with a positive deflection, not with the gamma patterned spiking (Buzsáki & Schomburg, 2015; Vaidya & Johnston, 2013). The spiking response to this low pass, dendrite, filtered input is likely then controlled by intrinsic cellular physiology characteristics, such as ion channel types. Though, across multiple brain states, specific interruption of gamma sub bands via optical stimulation of CA3 or EC blocks the respective gamma oscillation sub band in HPC CA1 or dentate gyrus (El-Gaby et al., 2021; Fernández-Ruiz et al., 2021; López-Madrona et al., 2020). Notably, these manipulations interrupted LFP power and cross frequency coupling between CA3/EC and their connected hippocampal CA1 layers. Behaviorally, these manipulations resulted in memory modality specific (object memory, place memory, context memory) deficits, while place field encoding was still conserved. The retention of local computation, while interrupting modality specific memory (dependent on the optically perturbed region), supports the idea that gamma serves as a communication frequency. Or rather, the oscillation sub bands do not represent the specific circuit information coming from CA3 or EC. These sub bands are the frequencies CA3 or EC circuits compute the information they encode and are the frequencies the information is relayed to the hippocampal circuits (Fernandez-Ruiz et al., 2023).

While an animal is running or in REM sleep the CA1 network is dominated by theta and its nested gamma frequencies. Once an animal stops running the hippocampal circuits shift from the theta/gamma regime and begins to spontaneously oscillate at their own relay

frequency, the sharp wave-ripple (SPW-R). These SPW-Rs are fast LFP events found in Str. Pyr of hippocampal CA1 during quiet restfulness or slow wave sleep (Buzsáki, 2015; Buzsáki et al., 1983) and are comprised of two independent LFP events that co-occur. 1) The sharp wave is a large negative deflection in the local field potential that represents a strong depolarizing signal to the CA1 region. Population bursting coming from CA3 Schaffer collaterals sends a surge of excitatory input to CA1 resulting in the sharp wave found in Str. Rad (Buzsáki, 1986; Buzsáki et al., 1983). 2) The ripple is the response of the CA1 pyramidal layer to the excitatory drive coming from the CA3 networks. In the pyramidal layer, reciprocal excitatory-inhibitory synaptic connectivity works together to create LFP oscillations at about 150 Hz (English et al., 2014; Gan et al., 2017; Stark et al., 2014). Immediately after an animal finishes a task SPW-Rs naturally occur more often (Eschenko et al., 2008). Upon closer inspection, the neurons that are activated during SPW-Rs after a task are more likely to be neurons that were active during the task itself (Gorriz et al., 2023). This phenomenon gives credence to the term replay, which is often used with SPW-Rs. SPW-Rs reactivate or 'replay' the same neurons in the exact same order they were originally active, functionally condensing a seconds to minutes long experience into a tens of milliseconds long package (Skaggs & McNaughton, 1996).

What is the function of this condensed SPW-R package? Multiple block and mimic studies have demonstrated the necessity and significance of the SPW-R for learning and memory. The first of which was a set of closed loop experiments conducted by Girardeau et al., 2009. Here they used a radial arm maze task where food rewards were placed at the end of

a set of arms. Rats were trained to find, learn, and remember the locations of the food rewards over multiple days. In a subset of rats, they had implanted a stimulating wire in the hippocampal commissure. Over multiple days, while the rats were asleep, after learning, an electrical stimulation was given whenever a SPW-R was detected, functionally terminating these SPW-Rs before they could come to completion. Over consecutive days, animals that had their SPW-Rs interrupted performed significantly worse when searching for food rewards on the radial arm maze. In 2019, Fernández-Ruiz et al. demonstrated the inverse by optogenetically elongating natural SPW-Rs. In an alternating M-maze task, they showed that animals performed significantly better over multiple days of SPW-R elongation compared to controls and animals that were given random optically induced SPW-Rs. Notably, SPW-R elongation significantly improved memory for only hippocampal dependent portions of the task and allowed for more neurons to become active during the SPW-R events (Fernández-Ruiz et al., 2019). These studies specifically tell us that SPW-Rs are necessary for memory guided behavior, but is the specific content, or sequence of cells active during SPW-Rs necessary for effective learning and memory or purely the SPW-R event itself? Gridchyn et al., 2020 aimed to answer this question by training rats to locate food rewards in two separate cheese board contexts. Context specific neural sequences were detected during inter-trial sleep just before SPW-Rs occurred. An optical stimulation to interrupt hippocampal activity was then delivered upon successful detection of sequences representing the target context. All other SPW-R events that did not exhibit neural sequences for the target context were spared. This intervention resulted in significantly decreased behavioral performance in the target

context but spared the behavioral performance in the control environment. Elegantly demonstrating the content, or specific neuronal sequences, within a SPW-R is vitally important for learning and memory, not just the LFP oscillation itself. Similar to gamma frequency being a reporter of functional interactions between CA3 or EC to CA1; the SPW-R is likely the frequency for which internal computations are conducted within the hippocampus and are transmitted to the rest of the neocortex.

Retrosplenial cortex high frequency oscillations

The logical next question is, what neocortical regions care about the SPW-R, or functionally decode the information within? Until recently, much work had gone into understanding the prefrontal cortex and how it interprets information coming from the hippocampus during SPW-Rs. Many studies have demonstrated hippocampo-cortical LFP-LFP, spike-LFP, spike-spike, BOLD, calcium sensor, and voltage sensor coupling (Abadchi et al., 2023; Dahal et al., 2023; Karimi Abadchi et al., 2020; Khodagholy et al., 2017; Pedrosa et al., 2022; Staresina et al., 2015). This growing body of work shows evidence for the retrosplenial cortex (RSC) being important for hippocampo-cortical dialogue.

The RSC is a large midline region that sits posterior to the splenium of the corpus collosum, per its namesake. Anatomically, it is separated into two sub regions known as the granular RSC (gRSC) for the granular nature of cell organization present in layer 2/3, and dysgranular RSC (dRSC) noted for the lack of a granular layer. In contrast to most 6 layered

neocortical regions, both RSC subregions consist of 4 layers, those being layer 1, 2/3, 5, and 6 (L1, L2/3, L5, L6). The earliest studies investigating the importance of the RSC in memory performance used various lesion methods to chemically, electrically, or physically lesion the RSC. These numerous studies reported conflicting evidence, likely due to variable animal strains, behavioral paradigms, lesion methods, and lesion sizes (Harker & Whishaw, 2002; Troy Harker & Whishaw, 2004; Vann & Aggleton, 2004). However, technological advances have allowed for more techniques to be used to study the RSC's function in spatial learning and memory. During sleep or anesthetized states immediately after a task, optogenetic reactivation of RSC neural ensembles coding for a fear memory task can protect memory guided behavior from hippocampal inactivation (de Sousa et al., 2019). Calcium imaging and voltage sensing have shown the RSC becomes activated just before SPW-Rs in the hippocampus and it reaches peak activity a couple hundred milliseconds after SPW-Rs (Abadchi et al., 2023; Karimi Abadchi et al., 2020; X. Liu et al., 2021). At the cellular level, 3 types of neurons have been identified in the gRSC, 1 inhibitory; fast-spiking neurons, and 2 excitatory; regular-spiking and low rheobase neurons. These low rheobase neurons are the most prevalent cell type in gRSC L2/3 and send projections out of the region (Brennan et al., 2020; Robles et al., 2020). Neural probe recordings have identified populations of gRSC neurons can distinguish between subtypes of SPW-Rs (Nitzan et al., 2020). Neural probe recordings have also identified place, head direction, boundary vector and border cells in the gRSC, which are all key for spatial navigation (Alexander, Carstensen, et al., 2020; Lozano et al., 2017; Mao et al., 2017, 2018; Shine et al., 2016; van Wijngaarden et al., 2020). In the local field potential, high frequency

oscillations (HFOs; ~150 Hz) have been found in superficial gRSC, occurring with hippocampal SPW-Rs and theta oscillations during quiet restfulness/ SWS or running/ REM sleep, respectively (Alexander et al., 2018; de Almeida-Filho et al., 2021; Ghosh et al., 2022; Nitzan et al., 2020; Opalka et al., 2020). gRSC theta oscillations follow hippocampal theta during awake and REM states, and HFOs during these states appear to be locked to the descending phase of both theta oscillations (Alexander et al., 2018; Arndt et al., 2024; Koike et al., 2017). HFO power increases with animal velocity, and is maximized during REM sleep (Ghosh et al., 2022). Ghosh et al., 2022 demonstrated these HFO events occur across the hemispheres in time with one another. Though, fascinatingly, the HFOs from each hemisphere are offset by 180 degrees. This offset may serve an integral role in functional computation within the gRSC, which potentially requires interhemispheric communication for the gRSC to interpret incoming information.

It seems to be well agreed upon that the RSC is important for learning and systems consolidation of memory, but the finer role of how it supports those functions is still unclear. One theory is the RSC can be viewed as a "relay hub" between internally and externally generated representations of experience. Or rather, to relate, to one another, key pieces of information about a memory that are generated and stored/ represented in distributed cell assemblies across the brain (Castiello et al., 2021; Stacho & Manahan-Vaughan, 2022; Vann et al., 2009). Here, internally generated representations of experience are defined as additional computational representations that require a confluence of multiple sensory modalities. For example, effective place cell mapping utilizes many sensory modalities such as visual flow,

intact vestibular cues, motion information, and olfactory cues (Chen et al., 2013; Fischler-Ruiz et al., 2021; O'Keefe, 1976; Save et al., 1998; Stackman et al., 2002). Other internal representations of experience include head direction, border, boundary vector, and grid cells. Externally generated representations of experience are defined as cues coming from sensory cortices, such as visual, motor, and auditory cortices. Effective coordination and communication between these distributed networks of spatial representation is necessary for the context of an environment to emerge. The RSC is optimally positioned to perform this contextual interpretation role and much work supports the RSC as a context encoder (Alexander et al., 2023; Alexander, Robinson, et al., 2020; Sun et al., 2021; Vann et al., 2009).

Projections from both internally and externally generating representations of experience target the gRSC, I will begin from the perspective of internally generated representations. gRSC L2/3 pyramidal cell spiking, compared to L5 pyramidal cells, covaries more with CA1 spiking. gRSC unit spiking transiently fluctuates between synchronized bursts of activity and desynchronized sustained spiking in both quiet restfulness and SWS. However, during quiet restfulness these bursts of activity occur with the onset of SPW-Rs, but during slow wave sleep the bursts terminate with end of SPW-Rs (Nitzan et al., 2020; Opalka et al., 2020). Subicular VGlut2^{+} bursty neurons in the dorsal subiculum are believed to drive HFOs in superficial gRSC. These bursty subicular neurons project into L1 and L2/3 of the gRSC evoking excitatory spiking of local pyramidal cells, but not L5 pyramidal cells, and optogenetic excitation of these neurons results in HFOs in superficial gRSC (Nitzan et al., 2020). Only two kinds of direct projections from the hippocampus to the gRSC have been identified. 1) Long

range inhibitory projections from neurons located on the Str. Rad and Str. LM boundary targeting gRSC L1 projecting dendrites of L5 pyramidal cells (Yamawaki et al., 2019). 2) Optostimulation of CaMKII expressing projections from rostral medial CA1, fasciola cinerea, targeting gRSC L2/3 resulted in activation of local inhibitory neurons and silencing of excitatory neurons (importantly, somatic locations of effected neurons are unknown) (Opalka et al., 2020). In support of these inhibitory projections, an additional experiment was conducted where optogenetic excitation of distal CA1 pyramidal cells induced large, rhythmic negative waves in superficial gRSC (Nitzan et al., 2020). The nature of these projection types either being inhibitory or activating local interneurons suggests an interesting role of possibly gating gRSC activity. This inhibitory input may act to restrict gRSC activity to occur at optimal times to best interpret incoming information from the hippocampal formation. Another possible function of this inhibition is feed forward inhibition. Feed forward inhibition is the subsequent activation of local inhibition following excitatory input, meant to refine further excitatory precision of the local network. In the gRSC network, feed forward inhibition may be a response to subicular excitatory input allowing the network to accurately decode information coming from the subiculum and hippocampus (Brennan et al., 2020, 2021). It is possible the HFOs present in superficial gRSC are driven by the interaction between this feedforward inhibition and the local low rheobase neurons found within L2/3. In the head direction (HD) system, excitatory cells from the anterodorsal nucleus of the thalamus (ADN) and dorsal subiculum send projections to gRSC L1 and L2/3 dendrites of low rheobase cells. Modeling suggests that depressing ADN input to low rheobase cells may improve head

direction and head velocity tuning in the gRSC (Brennan et al., 2020, 2021). The dorsal subiculum projections are potentially the same as the VGlut2^{+} bursty cells driving HFOs in superficial gRSC (Nitzan et al., 2020). Additionally, MEC projections target gRSC L1 and L2/3, with reciprocal connections from the gRSC to deep MEC (van Wijngaarden et al., 2020). These connections are important for gRSC boundary vector as well as border coding (Alexander, Carstensen, et al., 2020) (Figure 1).

From the perspective of regions creating externally generated representations of experience; monosynaptic projections from visual cortices target both dysgranular retrosplenial cortex (dRSC) and gRSC L1 and L5 (Fischer et al., 2020; van Groen & Michael Wyss, 1990; van Groen & Wyss, 1992; Van Groen & Wyss, 2003; Vogt & Miller, 1983). Notably, a majority of connections going into the dRSC come from the primary visual cortices, and these connections are important for the dRSCs ability to encode visual landmarks (Fischer et al., 2020; Powell et al., 2020). Most connections going into the gRSC come from secondary visual cortices, but the functional import of these connections has yet to be revealed (van Groen & Michael Wyss, 1990; van Groen & Wyss, 1992; Van Groen & Wyss, 2003; Vogt & Miller, 1983). From motor cortices, projections originate from secondary motor cortex (M2) (Vogt & Miller, 1983) and target M2 projecting neurons in both the dRSC L2 and 5 and gRSC L5 (Yamawaki et al., 2016). Importantly in this circuit, gRSC projections to M2 are weaker than dRSC projections. Chemogenetic inactivation and lesioning of both dRSC and gRSC result in impaired auditory cue induced memory recall in a trace fear conditioning paradigm (Todd et al., 2016). Regions encoding auditory signals send projections to both dRSC and gRSC

including both primary and secondary auditory cortices as well as the claustrum (Brennan et al., 2021). Notably, both dRSC and gRSC receive similar amounts of input from auditory cortices, and these connections are topographically mapped to the RSC (Todd et al., 2016) (Figure 1).

The confluence of input to the RSC from externally and internally generated representations lends much support to the hypothesis that the RSC is a relay hub between these representations. From this body of work, it appears connections from sensory regions encoding externally generated representations of experience are more numerous and stronger targeting the dRSC as compared to the gRSC. Inversely, regions encoding internally generated representations of experience are stronger and more numerous going into the gRSC. I hypothesize that the gRSC is responsible for decoding internally generating representations of space and correlating it to externally generated, sensory information sent to the dRSC. How are these pieces of information correlated or computed together into a coherent representation? As discussed above, we can turn to the local field potential for insight. Similar to the SPW-R in the hippocampus, the gRSC "utilizes" events in the same frequency range, the HFO. During hippocampal SPW-Rs, increased unit activity in the gRSC can distinguish between subtypes of SPW-Rs (Nitzan et al., 2020). gRSC HFOs, occurring during SPW-Rs or theta oscillations, are potentially how distributed representations of experience are correlated to one another. This supports my hypothesis that sensory information sent to the dRSC to be associated with internally generated representations sent the gRSC. This correlation could functionally allow for a contextual representation to emerge, memory encoding to occur, and

352 systems consolidation to progress. However, future work studying the interactions between
353 gRSC and dRSC networks is necessary, especially during SPW-R and theta associated brain
354 states.

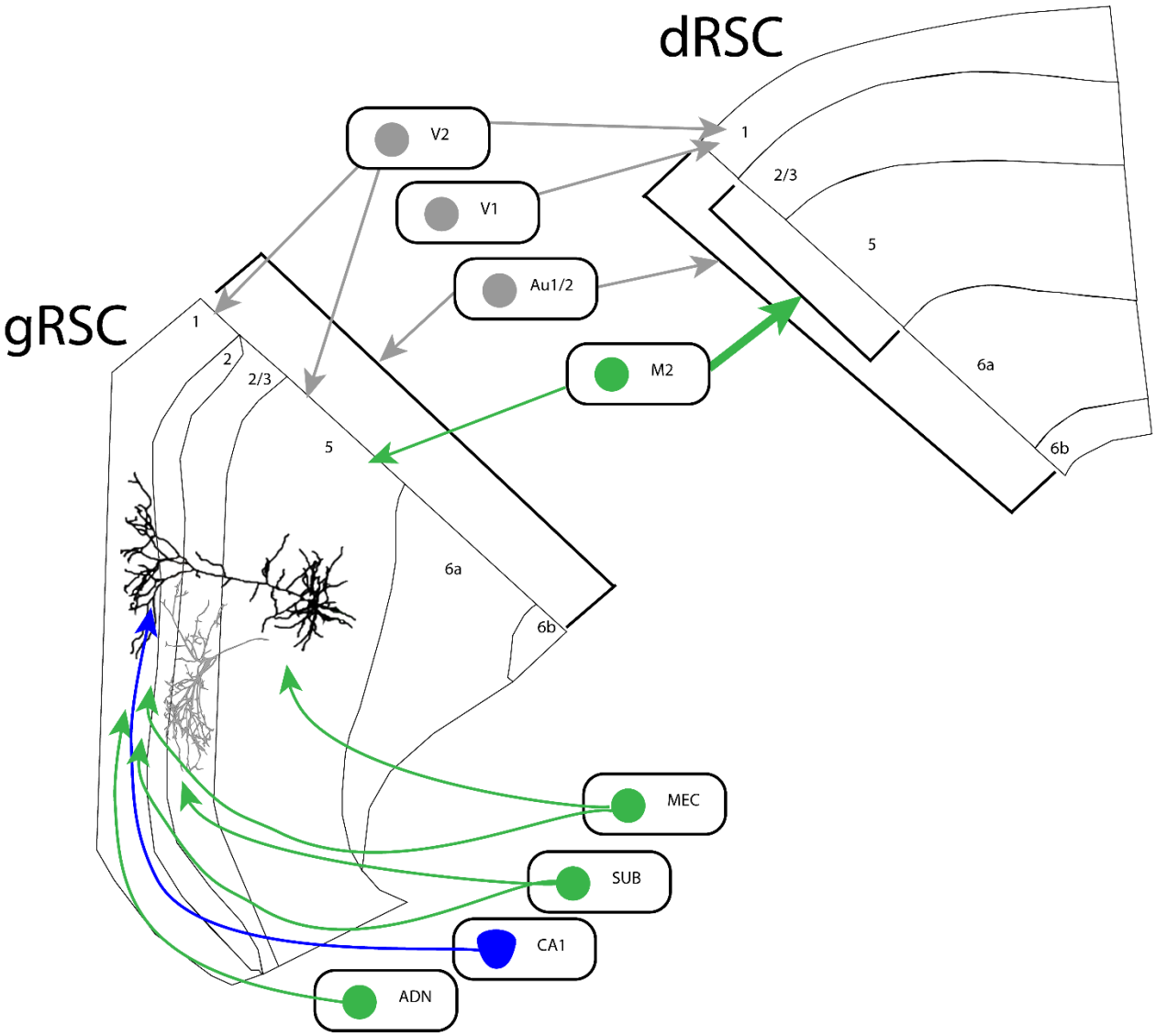

Figure 1. gRSC and dRSC input from internally and externally generated representations of experience: Note regions encoding internally generated representations of experience send projections only to gRSC, while sensory cortices coding for externally generated representations of experience send projections to both gRSC and dRSC. Green arrows are excitatory input, blue arrows are inhibitory input, grey arrows are unknown kinds of input. ADN – anterodorsal nucleus of the thalamus, CA1 – hippocampal CA1, Sub – dorsal subiculum, MEC – medial entorhinal cortex, M2 – secondary motor cortex, Au1/2 – primary and secondary auditory cortex, V1 – primary visual cortex, V2 – secondary visual cortex. This is a representation culminated from Vogt et al. 1983, Van Groen et al. 1990, 1992, 2003, Todd et al. 2016, Yamawaki et al. 2016, 2019, Fisher et al. 2020, Nitzan et al. 2020, Opalka et al. 2020, Wijngaarden et al. 2020.

Encoding and the theory of systems consolidation of memory

The theory of systems consolidation of memory posits that internal representations of experience in hippocampal (HPC) CA1 steer reorganization of distributed neocortical cell assemblies to associate preexisting experience with novel information. This gradual evolution of synaptic connectivity across the neocortex creates a long-term representation of the memory that is no longer dependent on hippocampal activity (Dudai, 2012; Squire et al., 2001, 2015). The first evidence for this theory came from the presentation of temporally graded retrograde amnesia. An animal's ability to remember a stimulus or event is improved the more distant in time or older the memory is from hippocampal lesioning/ inactivation. Temporally graded retrograde amnesia has been clinically described in humans for over 100 years (Ribot, 1882; RUSSELL & NATHAN, 1946), and many studies have demonstrated retrograde amnesia in numerous animal models such as rodents, cats, rabbits, and non-human primates (Squire et al., 2001).

Systems consolidation necessarily requires organized and persistent communication between the hippocampus and neocortex for events and memories to become hippocampal independent. In both humans and rodents, coordinated increases in hippocampal and downstream cortical activity have been described both during learning trials and within seconds of completing trials (Ben-Yakov et al., 2013; Ben-Yakov & Dudai, 2011; Diba & Buzsáki, 2007; Foster & Wilson, 2006). Additionally, tested individuals (humans and rodents) had improved memory response for the trials that had stronger inter regional communication during, and minutes after, the trial. (Staresina et al., 2013; Tambini et al., 2010). As time after

388 learning continues, cortical activation increases, hippocampo-cortical communication
389 continues, and task specific cortico-cortical communication increases; even without continued
390 reminders or reexperiencing the same context (Takehara-Nishiuchi & McNaughton, 2008;
391 Tambini et al., 2010; Tse et al., 2007, 2011; van Kesteren et al., 2010). These data demonstrate
392 the progressive strengthening of cortical networks after an experience or task has been learned
393 and the consequent shifting from the hippocampal representations to the neocortical
394 representations.

395 The communication between the hippocampus and cortex is meaningless without a
396 refined organizational scheme. For information to effectively be communicated with and
397 between synapsembles (groups of neurons interconnected with one another representing
398 similar information), the sender and receiver neurons must be in appropriate states to
399 effectively play their roles (Buzsáki, 2010). The simplest examples of this can be found in *in*
400 *vitro* studies of spike timing dependent plasticity (Markram et al., 1997, 2012). If the receiver
401 neurons are in a primed state, ready to respond or fire an action potential in response to the
402 sender neurons, the synapses between the neurons are strengthened. This strengthened
403 communication results in increased excitatory post synaptic potentials, more ion channels, and
404 larger synapses (Lu et al., 2001; Voglis & Tavernarakis, 2006). If the receiver neurons are not
405 prepared to fire action potentials in response to the sender neurons, the synapse is weakened.
406 This synaptic weakening is indicated by decreased excitatory post synaptic potentials, fewer
407 ion channels, and smaller synapses (Carroll et al., 1999; Voglis & Tavernarakis, 2006). What
408 does this idea of sender and receiver neurons look like when extrapolated into sender and

receiver synapsembles in different brain regions? Oscillatory synchrony between distributed synapsembles is likely the signature demarcating reliable transmission of information from one circuit to another. This means both the sender and receiver synapsembles need to be in a reliable state to send and receive information, respectively. Manipulation of local field potentials disrupts the required LFP-LFP synchrony and consequently blocks effective information transfer between regions or synapsembles, as demonstrated by Fernandez-Ruiz et al., 2021. In this case, LFP-LFP coupling between the hippocampus and downstream cortical regions is necessary for systems consolidation and hippocampo-cortical dialogue in general to occur. As described above, the SPW-R, and the spiking content within, is likely the hippocampal LFP event that guides the restructuring of cortical synapsembles; at least in offline brain states like quiet restfulness and SWS. However, during learning, cortical networks also encode information about experiences that are then recalled and strengthened as systems consolidation progresses (Lesburguères et al., 2011).

gRSC HFOs have been identified occurring during active navigation and REM sleep (when experiences are thought to be encoded), as well as during quiet restfulness and SWS with HPC sharp-wave ripples (when systems consolidation is thought to occur) (Alexander et al., 2018; de Almeida-Filho et al., 2021; Ghosh et al., 2022; Koike et al., 2017; Nitzan et al., 2020; Opalka et al., 2020). The occurrence of HFOs during different brain states that are known to support different computational functions for learning and memory is extremely interesting. This body of work suggests HFOs are recruited for both encoding and systems consolidation purposes.

It is possible that during active navigation and REM sleep, HFOs serve as an encoding signal to "prime" distributed cortical synapsembles as an animal goes through an experience as a memory encoding process. HFOs can occur at the peak of the gRSC and hippocampal theta oscillations (given the high phase coherence (Alexander et al., 2018)) during these states (Ghosh et al., 2022). Under the SPEAR model, established by Hasselmo et al., 2002, the peak of hippocampal theta, and its associated entorhinal cortex mid gamma input, is thought to be important for encoding processes (Colgin et al., 2009; Fernández-Ruiz et al., 2017; Hasselmo et al., 2002; Hasselmo & Stern, 2014; Mizuseki et al., 2009; Schomburg et al., 2014). During these same theta phases, gRSC HFOs can be found. It is possible during active navigation or REM sleep, gRSC HFOs work with hippocampal theta sequences, and EC input, to entrain cortical networks to encode experiences. Once the animal enters quiet restfulness and SWS systems consolidation processes begin. Spontaneously, hippocampal SPW-Rs replay the experience, evoking HFOs that then reactivate the previously primed cortical synapsembles representing the experience. However, this has not been shown and would require hippocampal activity and gRSC HFOs to be studied within a learning and memory dependent paradigm across brain/ behavioral states.

Summary

Learning and memory is necessary for every animal to survive and thrive. Hippocampal theta and gamma activity is required to organize neuronal sequences to encode spatial

information while an animal is actively navigating or during REM sleep (Zielinski et al., 2021). When an animal begins consummatory behavior during quiet restfulness or enters slow wave sleep, hippocampal circuits are spontaneously reactivated during SPW-Rs. SPW-Rs are believed to initiate systems consolidation and to be the signal that guides cortical reorganization as memories shift from short-term into long-term. The gRSC is a cortical region that receives memory specific input from both sensory cortices and internally generated representations from MEC, ADN, post subiculum, and HPC. gRSC HFOs have been correlated with both hippocampal SPW-Rs and theta activity across many brain and behavioral states. It is possible the gRSC serves as a relay hub between internally and externally generated representations of experience across the brain. HFOs within the gRSC may allow for coordination between these 2 information streams during both encoding and systems consolidation.

In this dissertation, I aimed to understand the hippocampo-cortical dialogue during gRSC HFOs across different brain states. To accomplish this, we studied the layer specific interactions supporting spontaneous gRSC HFO generation across brain states, whether the gRSC is capable of generating HFOs locally without patterned input, and the neural activity within the hippocampus during spontaneous HFO events in the gRSC. We accomplished this by recording LFP and single unit activity in awake head-fixed mice trained to run for water rewards in a 1-D linear virtual reality task. Silicon probes were implanted, underneath the central sinus, across the layers of the gRSC, and through ipsilateral HPC CA1. We found that activation of CaMKII expressing excitatory neurons in either layer 2/3 (L2/3) or layer 5 (L5) of

the gRSC induced HFO-like activity, though spontaneous HFOs and associated synaptic currents were only observed in L2/3. Excitatory and inhibitory monosynaptic connectivity was similar in L2/3 and L5. HFOs occurring without SPW-Rs were locked to the descending phase of theta oscillations, along with increased high gamma in CA1 stratum lacunosum moleculare (Str. LM). Additionally, medial entorhinal cortex (MEC) associated high gamma power in Str. LM was comodulated with HFO band power. HFO coupling with multiple HPC oscillations may be a general mechanism by which gRSC circuits process hippocampal inputs in support of hippocampo-cortical dialogue.

CHAPTER TWO: AWAKE HFOs ARE RESTRICTED TO LAYER 2/3

A modified version of this chapter was published at: Kaiser C. Arndt, Earl T. Gilbert, Lianne M.F. Klaver, Jongwoon Kim, Chelsea M. Buhler, Julia C. Basso, Sam McKenzie, Daniel Fine English, Granular retrosplenial cortex layer 2/3 generates high-frequency oscillations dynamically coupled with hippocampal rhythms across brain states, Cell Reports. https://doi.org/10.1016/j.celrep.2024.113910

Abstract

gRSC activity is necessary for spatial navigation and memory. Recent work has shown HFOs in the gRSC can be evoked with dorsal subiculum stimulation, and spontaneous HFOs coincide with HPC SPW-Rs (Nitzan et al., 2020; Opalka et al., 2020). Much is known about the neural circuitry supporting SPW-Rs (Buzsáki, 2015) however, comparatively little is known about HFO generation in the gRSC. To address this gap, we used a combination of high spatial density, anatomically registered silicon probe recordings and optogenetic manipulations. We demonstrate spontaneous gRSC HFOs and associated synaptic currents are produced exclusively in L2/3. Using layer specific optical excitation of channelrhodopsin expressing excitatory cells, both L2/3 and L5 are capable of generating induced HFOs (iHFOs). The capacity of both layers to produce iHFOs is potentially explained by a similar concentration of excitatory and inhibitory connections within each layer.

Introduction

The balance between excitatory (E) and inhibitory (I) currents within a local circuit supports fine timescale dependent organization of neural activity. This balance is specifically important for theta-nested gamma and SPW-Rs in the hippocampus (Buzśaki & Wang, 2012; English et al., 2014; Stark et al., 2014). The E-I balance necessary to support SPW-Rs has also been suggested in other cortical regions (Stark et al., 2014). Prefrontal cortex, posterior parietal, and retrosplenial cortex exhibit HFOs strongly coupling to HPC SPW-Rs (Khodagholy et al., 2017; Nitzan et al., 2020). The co-occurrence of HFOs and SPW-Rs has led to the idea that HFOs are a potential cortical circuit mechanism by which hippocampal SPW-R content is decoded, making the local circuit dynamics of HFO creation a topic of interest.

Historically, gRSC activity has been described using broadly defined locations such as "superficial" or "deep" (Alexander et al., 2018; Nitzan et al., 2020; Opalka et al., 2020). This has made understanding the synaptic interactions supporting HFOs difficult. To date, HFOs have been reported to occur in the superficial gRSC supported by an increased firing rate and phase locking of superficial pyramidal cells compared to deep pyramidal cells and interneurons (Nitzan et al., 2020). However, identifying a more spatially precise location of HFO activity is necessary for understanding the anatomical circuit organization that supports HFOs within the gRSC.

We addressed these gaps using anatomically registered laminar LFP and single-unit recordings combined with focal optogenetics in behaving mice. Using high density silicon

probe recordings, we found spontaneous HFO synaptic currents were localized to layer 2/3 (L2/3), even when events were detected in layer 5 (L5). We developed a device holder to allow for precise layer targeted implantation of chronic μLED probes in an acute setup. This modification of the probes allowed for optical activation of CaMKII-expressing excitatory neurons (ENs) in either L2/3 or L5 of the gRSC induced HFO-like activity, although spontaneous HFOs and associated synaptic currents were observed only in L2/3. The ability for both L2/3 and L5 is potentially supported by excitatory and inhibitory monosynaptic connectivity being similar in both layers.

Results

Spontaneous HFOs

LFP and single unit activity was obtained from mice (N = 7; F1 generation of crossing C57BL/6J with FVB/NJ) trained to run for water rewards in a head-fixed 1-D visual virtual environment. One high-density linear silicon probe (20 μm pitch spanning 1,200 μm) was implanted across the hemispheres beneath the central sinus spanning the layers of the gRSC, with a second probe inserted through ipsilateral HPC CA1 (Figure 2A). Probe locations were identified online using electrophysiological landmarks (see materials and methods below). Probe locations were post hoc identified using a chemically fluorescent stain (DiI) and electrolytic lesion in the tissue. Lesions were created by delivering electrical current through a subset of channels on the probe (Figure 2B). To examine layer-specific oscillatory power, we computed power spectral densities (PSDs) across anatomical space for entire recording sessions

(Figure 2C). HFO power was highest in L2/3 and weakly extended into L5. To anatomically localize current sources and sinks at the time of HFOs, we detected events in L2/3 and computed HFO-triggered current source densities (CSDs), which revealed rhythmic current sources and sinks localized to L2/3 (Figure 2D). Detecting HFOs from L5 LFP gave similar results, confirming that our finding is not due to incorrectly missing L5 HFOs (Figure 3).

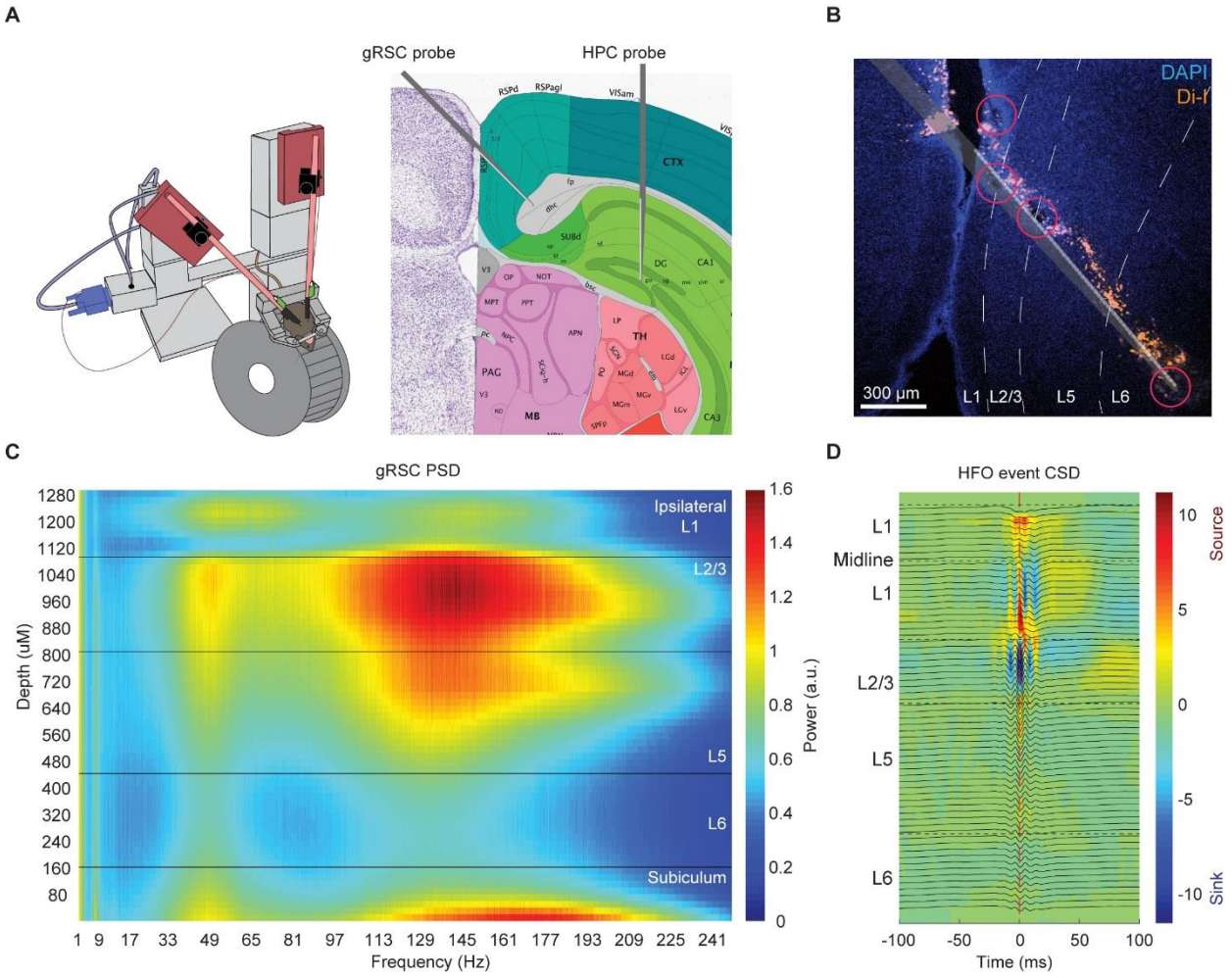

549 **Figure 2. HFO activity is highest in layer 2/3: A)** Acute head-fixed recording and multiprobe
550 implant locations in the gRSC and HPC CA1. Image of brain adapted from the Allen Mouse
551 Brain Atlas. **B)** Photomicrograph of the gRSC after a single-session recording showing probe
552 track (orange, DiI) and electrolytic lesions (red circles) delivered through the silicon probe at
553 specific channels to confirm layer locations. Scale bar, 300 µm. **C)** Representative power
554 spectral density across all layers of the gRSC for an entire recording. **D)** Representative event
555 triggered current source density for all detected HFOs from the L2/3 channel; time zero is the
556 peak of HFO events.

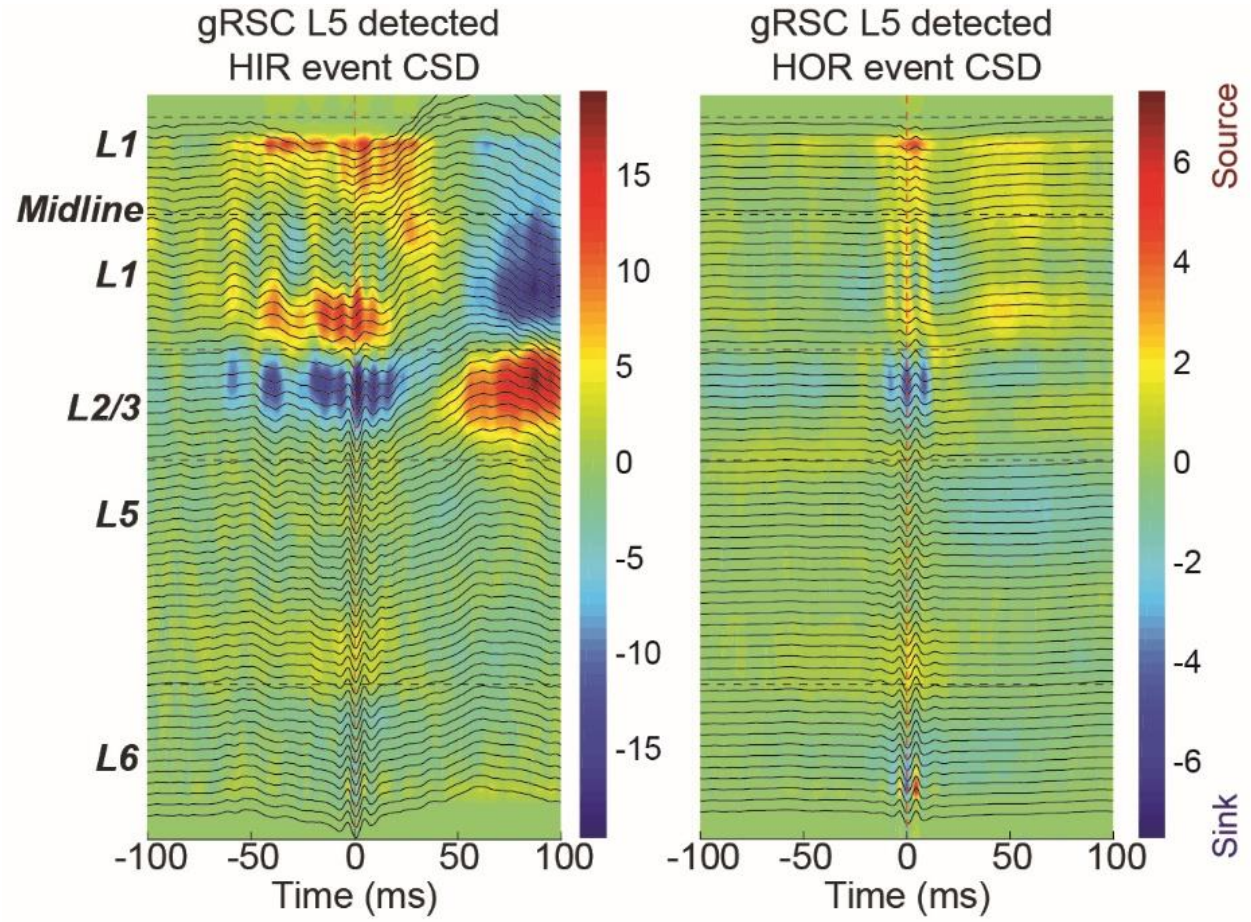

557 **Figure 3. L5 detected HFOs:** Current source density plots of HFO events detected in L5 of the
558 gRSC. Left; HIR events. Right; HOR events. Note for in both HIRs and HORs the current
559 sources and sinks are present flanking the L1-L2/3 border as when HFO events are detected in
560 L2/3.

Optical stimulation induced HFOs

Non-rhythmic activation of the CA1 pyramidal layer produces ripple-like events (similar in frequency to HFOs), but it is unknown whether the gRSC can intrinsically generate HFO-like events (Stark et al., 2014). Here, we sought to determine whether nonrhythmic optogenetic activation of either L2/3 or L5 neurons could produce HFOs, or whether rhythmic afferent input (e.g., from HPC/Sub) is required. To test this, we sought to use the 4 shank 32 channel μLED silicon probe (Wu et al., 2015). However, given the acute nature of these recordings we developed a device holder to convert the chronic device configuration into an acute device. This allowed for more precise control of implant geometries while still using previously purchased devices. The probe holder was designed in Inventor to be 3D printed in a Formlabs 3 printer using rigid resin but should be printable in any STL printer. Once printed, the μLED silicon electrodes were attached using 2-part epoxy. The probe holders were then permanently affixed to a steel rod for manipulation with a micromanipulator for acute implantation (Figure 4A). Probes were positioned with one shank placed in L2/3 and one in L5 of mice chronically expressing channelrhodopsin in CaMKII excitatory cells (N = 3 C57BL/6J-CamKII-Cre::C57BL/6J-Ai32; Figure 4B) (X. Wang et al., 2013). Single-shank illumination induced HFOs (iHFOs) in both L2/3 (Wilcoxon signed-rank test; p = 3.00e–66) and L5 (p = 6.79e–63) (100 ms half-sine wave pulses of 470 nm light applied semirandomly at 2-3 s intervals; Figure 4C). iHFOs had higher power in L2/3 compared to L5 (Wilcoxon rank-sum test; p = 3.58e–10; Figure 4D), consistent with results from our PSD analysis of spontaneous events. We next examined the response of the unstimulated layer (extralaminar).

582 Both L2/3 and L5 exhibited iHFOs in response to the extralaminar stimulation (L2/3 response
583 to L5 stim p = 6.08e–42; L5 response to L2/3 stim p = 6.45e–41; Figure 5A and B). Critically,
584 intralaminar (i.e., same layer) stimulation reliably induced higher-power iHFOs (L2/3 p =
585 2.97e–32; L5 p = 1.04e–7). The occurrence of weak but significant iHFOs in response to
586 extralaminar stimulation may be due to light spread or dendritic illumination. These results
587 suggest that whereas spontaneous HFOs are restricted to L2/3, nonrhythmic activation of
588 either L2/3 or L5 local circuits is sufficient to generate intralaminar iHFOs, although induced
589 HFO power was higher in L2/3.

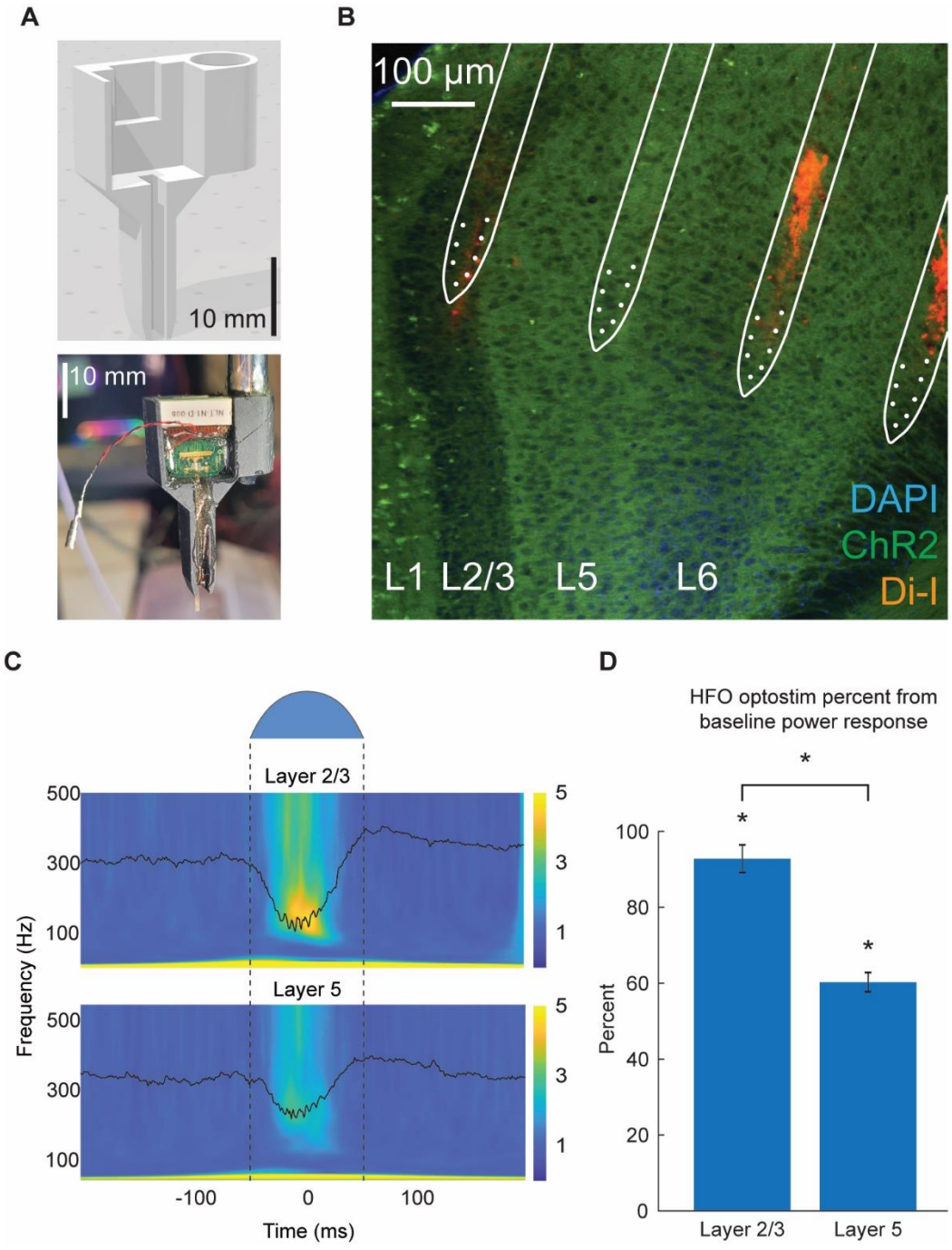
A
10 mm
10 mm
B
100 µm
DAPI
ChR2
Di-I
L1 L2/3 L5 L6
C
Layer 2/3
Layer 5
Frequency (Hz)
500
300
100
5
3
1
-100
0
100
Time (ms)
D
HFO optostim percent from baseline power response
Percent
100
80
60
40
20
0
Layer 2/3
Layer 5
*

590

Figure 4. gRSC L2/3 and L5 are both capable of generating HFOs: A) Photomicrograph of the gRSC of CaMKII-Cre::Ai32 mice. White overlay of Neurolight Technologies' microscopic light emitting diode probe. Channelrhodopsin (green) expressed in excitatory cells. DiI (orange) used to mark the tracks of the probe shanks. Scale bar, 100 μm. **B)** Top: shape of 100 ms light stimulation pulse delivered to each layer of the gRSC. Light intensity was determined empirically in L2/3 and set to a level that reliably evoked HFOs. Center: representative L2/3 optical stimulation event-triggered PSDs (100–150 pulses to each layer) Z scored and normalized to 500 ms before analysis window shown. Overlaid traces are the event-triggered average LFP. Time zero is the peak of the stimulation pulse. Bottom: same as center, but for L5. **C)** Percentage from baseline (100 ms before stimulation) power response in the 100–250 Hz range. Both L2/3 ($p = 3.00e{-}66$) and L5 ($p = 6.79e{-}63$) reliably generated HFOs during stimulations (Wilcoxon signed-rank test, 3 animals, $n = 400$ total light pulses to each layer). L2/3 responded significantly more than L5 to optical stimulation ($p = 3.58e{-}10$; Wilcoxon rank-sum test). Error bars show the SEM.

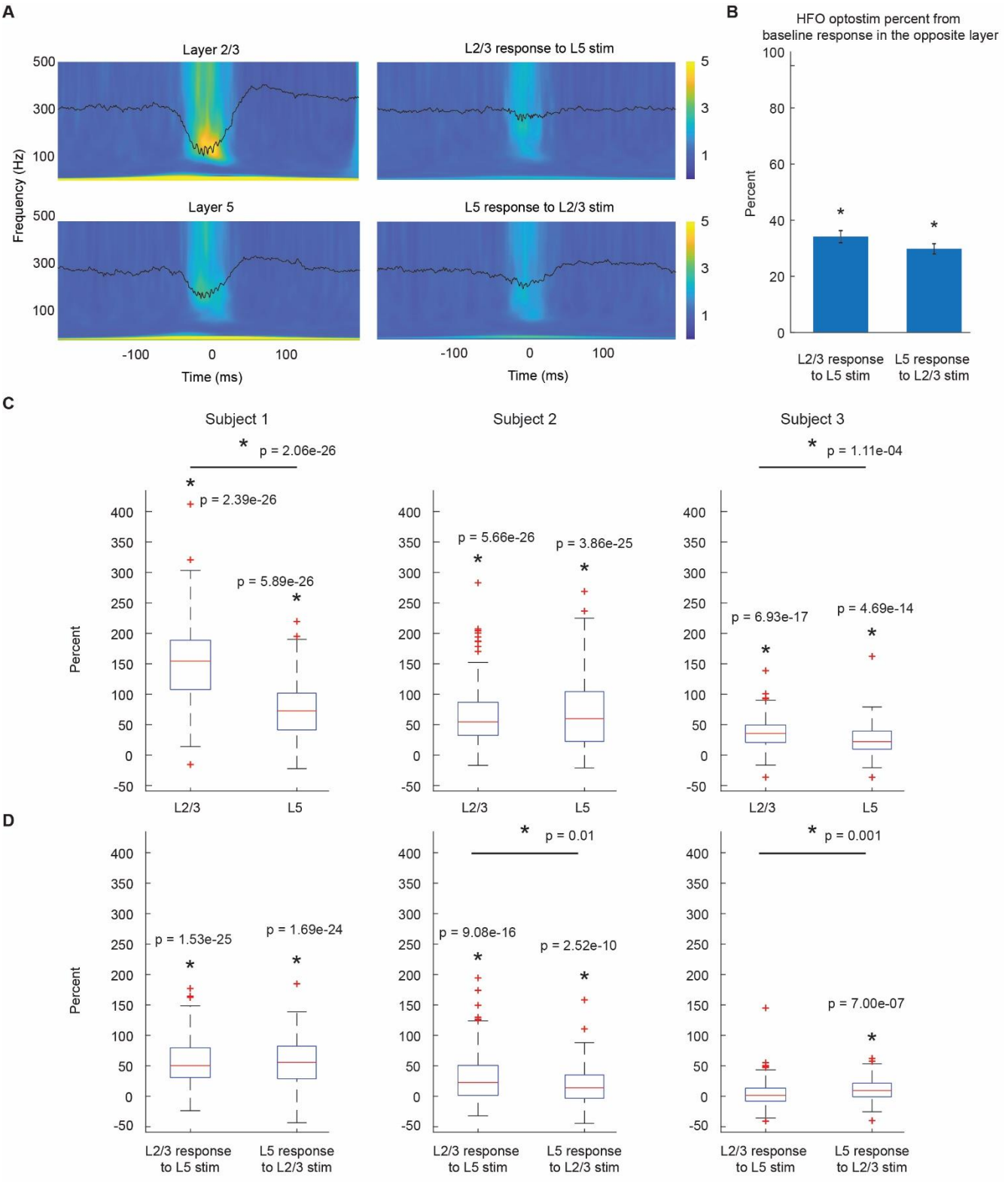
A
Layer 2/3
L2/3 response to L5 stim
Layer 5
L5 response to L2/3 stim
Frequency (Hz)
500
300
100
5
3
1
-100
0
100
Time (ms)
B
HFO optostim percent from baseline response in the opposite layer
Percent
100
80
60
40
20
0
L2/3 response to L5 stim
L5 response to L2/3 stim
C
Subject 1
Subject 2
Subject 3
p = 2.06e-26
p = 2.39e-26
p = 5.89e-26
p = 5.66e-26
p = 3.86e-25
p = 1.11e-04
p = 6.93e-17
p = 4.69e-14
Percent
L2/3
L5
D
p = 0.01
p = 0.001
p = 1.53e-25
p = 1.69e-24
p = 9.08e-16
p = 2.52e-10
p = 7.00e-07
L2/3 response to L5 stim
L5 response to L2/3 stim

605

Figure 5. Opposite layer response to optostimulation: A) Left; same PSDs from Fig. 2B. Right; Representative optical stimulation event-triggered PSDs (100-150 pulses to each layer z-scored and normalized to the 500 ms before analysis window shown. Top right: L2/3 response to L5 optical stimulation. Bottom right: L5 response to L2/3 optical stimulation. **B)** Mean percent from baseline power response to stim in the 100-250 Hz range. Both L2/3 ($p = 6.08e-42$) and L5 ($p = 6.45e-41$) reliably generated HFOs during stimulations of the other layer (baseline compared to stim; Wilcoxon signed rank test, 3 animals, 100-150 light pulses to each layer in each animal). All error bars show the SEM. **C)** Optostimulation pulse box plots split by session (400 stims; 150, subject 1; 150, subject 2; 100 subject 3) corresponding to bar graph in Fig. 2C. **D)** Same as in C but data points correspond to B.

Monosynaptic connectivity

To determine whether differences in connectivity patterns could explain why HFOs are localized to L2/3, we quantified putative excitatory and inhibitory monosynaptic connections. Putative excitatory and inhibitory units were first identified in CellExplorer (Petersen et al., 2021) using ACG*tau* rise and trough to peak time (Figure 6). examining auto- and crosscorrelograms for spike trains of gRSC neurons (Figure 7A), both within and between layers (Figure 7B). A total of 65.6% of monosynaptic connections were observed to be intralaminar. Given that L2/3 and L5 are capable of generating local HFOs and local monosynaptic connections are thought to support high-frequency activity, (Stark et al., 2014) we quantified the percentage of ENs and Ints with a connection to another cell within the presynaptic cell's layer: E-I, I-I, and I-E. Connection probabilities were not different between L2/3, L5, and L6 (ANOVA, E-I $p = 0.90$; I-I $p = 0.52$; I-E $p = 0.47$; Figure 7C). L1 was excluded from this analysis because no intralaminar monosynaptic connections were identified. E-E connections were excluded because only three putative connections were identified (potentially due to the fact that E-E connections are more difficult to identify). Thus, similar excitatory and inhibitory connectivities are present in each layer, potentially explaining our ability to drive iHFOs in both lamina (Figure 4).

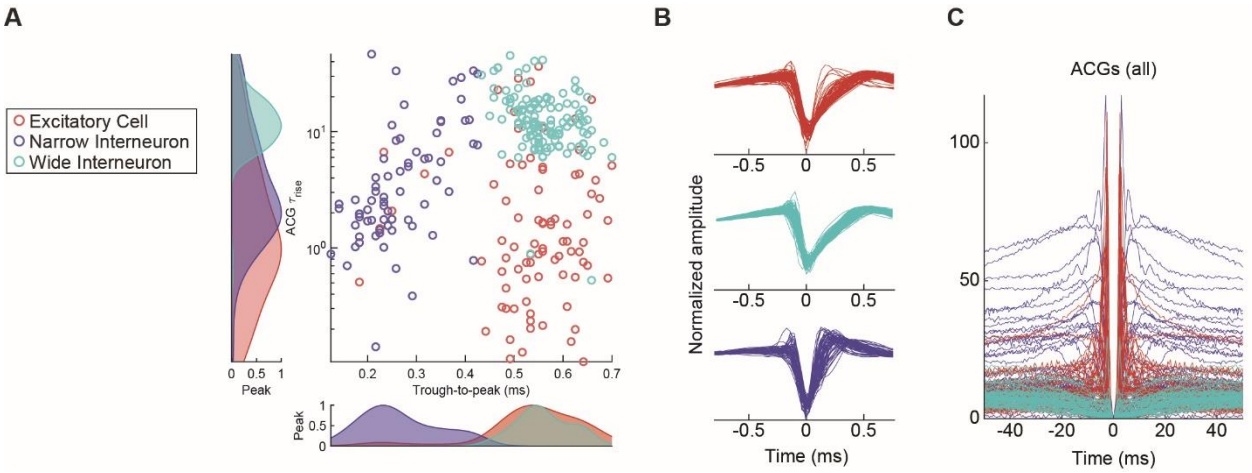

633 **Figure 6. Cell type classification: A)** Metrics used to classify each cell as a wide (light blue, n =
634 128) or narrow (dark blue, n = 69) interneuron, or an excitatory cell (red, n = 85). **B)** Wave
635 forms of each cell type. **C)** Autocorrelograms for each recorded unit.

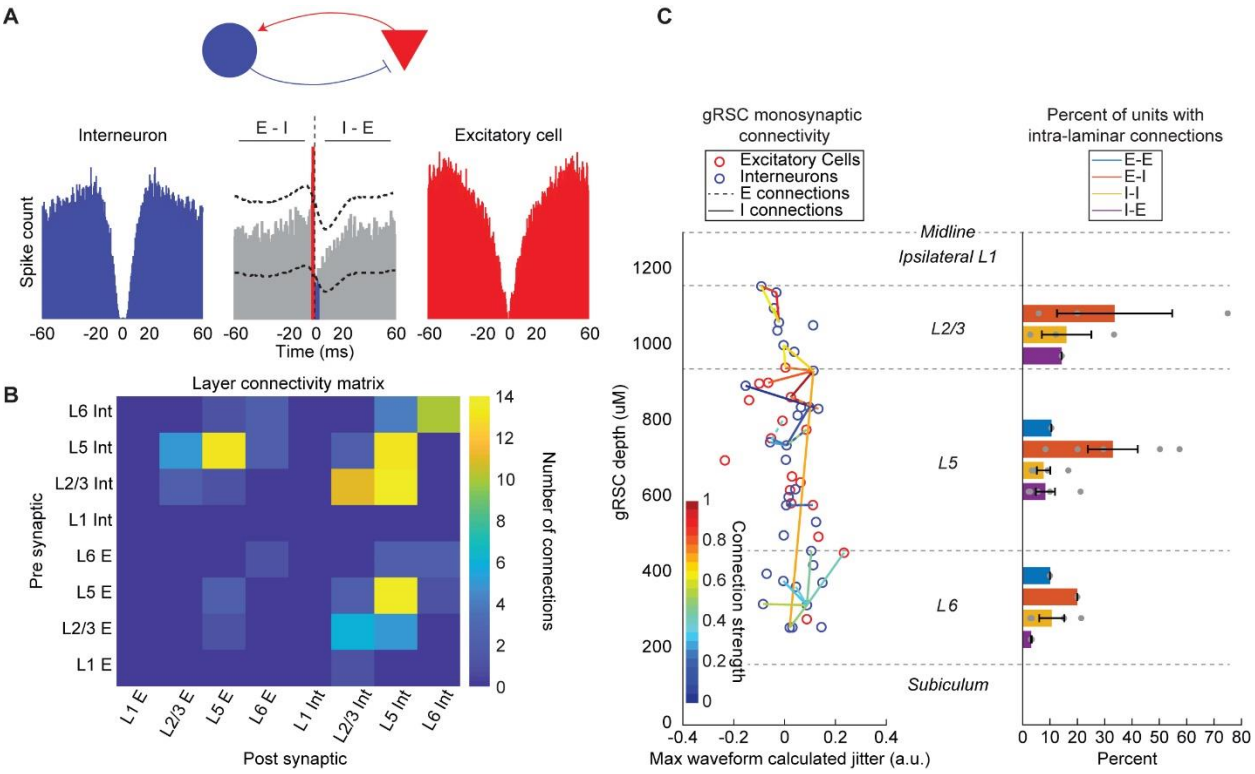

Figure 7. Inter- and intralaminar monosynaptic connections in the gRSC: A) Example monosynaptic excitatory and inhibitory connection between a putative excitatory and inhibitory cell. Center: crosscorrelogram between the Int and excitatory cell. The peak before zero shows excitatory drive of the Int (red bars) and the trough after zero shows the inhibition of the EN. Horizontal dotted lines are the 95% confidence interval of the average cross-correlation at each time point. **B)** Connectivity matrix for the number of monosynaptic pairs between ENs and Ints across the layers of the gRSC from 7 recordings of 4 mice. **C)** Left: representative monosynaptic connectivity map showing the putative locations of each unit and their monosynaptic connections across the layers of the gRSC. Right: percentage of each cell type with putative intralaminar connections in each layer from n = 7 recordings from 4 animals. Bars not shown in each layer had no detected monosynaptic connections of that type. An ANOVA was used to compare the percentage of cells with each monosynaptic connection type in each layer. Error bars show the SEM.

Discussion

HFOs have been reported to occur in the superficial gRSC (Ghosh et al., 2022; Nitzan et al., 2020). Other studies have used tetrode implants randomly targeted to all layers (biased to deep) of the gRSC and have reported HFOs (Alexander et al., 2018; Opalka et al., 2020). The anatomically ambiguous nature of these previous studies has left the cellular basis supporting HFO generation unclear. Here, we aimed to address this gap by using a combination of high density linear and μLED silicon electrode recordings. We mapped the laminar electro-anatomy of the gRSC and found that spontaneous HFOs occur exclusively in L2/3, supported by CSD analysis. These findings were consistent for events detected in L5 showing synaptic currents also present in L2/3, suggesting HFOs present in L5 are a consequence of volume conduction (the passive spread of electrical currents, not associated with active input from the local region to generate the electrical currents).

L2/3 is additionally the location of afferent inputs from ADN, dorsal subiculum, MEC, and HPC, all regions responsible for encoding internally generated representations of experience. Activation of dorsal subiculum resulted in evoked HFOs in the gRSC L2/3 (Nitzan et al., 2020). Prior to this work, it remained unclear if nonrhythmic activation of local circuits could produce HFOs or if they require activation of upstream circuits to create the oscillation.

To address whether local gRSC circuits naturally support HFO frequencies we took advantage of the precise geometry of μLED silicon probes (Wu et al., 2015). We found that focal activation of both L2/3 and L5 resulted in iHFOs, albeit L5 HFOs were weaker than those

669 in L2/3. Therefore, each layer is able, with strong afferent drive, to generate an HFO, although
670 L5 typically does not. However, even iHFO power differed between layers, suggesting other
671 potential variations in rhythmogenesis. E-I connections, important for rhythmogenesis, were
672 not found to be different between layers. This analysis is known to be biased to detect strong
673 connections; therefore, it is possible that other differences exist in the microcircuitry, and this
674 should be explored in multipatch in vitro preparations. The lack of spontaneous HFOs in L5
675 may be due to differences in excitatory drive, recurrent E-I connectivity, cell density, and/or
676 cellular physiology (e.g., input resistance such as low rheobase cells in L2/3 (Brennan et al.,
677 2020, 2021)). Our results suggest that variations in afferentation likely play the dominant role,
678 because the latent possibility for HFO genesis was revealed with artificial optogenetic drive.
679 However, this shouldn't rule out other possibilities of cell type or local network differences,
680 where sufficient excitatory input is capable of evoking iHFO oscillations in layers they don't
681 naturally occur.

682 Even though we were able to drive iHFOs in both L2/3 and L5, spontaneous HFOs
683 appear to occur exclusively in L2/3 as demonstrated by the presence of current sinks. L2/3 is
684 also where low rheobase (LR) excitatory neurons are located (Brennan et al., 2020; Robles et
685 al., 2020). Optical activation of axon terminals from both ADN and dorsal subiculum results in
686 excitation of these LR neurons (Brennan et al., 2021). It is possible that LR neuron activity is
687 required for the occurrence of spontaneous HFOs and potentially why HFOs occur exclusively
688 in L2/3, but not L5. If this is the case, HFOs, and consequently LR neuron activity, may be

critical for the contextual association between internally and externally generated representations of experience. We believe these questions are of vital importance in understanding the gRSCs role in learning and memory. Future studies using *in vitro* and *in vivo* preparations should focus on the necessity of LR neurons in the occurrence of HFOs as well as the necessity of LR and HFO activity in learning and memory tasks.

CHAPTER THREE: HFO INTERACTIONS WITH THE HIPPOCAMPUS

A modified version of this chapter was published at: Kaiser C. Arndt, Earl T. Gilbert, Lianne M.F. Klaver, Jongwoon Kim, Chelsea M. Buhler, Julia C. Basso, Sam McKenzie, Daniel Fine English, Granular retrosplenial cortex layer 2/3 generates high-frequency oscillations dynamically coupled with hippocampal rhythms across brain states, Cell Reports. https://doi.org/10.1016/j.celrep.2024.113910

Abstract

Numerous studies have reported high frequency oscillations are found within the gRSC during all brain states when both HPC SPW-Rs and theta/ gamma oscillations occur (Alexander et al., 2018; Ghosh et al., 2022; Khodagholy et al., 2017; Koike et al., 2017; Nitzan et al., 2020; Opalka et al., 2020). gRSC population unit activity can differentiate between subclasses of SPW-Rs. Specifically, subsets of gRSC neurons respond to specific SPW-R subtypes that encode differing information (Nitzan et al., 2020). However, it has been reported that HFO power in the gRSC of both mice and rats is strongest during REM sleep (Ghosh et al., 2022; Koike et al., 2017). Thus far, no study has focused on the gRSC and HPC LFP dynamics during HFOs occurring with and without SPW-Rs. Here we aimed to illuminate this gap by using an *in vivo* awake head fixed dual acute silicon probe setup, where probes were simultaneously implanted into the gRSC and hippocampal CA1. We show HFOs occurring with SPW-Rs (HIRs) are higher power, frequency, and amplitude compared to HFOs outstide of SPW-Rs (HORs). Unit activity trends toward being more HOR modulated. HORs are locked

to the descending phase of both local and HPC theta. Supported by independent component analysis, gRSC HOR frequency is strongly coupled with high gamma of the CA1 stratum lacunosom moleculare component; which is known to be generated by the medial entorhinal cortex.

Introduction

The theory of systems consolidation of memory posits that internal representations of experience in HPC CA1 guide cortical neuroplastic changes within synapsembles to encode long term memories of events (Dudai, 2012; Squire et al., 2001, 2015). When animals actively explore their environment, encoding is thought to dominate over retrieval. These moments are associated with high cholinergic tone and strong power in the theta and gamma bands, which can be observed in the LFP, spiking of neuronal populations, and membrane potentials of individual neurons in both HPC and downstream cortical networks (Buzsáki, 2002; English et al., 2014; Harvey et al., 2009; Isomura et al., 2006; Sirota et al., 2008). In contrast, when cholinergic tone diminishes, theta power decreases and SPW-Rs (Haam & Yakel, 2017; Hasselmo, 1999; Vandecasteele et al., 2014) can be observed in the CA1 LFP, reflecting 100–250 Hz oscillations in neuronal membrane potentials and spiking activity (Buzsáki, 2015; English et al., 2014; Harvey et al., 2009; Isomura et al., 2006; Sirota et al., 2008; Stark et al., 2014). CA1 theta oscillations organize place cells into assemblies during experience, and by modifying synaptic connectivity, are believed to enable subsequent SPW-Rs to function as a "teaching signal" (C. Liu et al., 2023) to induce plasticity in downstream cortical regions and

consolidate the memory of the experience (Dudai, 2012; McKenzie et al., 2020; Squire et al., 2015).

A growing body of work suggests the gRSC is a region necessary for systems consolidation to occur (Alexander et al., 2023; Alexander, Robinson, et al., 2020; Sun et al., 2021; Vann et al., 2009). Healthy gRSC activity is necessary for effective spatial navigation as well as learning and memory. Changes in gRSC oscillatory activity are observed in several neurological and neuropsychiatric disorders (Mitelman et al., 2005; Nestor et al., 2003; Nugent et al., 2006). In animal studies, lesioning or removal of the gRSC results in impaired learning and memory performance, while optical stimulation of the gRSC can recover memory deficits induced by HPC inactivation (de Sousa et al., 2019). gRSC activity coincides with hippocampal SPW-Rs during quiet restfulness and slow wave sleep or theta and gamma oscillations during active running or REM sleep (Alexander et al., 2018; de Almeida-Filho et al., 2021; Ghosh et al., 2022; Khodagholy et al., 2017; Koike et al., 2017; Nitzan et al., 2020; Opalka et al., 2020). During these periods of hippocampo-cortical coactivity, high frequency oscillations have been observed within the gRSC in all brain states. gRSC HFOs occur often with SPW-Rs and gRSC population unit activity can discriminate between types of SPW-Rs (Nitzan et al., 2020; Opalka et al., 2020).

Here, we aimed to understand the coupling of hippocampal oscillations to local gRSC HFOs across awake brain states. To accomplish this goal, we used anatomically precise probe implants to record LFP and single unit activity in an awake, head-fixed setup. Recorded HFOs

were split into groups occurring with SPW-Rs and those occurring without. Synaptic currents supporting both groups were present within L2/3. L5 units increased their firing rate more during HFOs outside of ripples (HORs). HORs were locked to the descending phase of theta oscillations, along with increased high gamma in stratum lacunosum moleculare (Str. LM). In addition, MEC-associated high gamma power in Str. LM was comodulated with HFO band power. HFOs during different brain states, coupling with multiple HPC oscillations, may be a general mechanism by which gRSC circuits process HPC inputs to support hippocampo-cortical dialog.

Results

Characteristics of HIR and HORs

There is a body of prior work showing that gRSC HFOs are coupled with both CA1 SPW-Rs and theta oscillations, particularly in rapid eye movement (REM) sleep (Abadchi et al., 2023; Alexander et al., 2018; de Almeida-Filho et al., 2021; Ghosh et al., 2022; Koike et al., 2017; Nitzan et al., 2020). Because SPW-Rs and theta occur in antagonistic states, it is unclear whether these HFOs are equivalent events. To compare the physiology of these events, we separately analyzed HFOs that did or did not occur in time with CA1 SPW-Rs. HFOs occurring within ±50 ms of a CA1 SPW-R were designated as in-SPW-R events (HIRs) and those outside this window as outside-SPW-R events (HORs; Figures 8A and 8B). HIRs had significantly higher amplitude, power, and frequency (7,720 HIRs, 71,965 HORs; Wilcoxon rank-sum test; $p = 5.21e{-}138$, $1.21e{-}280$, and $4.82e{-}93$, respectively), whereas HORs were significantly longer

780 (Wilcoxon rank-sum test; p = 1.16e–8; Figures 8C, 8D, and 9A). Given that we observed a
781 higher number of HORs, we took a random sample of HORs matching the number of HIRs
782 and reanalyzed this subset of the data, which yielded results that were consistent with the full
783 datasets (Figure 9B).

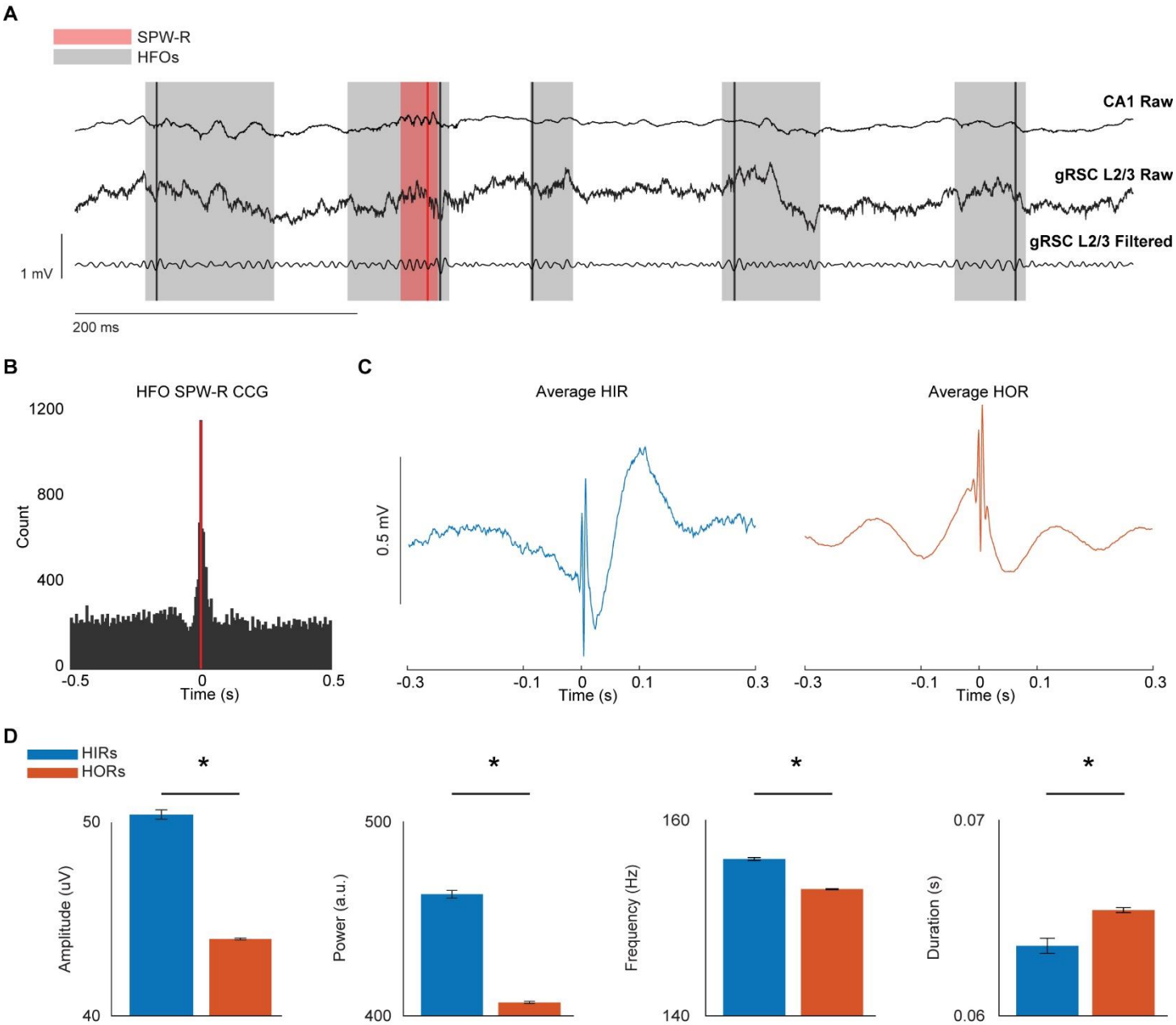

784 **Figure 8. HFOs are identified during and outside of SPW-Rs: A)** Example traces and detected
785 SPW-Rs (red) and HFOs (gray) in CA1 and gRSC, respectively. Lines mark the peak of the
786 detected event; shaded areas mark the duration of the detected event. **B)** SPW-Rs-HFO
787 crosscorrelogram. Red line marks the peak of detected SPW-Rs. **C)** Left: representative average
788 of HFOs in ripples (HIRs; n = 513 events). Right: same as left for HFOs out of ripples (HORs;
789 n = 14,986 events). **D)** Comparison of peak amplitude (p = 5.21e–138), peak power (p =
790 1.21e–280), peak frequency (p = 4.82e–93), and duration (p = 1.16e–8) (left to right) between
791 HIRs and HORs across 4 recordings from 4 animals (n = 7,720 HIRs; n = 71,965 HORs). All of
792 the tests used Wilcoxon rank-sum test. Error bars show the SEM.

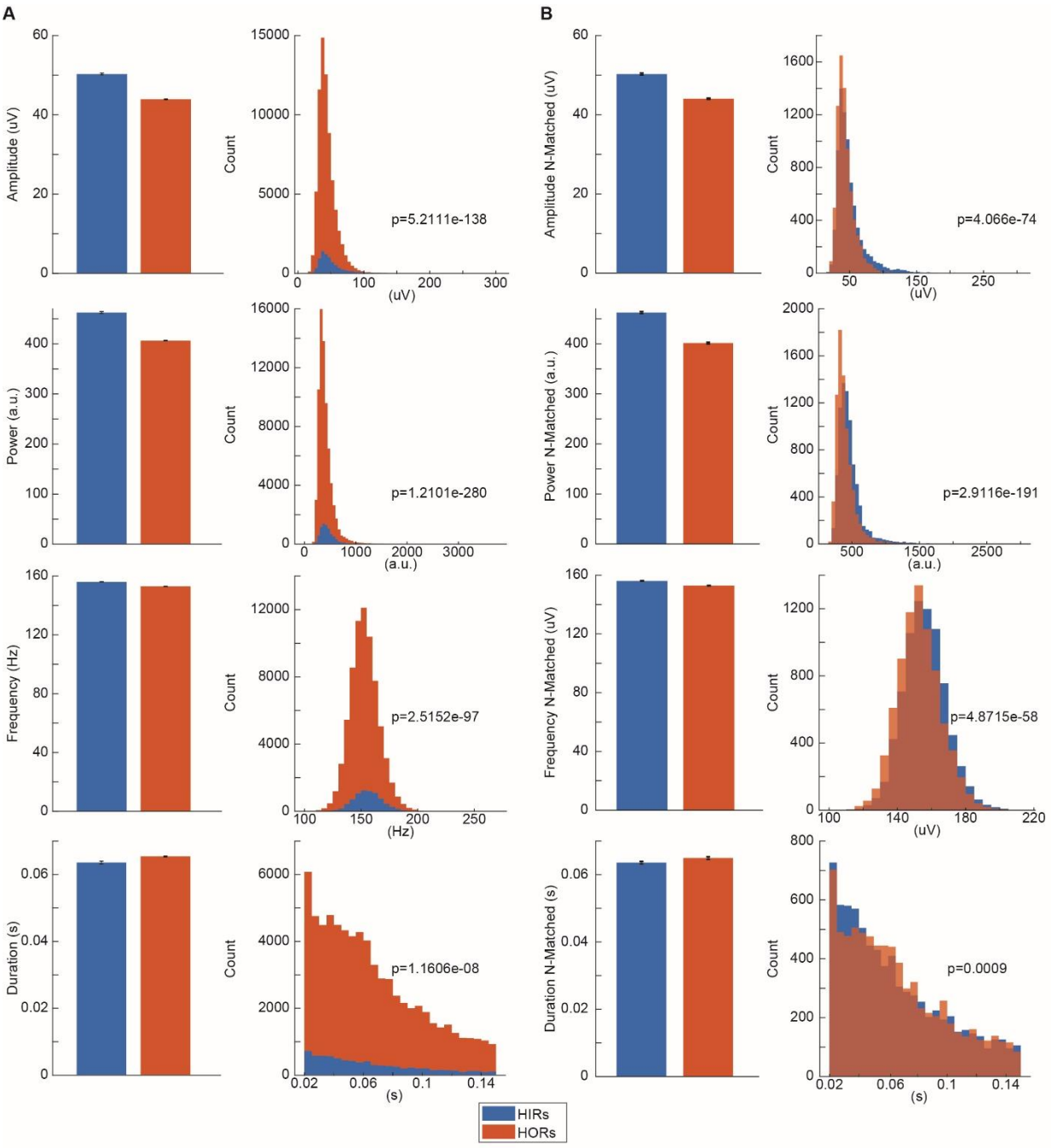

Figure 9. High frequency oscillation features in and out of sharp wave-ripples: A) All detected HIR (blue; n = 7720 events) and HOR (orange; n = 71965 events) events showing comparison of peak amplitude, peak power, peak frequency, and duration. Right shows the distributions of HIRs and HORs corresponding to Figure 3. HIRs had higher amplitude, power, and frequency, and HORs had longer duration. **B)** The same as in A, but a subset of randomly selected HOR events to match the number of detected HIRs were used for statistical comparison. All metrics were consistent with that of all event comparisons in A. All comparisons made with the Wilcoxon rank sum test. Centers show the mean and error bars show the SEM.

Unit responses to HIR and HORs

HFOs are thought to arise due to interactions between excitatory and inhibitory cell interactions (Stark et al., 2014). Therefore, we next quantified the spiking activity of putative ENs (n = 85 units) and interneurons (Ints, n = 197 units) using CellExplorer (Petersen et al., 2021) (Figures 6). Neurons were assigned to layers by estimating their position using the recording site with maximum spike amplitude. L5 ENs and Ints both increased their firing rate more during HORs than HIRs (ENs, p = 0.0036; Ints, p = 0.0041; t test HOR gain minus HIR gain); conversely, L1 Ints increased their firing rate more during HIRs than HORs (p = 0.045) potentially due to different neuromodulatory tone. In contrast, the gain in L2/3 firing rate was not significantly different across HIRs and HORs; however, there was a nonsignificant bias toward HORs (Figure 10).

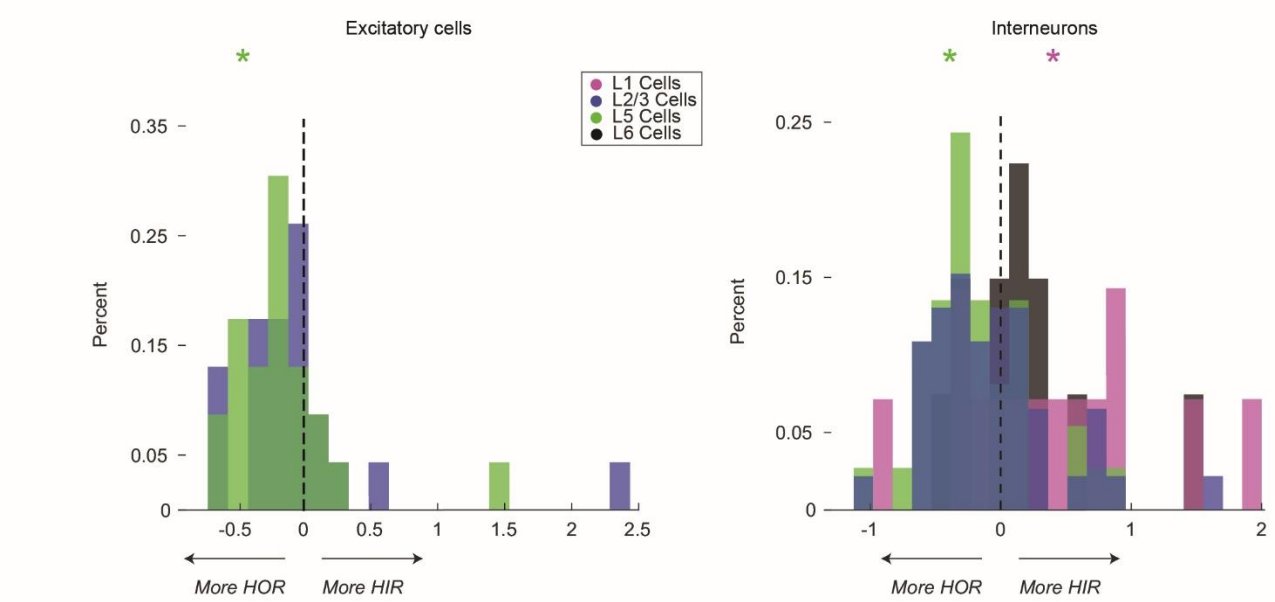

Figure 10. Unit firing rate responses to HIRs and HORs: Gain in firing rate for putative excitatory cells (left) and interneurons (right) during HIRs and HORs. X axis is the difference between the gain in firing during HIRs and HORs. Colored asterisks correspond to the layer they were recorded in and designates whether those units fired more during either event type. Layers without asterisks did not have cells that fired more during either HIRs or HORs. L5 ENs ($p = 0.0036$ and Ints ($p = 0.0041$) fired more during HORs and L1 Ints ($p = 0.045$) fired more during HIRs (t-test of HIR gain minus HOR gain). Unit counts are as follows: excitatory neurons (L2/3 = 23, L5 = 23) inter- neurons (L1 = 14, L2/3 = 46, L5 = 37, L6 = 12).

gRSC HFOs coincide with L2/3 CSD sinks across network states

We next investigated LFP and synaptic activity supporting natural HFO generation in the gRSC. HIR and HOR event-triggered PSDs revealed differences in associated rhythmic network activity. HIRs were associated with a negative LFP deflection in L2/3, suggesting local neuronal depolarization (Figure 11A). HORs occurred when gRSC and CA1 exhibited LFP theta oscillations, preferentially occurring at the descending phase of the oscillation (Rayleigh's test, $p < 1.0e{-}50$ for both HPC and gRSC; Figure 11B). This rhythmic theta activity is clearly present in the HOR-triggered LFP (Figure 8C) and PSD (Figure 11A). Although the rate of HORs was similar for periods of ambulation and stillness ($p > 0.05$), nearly all of the HIRs occurred when the animals were still (Wilcoxon rank-sum test, $p = 0.05$; Figure 11C). In addition, running speed and theta power were higher during HORs than during HIRs (Figure 12). CSDs revealed rhythmic current sources and sinks located on the border between L2/3 and ipsilateral L1 for both HIRs and HORs (Figure 11D). To determine whether these results were biased by the detection of HFOs in L2/3 and not L5 (a smaller-amplitude HFO is seen in L5 at the same time), we detected HFOs from L5. Current sources and sinks localizations did not depend on the layer used to detect HFOs (Figure 3), suggesting that apparent L5 HFOs reflect volume conduction.

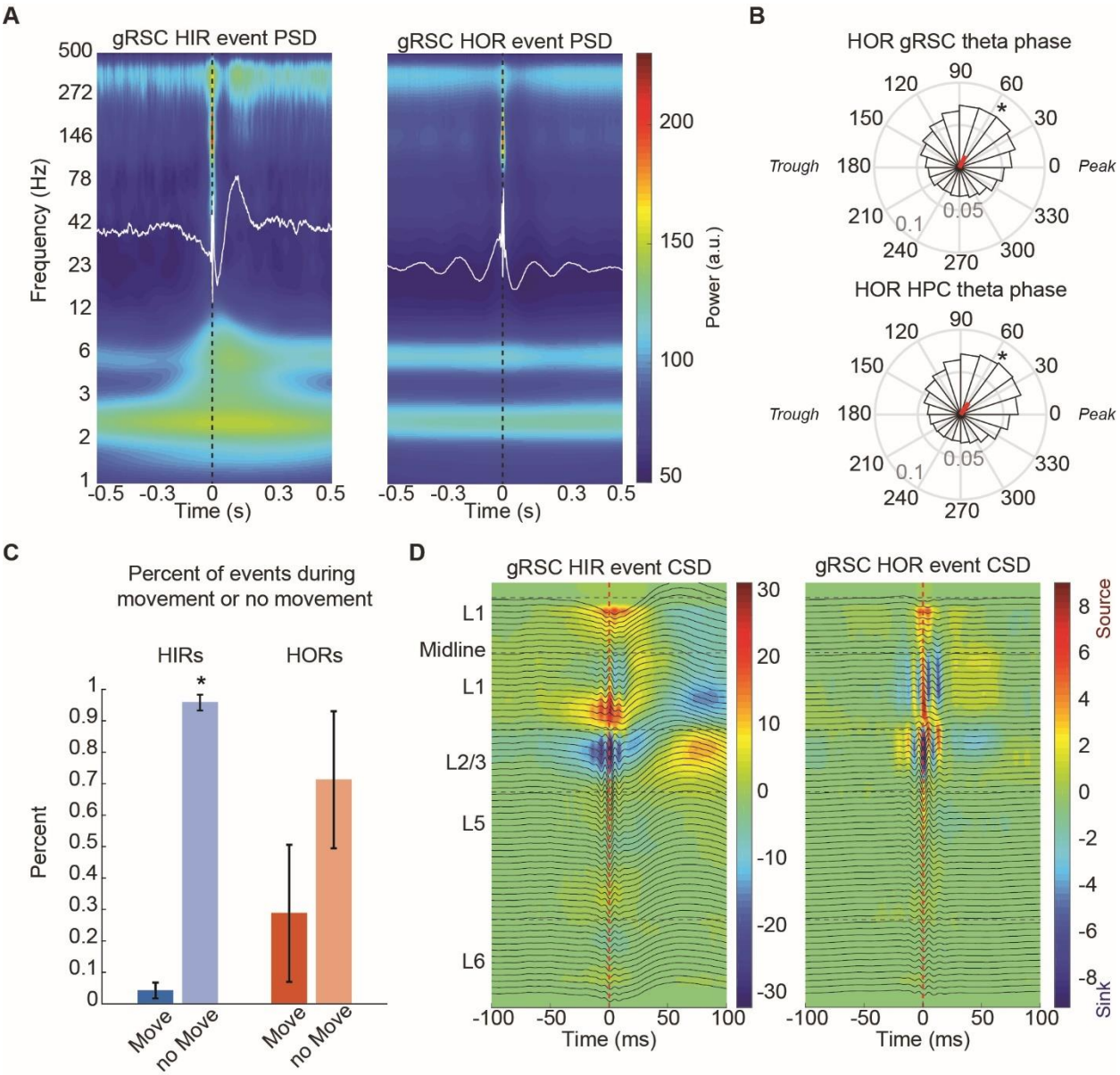

838 **Figure 11. gRSC HFO activity is on the border of L1–L2/3, and HORs occur on the descending**
839 **phase of local and HPC theta: A)** Left: representative HIR (n = 513 events) event-triggered PSD
840 in the gRSC. The peak of each event is centered on zero. Right: same as left, but for HORs (n
841 = 14,986 events) from the same session. **B)** Polar plots of HOR (4 recordings from 4 mice, n =
842 87,369 events) preference to local gRSC theta (top; Rayleigh's test $p < 1.0e{-}50$, resultant vector
843 length = 0.208) and HPC theta (bottom; Rayleigh's test $p < 1.0e{-}50$, resultant vector length =
844 0.23). **C)** Percentage of HIRs (blue) and HORs (orange) that occur when the animal is moving
845 or stationary (Wilcoxon rank-sum test $p = 0.05$, n = 3 recordings from 3 mice). Error bars show
846 the SEM. **D)** Left: representative HIR event-triggered CSD centered the same as in (A) and
847 using the same events as in (A). Right: same as left, but for HORs from the same session.

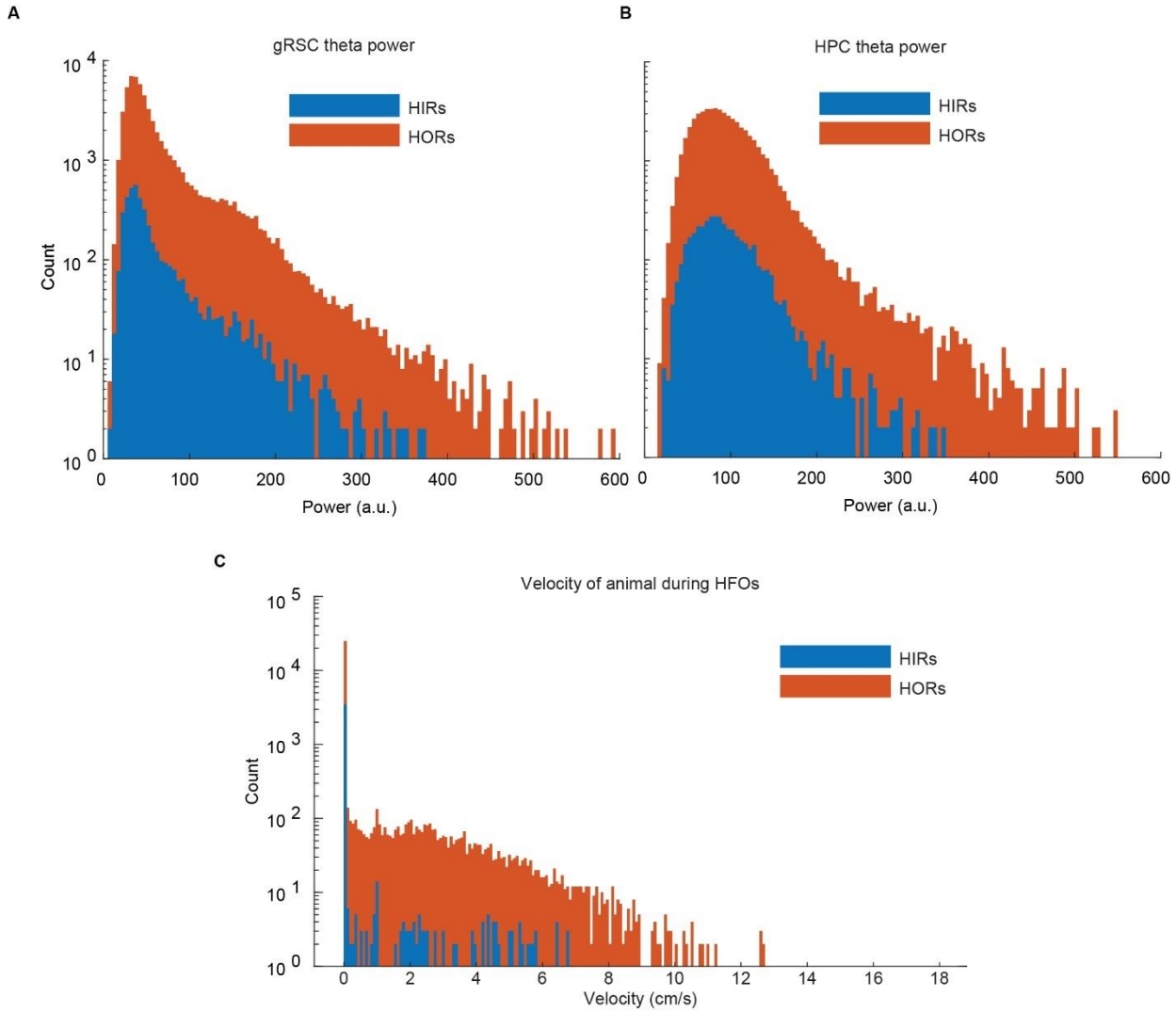

Figure 12. gRSC, HPC theta power and animal velocity during HFOs: A) RSC theta power during HFOs for 5 animals, n = 8227 HIRs, and n = 119970 HORs. There was higher gRSC theta power during HORs than during HIRs (p = 2.38e-06; Wilcoxon rank sum test). **B)** Same as in A but for HPC theta power. There was higher HPC theta power during HORs than during HIRs (p = 0.02; Wilcoxon rank sum test). **C)** Same as in A and B but for animal velocity for 3 animals, n = 7204 HIRs, and n = 56979 HORs corresponding to Fig. 5C. Animal velocity was significantly higher during HORs than HIRs (p = 3.23e-17; Wilcoxon rank sum test).

Str. LM high-frequency gamma oscillations are comodulated with HFOs

To determine the oscillatory activity of CA1 circuits during HIRs and HORs, we computed event-triggered PSDs and CSDs from the CA1 pyramidal layer LFP (Figures 13A and B). In HIRs, SPW-R frequency and delta power were elevated (Figure 14), and characteristic current sources and sinks were present in stratum pyramidale (Str. Pyr) and stratum radiatum (Str. Rad), respectively (Figures 6A and B, left). In HORs, CA1 pyramidal layer LFP exhibited a sustained increase in theta power and theta-nested gamma (Figure 14). CA1 theta activity was associated with expected current sources and sinks in the pyramidal layer and Str. LM, respectively (Figure 14B) (Brankačk et al., 1993; Fernández-Ruiz et al., 2017). Using independent component analysis, we identified independent components (ICs) previously established to reflect CA3 input to the Str. Rad and MEC input to Str. LM (Figures 14C and D), here referred to as ICRad and ICLM, respectively (Fernandez-Ruiz et al., 2023; Fernández-Ruiz et al., 2012, 2017; Schomburg et al., 2014). gRSC HFO frequency and ICLM high gamma were strongly comodulated (Figure 14E). Notably, the ICLM high gamma comodulation was higher than the ICLM low gamma and ICRad low and high gamma ($p < 5.96$ e–8 for all tests). The strong correlation between ICLM and gRSC rhythmic activity suggests privileged communication between the entorhinal cortex, CA1, and gRSC during descending phases of the theta rhythm.

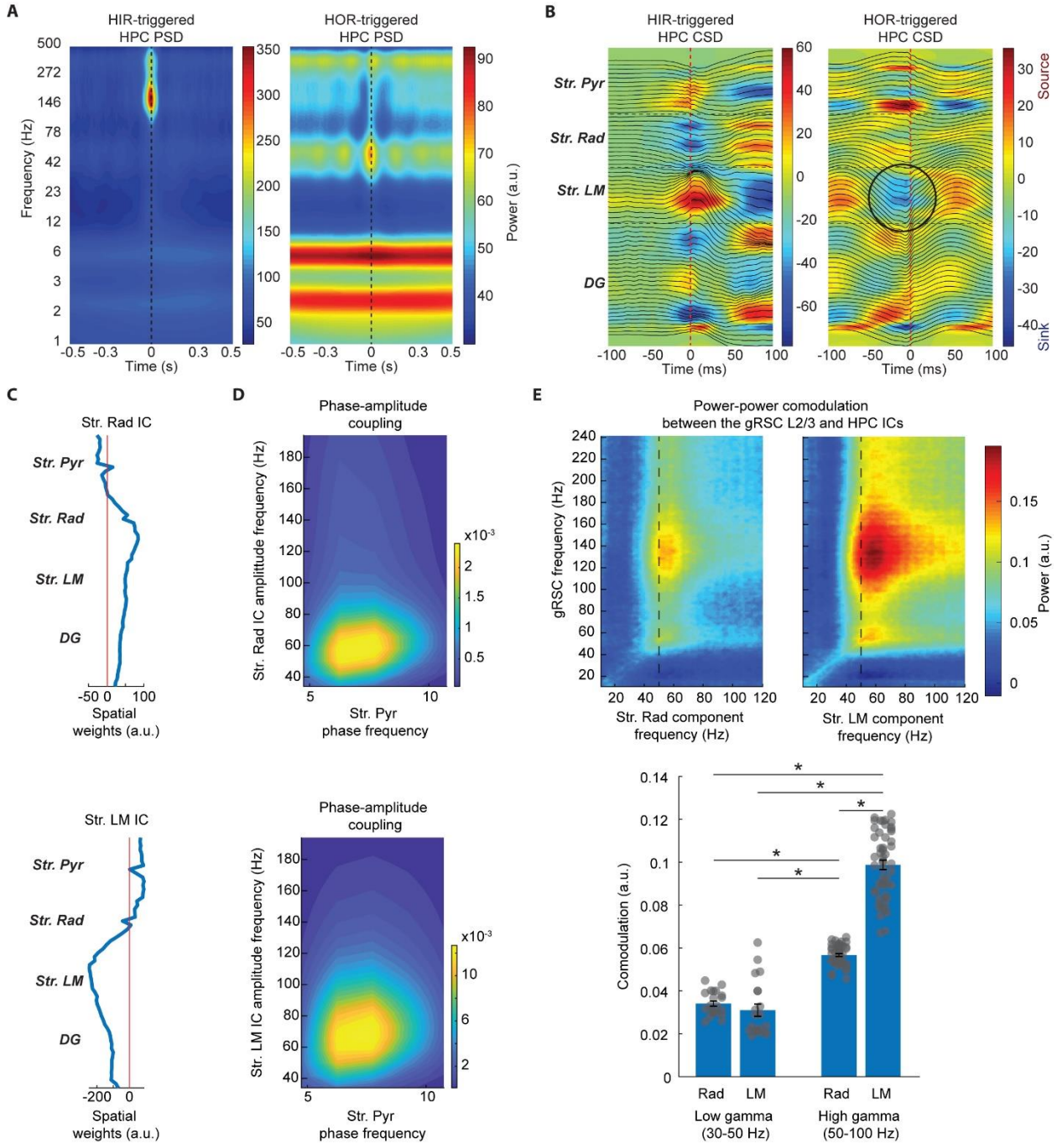
A
HIR-triggered
HPC PSD
HOR-triggered
HPC PSD
Frequency (Hz)
Time (s)
Power (a.u.)
B
HIR-triggered
HPC CSD
HOR-triggered
HPC CSD
Str. Pyr
Str. Rad
Str. LM
DG
Time (ms)
Source
Sink
C
Str. Rad IC
Spatial
weights (a.u.)
Str. LM IC
D
Phase-amplitude
coupling
Str. Rad IC amplitude frequency (Hz)
Str. LM IC amplitude frequency (Hz)
Str. Pyr
phase frequency
E
Power-power comodulation
between the gRSC L2/3 and HPC ICs
gRSC frequency (Hz)
Str. Rad component
frequency (Hz)
Str. LM component
frequency (Hz)
Comodulation (a.u.)
Rad
LM
Low gamma
(30-50 Hz)
High gamma
(50-100 Hz)

873

Figure 13. HPC spectral coupling dynamics of gamma and SPW-Rs with gRSC HFOs: A) Left: HPC activity during representative HIR (n = 513 events) event-triggered PSD in the HPC channel used to detect SPW-Rs. Zero is centered on the peak of the HIR. Right: same as left, but for HORs (n = 14,986 events). **B)** Left: representative HIR event-triggered CSD centered the same as in (A) and using the same events as in (A). Right: same as left but for HORs. Black circle marks current sink in Str. LM. **C)** Top: representative spatial loading of the IC_{Rad} following independent component analysis. Bottom: same as top, but for the IC_{LM}. **D)** Top: representative phase amplitude coupling between the IC_{Rad} amplitude and Str. Pyr theta phase. Bottom: same as top for $IC_{LM.}$ Note that colorbar axes are different between top and bottom to aid in visualization of the lower amplitude IC_{Rad}. **E)** Top: representative power-power comodulation between the gRSC L2/3 and the IC_{Rad} (left) and IC_{LM} (right). Bottom: the average power-power comodulation of gRSC L2/3 (120–180 Hz) and HPC ICs of 4 recordings from 4 animals split between low gamma (n = 20 frequency bins of 30–50 Hz) and high gamma (n = 50 frequency bins of 50–100 Hz), as shown at top by the dashed vertical line. The LM high gamma component has significantly higher comodulation with gRSC HFO than the RAD low gamma (ANOVA with multiple comparison t tests, asterisks indicate $p < 5.96\ e{-8}$). Error bars show the SEM.

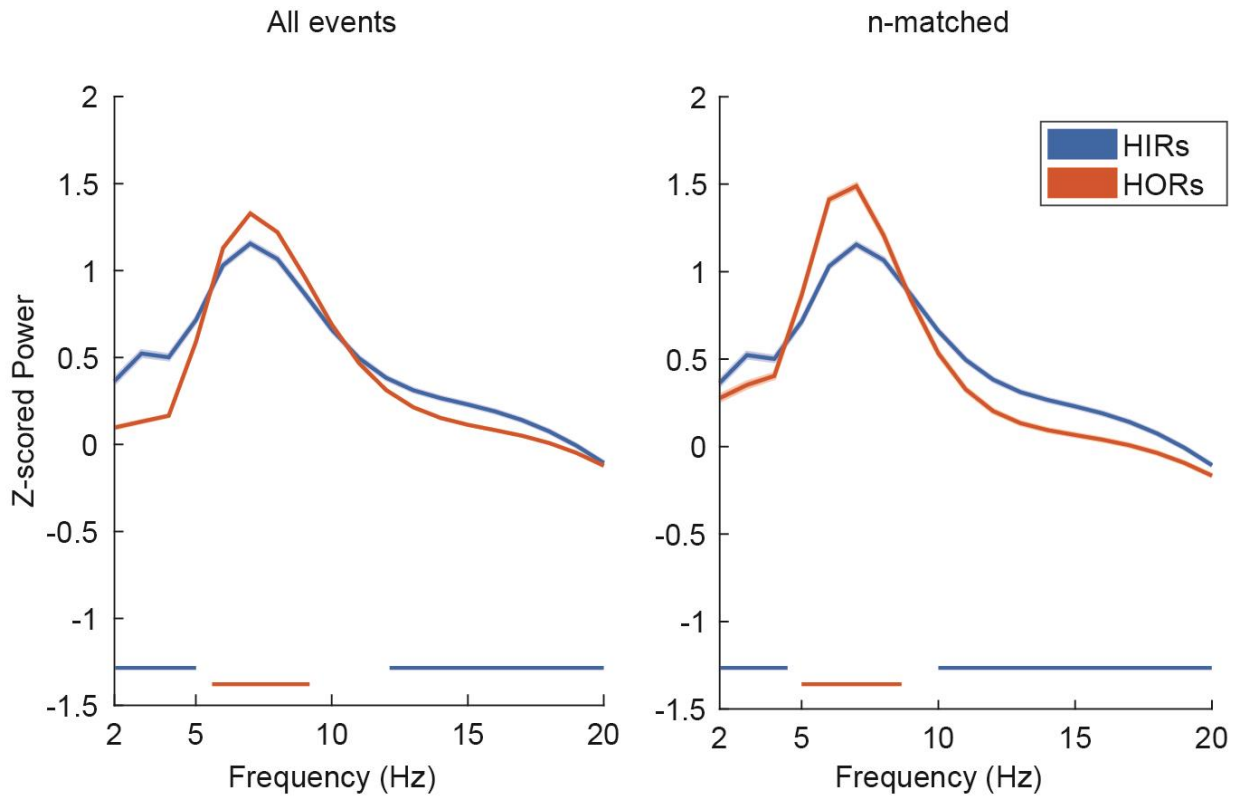

Figure 14. L5 detected HFOs: Current source density plots of HFO events detected in L5 of the gRSC. *Left;* HIR events. *Right;* HOR events. Note for in both HIRs and HORs the current sources and sinks are present flanking the L1-L2/3 border as when HFO events are detected in L2/3.

Discussion

In rodents and humans, high-frequency cortical oscillations are prevalent during periods of HPC SPW-Rs and theta oscillations in cortical regions receiving excitatory drive from the hippocampal formation (Dickey et al., 2022; Khodagholy et al., 2017; Norman et al., 2019; Staresina et al., 2015; Vaz et al., 2019) which suggests flexible coupling of these events to different hippocampal oscillations (Alexander et al., 2018; Cardenas et al., 2023; Nitzan et al., 2020; Opalka et al., 2020). Here, we investigated gRSC HFO properties across brain states, and we demonstrated interactions with CA1 gamma oscillation current generators during HFOs occurring outside of SPW-Rs.

We found that spontaneous HFO events, across different brain states are generated in L2/3. This is supported by our CSD analysis showing that during all events (HIRs and HORs), the current sources and sinks remain in L2/3, even when we detected events in L5. Recently, gRSC "splines," with similar frequencies to HFOs, have been described in superficial gRSC, phase locked to the peak of theta oscillations during running and REM sleep. We believe these splines and our recorded HORs are likely the same physiological event as they are both found in superficial (L2/3) gRSC with very similar synaptic current activity, as well as being locked to similar phases of the theta oscillation during similar brain states. HIRs preferentially occurred when animals were stationary, whereas HOR prevalence was less dependent on behavior (consistent with previous reports) (Alexander et al., 2018). Although the theta oscillation is typically associated with running behavior, type 2 (atropine-sensitive) theta oscillations can occur independent of movement, potentially underlying unique

computation/brain states (Buzsáki, 2002; Buzsáki et al., 1983; Kamondi et al., 1998). It is possible that HORs consist of multiple subgroups of HFOs, potentially dependent on distinct theta oscillations resulting in unique state specific computation (Buzsáki, 2002; Kocsis et al., 1999). One potential mechanism resulting in multiple types of HORs could be the dynamic cholinergic inputs into the gRSC (Anzalone et al., 2009; Murakami et al., 2013; Robertson et al., 2009). Historically, theta oscillations have been split into 2 types. The cholinergic antagonist atropine has been shown to disrupt HPC type 2 theta oscillations during quiet restfulness, but not type 1 theta oscillations during active locomotion (Buzsáki et al., 1983). Type 1 theta is thought to be important for encoding of spatial information during active navigation, while type 2 theta is hypothesized to be a marker of arousal and attentiveness during immobility (Mikulovic et al., 2018; Montoya et al., 1989; Sainsbury et al., 1987). It is possible that particular theta and acetylcholine dynamics promote HOR occurrence and may allow for unique computation during different behaviors such as spatial encoding during active locomotion and attentiveness during immobility. Additional studies focused on the behavioral correlates of HFO generation across brain states in task specific manners will shed light onto the specific function of gRSC network activity during these oscillations. For example, interruption of cholinergic input to the gRSC may inhibit attentive behaviors, or closed loop inhibition of HFOs triggered on theta or SPW-Rs may inhibit learning and memory processes (discussed more in the next chapter).Because we observed HFOs in both theta and SPW-Rs, we suggest that they are a general mechanism by which gRSC circuits process HPC and potentially entorhinal cortex inputs (Figure 15) (Ghosh et al., 2022).

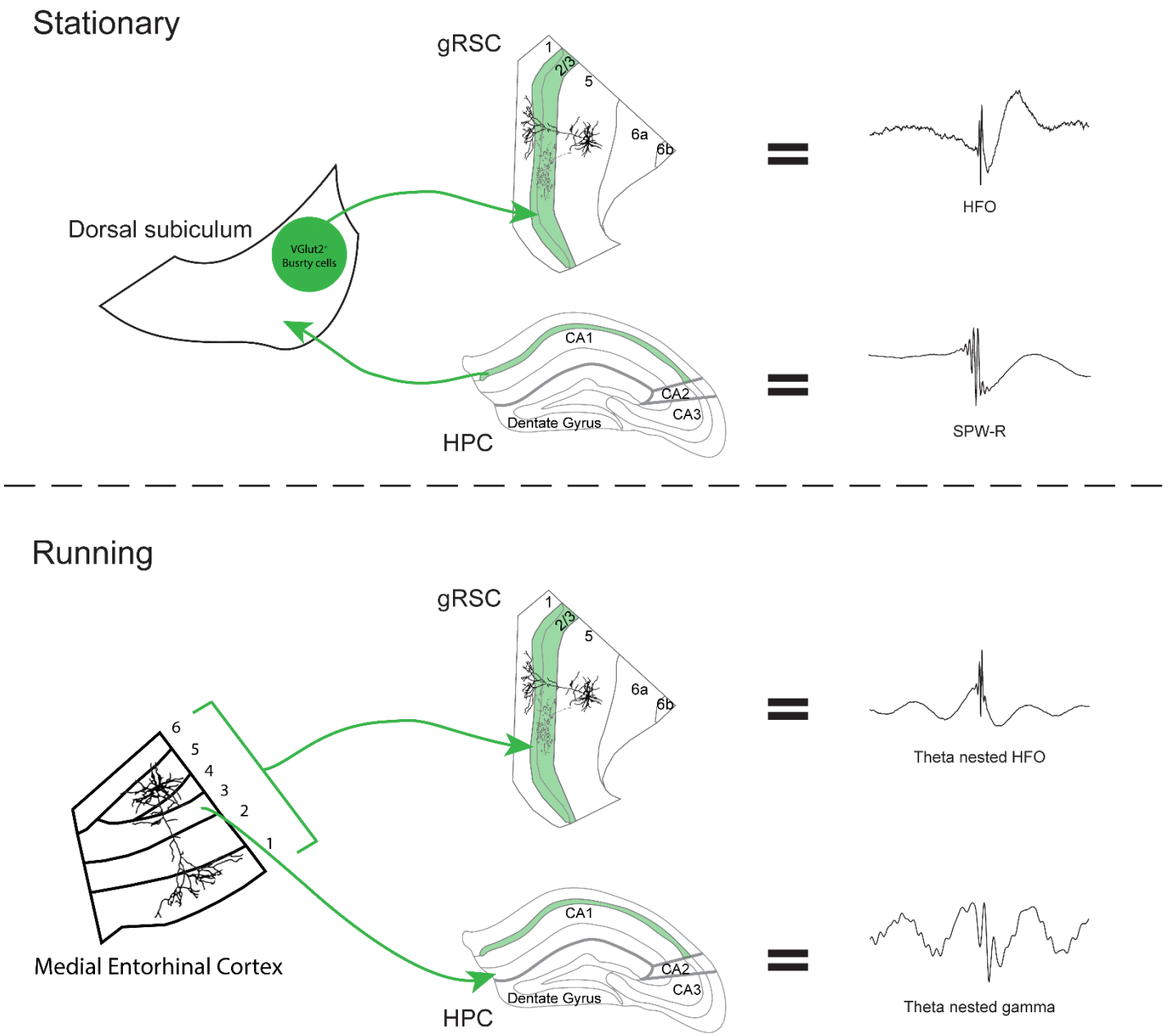

Figure 15. Proposed mechanism modulating HORs and Str. LM gamma synchrony: *Top*: Pathway from hippocampus to dorsal subiculum to gRSC via VGlut2+ positive bursty cells driving gRSC HFOs in time with hippocampal SPW-Rs. This is supported by work from Nitzan et al 2020 and Opalka et al 2020. *Bottom*: Proposed pathway from work discussed here of excitatory input from medial entorhinal cortex driving comodulation between CA1 Str. LM high gamma and gRSC HORs.

CHAPTER FOUR: CONCLUDING DISCUSSION AND FUTURE WORK

Introduction

The retrosplenial cortex serves a vital role in learning and memory (Alexander et al., 2023; de Sousa et al., 2019; Mitchell et al., 2018; Mitelman et al., 2005; Nestor et al., 2003; Nugent et al., 2006; Vann et al., 2009) however, the field has yet to reach a consensus on the RSC's precise function. Previous work has shown that HFOs are present in the superficial layers of the gRSC, occurring in time with hippocampal SPW-Rs and theta oscillations (Alexander et al., 2018; de Almeida-Filho et al., 2021; Ghosh et al., 2022; Khodagholy et al., 2017; Koike et al., 2017; Nitzan et al., 2020; Opalka et al., 2020). These findings suggest HFOs are a potential mechanism by which information from cortical and subcortical regions is processed for memory encoding and consolidation. In this dissertation, I aimed to understand the hippocampo-cortical dialogue during gRSC HFOs across different brain states. To accomplish this we studied the precise laminar organization of synaptic currents generating HFOs in the gRSC, whether gRSC neural activity naturally oscillates at HFO frequency, and how HPC gamma generators couple with gRSC HFOs outside of SPW-Rs.

HFO generation

Intralaminar Connectivity

To support and maintain high frequency oscillations, such as hippocampal SPW-Rs, intricate and precise local excitatory and inhibitory interactions are required (Buzsáki, 2015; English et al., 2017; Stark et al., 2014). In gRSC L2/3, a special class of excitatory neuron is most prevalent, low-rheobase (LR) cells (Brennan et al., 2020, 2021; Robles et al., 2020). The spiking properties, notably the ability to fire at high frequencies, low rheobase, high input resistance, and low spike frequency adaptation, of LR neurons are optimal for encoding information sent to the gRSC and for supporting excitatory currents of spontaneous HFO generation. LR neurons comprise the largest proportion of neurons in gRSC L2/3 and are potentially the primary driver of excitatory currents onto local fast spiking interneurons. Brennan et al., 2020 showed, in slice preparation, that the only local excitatory connectivity originates from 17% of all LR cells who synapsed onto deeper located fast spiking inhibitory cells. 52% of these fast-spiking inhibitory cells also had connections onto LR cells. Brennan et al., also showed that much of the local network is supported by feed forward inhibition potentially allowing the gRSC circuit to utilize interneuron-gamma and/or pyramidal-interneuron gamma mechanism to create high frequency oscillations (Buzsáki, 2015; Buzśaki & Wang, 2012; Stark et al., 2014; Tiesinga & Sejnowski, 2009). In our optical stimulation experiments, we likely excited many of these LR cells in L2/3, recruiting the local circuit to oscillate at high frequencies.

There still remains discrepancies in this theory of LR neurons being important for HFO generation in L2/3, however. The first of which is we were able to evoke HFOs in L5, yet LR

cells are only present in L2/3 and not L5. It is possible our L5 optical stimulation excited LR axons going through L5 targeted to deeper interneurons resulting in L5 interneuron recruitment and HFO generation. However, these are speculations that require more studies to accurately address. Secondly, many other cortical regions have been found to exhibit similar high frequency oscillations (Averkin et al., 2016; Grenier et al., 2001; Khodagholy et al., 2017; Manabe et al., 2011; Vaz et al., 2019). Yet, LR cells have not been identified in any of these other brain regions suggesting the LR cells are not the main source supporting high frequency oscillations. An alternative hypothesis can come from the perspective of inhibition. Fast spiking interneurons are present across the brain and are known to be necessary for SPW-Rs (Buzsáki, 2015; Schlingloff et al., 2014) and cortical HFOs (Grenier et al., 2001). It is possible the local fast spiking interneurons in the gRSC are the major source of gating HFO frequency and occurrence (Brennan et al., 2020). However, additional *in vivo* experimentation is required to fully understand the cellular basis governing HFO generation in the gRSC.

Cholinergic system

Atropine is a common acetylcholine receptor antagonist and has been used extensively to study hippocampal theta oscillations (Buzsáki et al., 1983; Hasselmo, 1999; Herreras et al., 1988). Hippocampal theta oscillations can be separated into 2 types. Type 1 is atropine resistant theta which is present during active locomotion and linked to sequential place cell activity. Type 2 is atropine sensitive theta, which is present during quiet restfulness (Buzsáki, 2002; Vanderwolf, 1988). The medial septum-dorsal band of broca (MS-DBB) is a large generator of

hippocampal theta oscillations through its cholinergic inputs (Buzsáki, 2002). Inactivation of the MS-DBB disrupts both hippocampal and entorhinal cortex theta oscillations (Buzsáki, 2002). Additionally, systemic administration of acetylcholine receptor antagonists results in disruption of theta-gamma phase amplitude coupling within the MEC (Newman et al., 2013). The MEC sends projections to the gRSC that are important for encoding boundaries of environments (van Wijngaarden et al., 2020). The MS-DBB also sends cholinergic projections to the gRSC L2/3, which are implicated in amyloid beta accumulation in Alzheimer's disease (Robertson et al., 2009). Given the importance of cholinergic inputs to the HPC and MEC for effective place coding and coordination of LFP, it appears likely that cholinergic inputs to the gRSC also play an important role for maintaining unit and LFP activities. This hypothesis is also supported by the strong phase coherence of gRSC and HPC theta oscillations, if theta frequency shifts, I would expect to see a similar frequency shift in gRSC (Alexander et al., 2018). We show that HIRs occur when animals are stationary, as expected from the occurrence of SPW-Rs. However, HORs do not occur more during quiet restfulness or active locomotion, suggesting HORs here are potentially comprised of multiple groups of events. Some HORs may be occurring during SPW-Rs that were not captured in the CA1 network we recorded form. Some HORs are likely apart of type 1 theta during active locomotion and are likely important for encoding of experiences. Lastly, some HORs are likely occurring during type 2 theta during restfulness. These multiple groups of HORs are potentially modulated by cholinergic input to the gRSC and may be separable based on variable activity of cholinergic inputs during different brain states.

gRSC's role in a larger circuit

Input from internally generated representations of experience

The gRSC receives strong input from many brain regions responsible for encoding internally generated representations of experience, such as the hippocampus, dorsal subiculum, ADN, and MEC (Alexander, Carstensen, et al., 2020; Lozano et al., 2017; Mao et al., 2017, 2018; Shine et al., 2016; van Wijngaarden et al., 2020). Much of this input likely affects LR neuron tuning and the generation of HFOs. In *In vitro* preparations, LR neurons receive strong excitation from dorsal subiculum and ADN which are important for head direction and head velocity (Brennan et al., 2021). Optical excitation of dorsal subiculum drives L2/3 HFO activity (Nitzan et al., 2020). Stimulating CA1 to evoke HFOs likely requires subiculum activity, as only stimulation of distal CA1 resulted in large negative waves in gRSC L2/3. To date, the only direct monosynaptic connections from CA1 to the gRSC are inhibitory in nature or activate local interneurons in the gRSC (Opalka et al., 2020; Yamawaki et al., 2019). This incoming inhibition potentially serves the purpose of gating gRSC HFO activity, during different states, to occur at the precise moments in time to receive incoming information potentially from the subiculum (during SPW-Rs or theta oscillations) (Nitzan et al., 2020). Or put another way, the hippocampal writer network may send excitatory signals to the subiculum at the same time as inhibitory signals to the gRSC, gating the gRSC receiver network to be in an optimal state to encode the incoming information from the subiculum. The MEC sends, likely excitatory, monosynaptic projections to gRSC L2/3 and L5 that are necessary for effective encoding of environment boundaries (van Wijngaarden et al., 2020).

Optical inhibition of these projections disrupts information transfer from MEC to the gRSC resulting in impaired boundary coding of gRSC neurons. Using independent component analysis, we show that CA1 Str. LM high gamma, thought to originate from the MEC, is highly correlated with gRSC HFOs in L2/3. MEC input to L2/3 may modulate HFO activity during active navigation theta states. Future studies should aim to dissect this circuit across brain states (described in more detail below).

Cross hemisphere interactions

We show that synaptic currents supporting HFO generation are located across the boundary between L1 and L2/3, and current sources span both ipsilateral and contralateral L1. Notably, these currents are in the same position across brain states during both HIRs and HORs, suggesting similar network recruitment for different brain states and associated computation. Previously reported splines, events with similar frequency to HFOs, that lock to the peak of theta specifically during active locomotion and REM sleep are likely the same events, or at least of portion of them, reported here as HORs (Ghosh et al., 2022). A key feature of splines is their 180-degree phase offset between the gRSC hemispheres, suggesting a novel and complex computation strategy for encoding information in the gRSC between the hemispheres. In our recordings, we didn't position probes spanning contralateral L2/3 so we weren't able to capture this phase offset, though, CSD analyses shown here and in Ghosh et al., 2022 appear similar. The extent to which this cross-hemisphere interaction is important

for information coding remains unknown, as well as whether or not this unique computation is consistent across all states, such as during HIRs (discussed more below).

Future experiments and speculations

LR neuron importance for HFO/ spline generation

LR neurons have been shown to receive strong excitatory input from the ADN and dorsal subiculum suggesting LR neurons may encode information coming from these brain regions(Brennan et al., 2020, 2021). Optical excitation of the dorsal subiculum VGlut2^{+} bursty neurons is sufficient to evoke HFO like activity in gRSC L2/3, where naturally occurring HFOs and LR cells are found (Nitzan et al., 2020). Via this pathway it is possible that LR cells encode aspects of experience, such as head direction or location, during HFOs and splines. Future studies may look to genetic techniques to target and manipulate these neurons in awake behaving animals to perturb both local and interregional communication. Understanding the importance and role of LR cell activity in HFO/spline generation will give insights into the gRSC's role in learning and memory processes.

HFO and sequential unit activity necessary for learning and memory

SPW-Rs and their sequential spiking content within, are necessary for learning and memory (Girardeau et al., 2009; Gridchyn et al., 2020). gRSC population activity can detect subclasses of SPW-Rs (Nitzan et al., 2020), however 2 ideas remain untested. What unit coding strategy is used within HFOs and are HFOs necessary for learning and memory. Identifying

the coding strategy used during HFOs will require denser recordings to capture larger numbers of neurons across all layers in both hemispheres. To test the necessity of HFOs, closed-loop inhibition of both gRSC hemispheres, triggered on SPW-Rs, is an important place to start. This will give the field insights into gRSC and hippocampal interactions and their necessity for learning and memory processes. Additionally, the closed-loop strategy could be triggered upon theta peaks during running to test the necessity of HFOs during encoding processes.

MEC modulation of HPC to gRSC interaction

We show that gRSC HFOs are highly comodulated with Str. LM high gamma, which is known to be generated by MEC inputs (Colgin et al., 2009; Fernández-Ruiz et al., 2017; Schomburg et al., 2014). It is possible MEC inputs pace hippocampo-retrosplenial interactions. Perturbing these interactions is necessary for understanding this interregional communication. I propose a set of experiments disconnecting the gRSC from MEC inputs. This could be achieved by injecting retrograde AAV coding for Cre into the gRSC, combined with AAV injection into the MEC which codes for a Cre dependent caspase 3. This series of viral injections will selectively eliminate MEC projections targeting the gRSC. For fine timescale manipulations, studies could use the same approach described by Wijngaarden et al., 2020, or the dual AAV injection described above, but using a Cre dependent inhibitory rhodopsin injected into the MEC and use opto-stimulation to inhibit these projections from interacting with gRSC activity. These manipulations will provide a better understanding of the MECs role

in the multi-synaptic loop between the hippocampus, gRSC, and MEC over both long and short timescales as well as across brain states.

Inter-hemispheric computation during different states

Splines are specific HFOs found in gRSC L2/3, which we likely recorded some splines in our HORs, and are present during active navigation and REM sleep at the peak of local theta. Their most salient feature is the 180-degree phase shift they exhibit with splines co-occurring in the opposite hemisphere (Ghosh et al., 2022). This interhemispheric phase offset has not been reported in other structures across the brain before, so little is known about how these interactions are generated or important for information processing. I would like to theorize a few ways this phenomenon may be important for information processing within the gRSC. Potentially, this interaction is a necessary process during learning tasks, where by interrupting this communication, gRSC processing is halted entirely causing results similar to lesioning experiments (Vann & Aggleton, 2002, 2004). To test this, we could utilize the Cre dependent inhibition or cellular ablation (discussed in the previous section) to disconnect the hemispheres. Alternatively, this unique interhemispheric computation may allow for redundancy in information processing where neurons encoding similar information in both hemispheres are active simultaneously during HFOs (for example, cells A,B,C,D are active in one hemisphere and cells A',B',C',D' are active simultaneously in the other hemisphere). If we were to disrupt this interhemispheric communication by inhibiting one hemisphere during a learning task, the animal's performance may be entirely conserved. Another possibility is

parallel computation where each hemisphere processes unique pieces of information from the experience that is then correlated with one another during HFOs (for example cells A,C,E,G are active in one hemisphere while cells B,D,F,H are simultaneously active in the other hemisphere). Inhibition of one hemisphere during a learning task could result in decreased performance, but still better than that of removing the RSC. Understanding how gRSC computation may utilize interhemispheric communication to interpret incoming information streams is vital for uncovering its full role in learning and memory processes.

Acetylcholine modulation of gRSC HORs

We show that gRSC HORs are locked to the peak of local and hippocampal theta (Alexander et al., 2018; Arndt et al., 2024; Ghosh et al., 2022). However, we captured a population of HORs that occurred when the animal was stationary, suggesting 2 subgroups of HORs. Hippocampal theta oscillations can be separated into 2 groups, atropine resistant theta, which occurs during running, and atropine sensitive theta, which occurs during quiet restfulness states (Buzsáki et al., 1983). Importantly, when atropine, an acetylcholine receptor antagonist, is administered directly to the hippocampus or intraperitonially atropine sensitive theta goes away, but atropine resistant theta persists. It is possible that HORs are comprised of atropine sensitive and atropine resistant variants which may also underlie novel computation. Recently, a unique device capable of simultaneous LFP and unit recording, optogenetic manipulation, and drug delivery was developed (T-DOpE probe; Kim et al., 2024). Using this

probe, I propose recording gRSC HFOs during a range of behavioral states to capture baseline events. Then, a few hours after baseline, deliver atropine via the T-DOpE probe while continuing to detect HFOs. Local administration of acetylcholine receptor antagonists could interrupt theta and associated HORs during different states. If cholinergic input in the gRSC functions similarly, I would expect to see an abolishment of theta and associated HORs only while stationary. However, during running, theta and associated HORs may be preserved. This approach would provide the field with a larger view of the cholinergic systems role in encoding, and how it may modulate communication between the gRSC, hippocampus and MEC.

The work presented here is merely a small step toward understanding hippocampo-cortical dialogue during learning and memory processes. The next couple decades are sure to be exciting in this area of study as we work toward unraveling these complex interactions.

MATERIALS AND METHODS

Experimental model and study participant details

All data used in this study was collected in 12 sessions from N = 10 male and female mice, aged 8–20 weeks. For optical stimulation of the gRSC layer experiments we used N = 3 C57BL/6J-CamKii-Cre::C57BL/6J-Ai32 mice, for all other experiments N = 7 C57BL/6J::FVB/NJ were used as they show better behavioral performance (Sloin et al., 2022). All animals regardless of sex were selected based on availability, additionally based on our data, we do not anticipate sex dependent differences. Animals were housed in a 12 h reverse light-dark cycle. All experiments were approved by the Virginia Tech IACUC.

Surgeries and habituation

Mice were anesthetized with isoflurane for all surgeries and received both local (bupivacaine 0.1 mL at a 0.5% concentration) and systemic (meloxicam 1 mg/kg) analgesia. In the first surgery, a ground wire was implanted parallel with the surface of the cerebellum and a titanium head-bar was fixed above the skull and connected to the ground wire. The entire skull was then covered with dental cement (UNIFAST LC acrylic cement). Animals were monitored daily post-surgery. All animals were habituated to head fixation over the course of 1–2 weeks and were permitted ad libitum access to food and water. 1 week before recordings were conducted, all animals were water deprived to motivate them to run for water rewards in a 1-D virtual reality system. Mice learned this behavior in 7 days. The day before recording,

craniotomies were made above the HPC and gRSC as follows (all measurements are made with respect to bregma). HPC: 1.5 mm M/L by –1.75 A/P; gRSC linear probe recordings: .5 mm M/L on contralateral side of HPC craniotomy by –2.4 to –2.7 mm A/P; gRSC opto-stimulation recordings: .5–1.25 mm M/L by –2.4 to –2.7 mm A/P. All animals were perfused within 24 h of the end of the recording and 48 h after perfusion brains were sectioned, mounted, and imaged.

gRSC and HPC recording setup

Male and female, C57/B6J and C57BL/6J FVB/NJ mice (N = 7) were used in these experiments. 64 channel silicon probes (linear layout, 20 μm pitch; H3 Cambridge Neurotech) were inserted at a 42-degree angle into the contralateral hemisphere then passed across the midline into the gRSC, then a second such probe was implanted at 90 degrees into ipsilateral HPC CA1. Probe positions were determined online using electro-anatomical landmarks and confirmed by imaging of fluorescent probe tracks (probes are painted with Di-I before recording). Electro-anatomical landmarks used to identify location were a combination of superficial layer key LFP "events" and the presence of many recorded neurons deeper in the RSC. The midline is identified by a single band of large negative deflections with very few units active on either side for a few hundred micrometers given the low number of neurons in L1. L2/3 is then marked by the reemergence of dense unit activity and visible high frequency oscillations. The transition into L5 is marked by a diminishment of HFO activity and a

reduction of unit activity. For a subset of experiments electrolytic lesions were made using selected channels to further confirm the layer from which each electrode was placed during the experiment.

gRSC Optostimulation recording setup

Male and female, C57BL/6J-CamKii-Cre C57BL/6J-Ai32 mice (N = 3) were used in these experiments. All mice were head-fixed as described above, and Neurolight Technologies μLED probes were then implanted in the gRSC such that each shank was within each layer of the gRSC. To accomplish this the probe was set at a 15-degree angle from the midline. Electro-anatomical landmarks were used to identify recording depth during probe implant. Once the probe was in place optical stimulation intensity was empirically determined and set to an intensity that reliable evoked HFOs in L2/3. We then chose one higher and one lower intensity and gave 100–150, 100 ms pulses of each low, medium, and high intensity stimulations each with a randomized delay of 1–3 s between stimulations (only medium intensity stimulations shown in text; Figure 2). Di-I fluorescence was used to post hoc identify probe implant locations.

Tissue processing and immunohistochemistry

Within 24 h after recordings, animals were perfused using 4% paraformaldehyde. Brains were extracted and sliced 48 h after perfusion. Sections were mounted with DAPI containing mounting solution and imaged using a confocal microscope.

Data acquisition

Silicon probes from Cambridge Neurotech∗, IDAX∗, or Neurolight Technologies∗∗ were used to obtain LFP and single unit recordings. Electrophysiology data were acquired using an Intan RHD2000 recording system (sampled at 30 kHz).

∗ = gRSC and HPC dual recordings.

∗∗ = opto-stimulation recordings.

Quantification and statistical analysis

All recordings were down sampled to 1.25 kHz to analyze LFP activity. Statistical analyses were conducted using MATLAB (Statistical Toolbox, Circular Statistics Toolbox, CellExplorer, and Buzcode Toolbox). Sample sizes were not determined by any statistical analyses but are consistent with sample sizes used in previously published studies in the field. Specific information about statistical tests can be found in the respective figure legends. Additional details on each piece of analysis can be found below.

gRSC Optostimulation percent from baseline power response

For each stimulation, the percent change from baseline was calculated as the power response within stimulation minus the baseline power response (100 ms window before the stimulation) divided by the baseline. Wilcoxon signed-rank test was used to test if each individual layer had a significant response to the stimulation. Wilcoxon rank-sum test was used to compare the responses between layers/groups (Figures 4 and 5).

HFO and SPW-Rs event detection

For high frequency oscillation detection, channels from the gRSC were chosen with the highest power in the ~150 Hz range across the duration of the entire recording. For sharp wave-ripple detection, channels from the HPC with the highest power in the ~150 Hz range were chosen by visual inspection. Selected channels were bandpass filtered between 100 and 250 Hz. HFO events were identified as events no longer than 150 ms that surpassed 1 standard deviation above the mean of the rectified and filtered signal. SPW-R events were identified as events no longer than 150 ms that surpassed 3 standard deviations above the mean of the rectified and filtered signal. Each group of events detected from each recording were visually inspected using Neuroscope2. HFO events were then split into HIRs and HORs. HIRs are HFOs that occur within +/– 50 ms of an HPC SPW-R, and HORs were all other events outside +/–50 ms of SPW-Rs. The Wilcoxon rank-sum test was used to compare HIRs and HORs for all peak

amplitude, power, frequency and duration metrics (Figures 8 and 9). A Kolmogorov-Smirnov test was used to check the frequency distributions did not come from a normal distribution.

Unit classification, monosynaptic connection identification, and HFO response

Unit activity was extracted from the raw 30 kHz recordings using Kilosort1 and manually curated in Phy2. Units were putatively labeled excitatory or inhibitory units using CellExplorer.34 Putative monosynaptic connections were also determined in CellExplorer using established methods and manually checked for accuracy (Barthó et al., 2004; English et al., 2017; Gerstein & Clark, 1964). Gain in single unit firing rate to HORs and HIRs was calculated as the average in-event firing rate divided by the baseline firing rate outside of all events. Firing rate increases in HIRs versus HORs was calculated using a t test after subtracting the HIR firing rate gain from the HOR firing rate gain (Figure 10). Percentages of cells making monosynaptic connections were calculated by finding the number of ENs (E-E or E-I) and Ints (I-E or I-I) making intra-laminar connections. The number of units making these connections was then divided by the total number of that presynaptic unit type found in the layer. An ANOVA was used to compare the percent of cells with each monosynaptic connection type in each layer (Figure 7).

Spectral analysis

For the averaged and aligned whole recording power spectral density (PSD; Figure 2) all channels were whitened, and low pass filtered at 250 Hz. A fast Fourier transform was then computed and smoothed using a Savitzky-Golay filter for each channel. For event triggered PSDs (Figures 11 and 13) channels used to detect HFOs and SPW-Rs were selected and whitened. A sliding 16 ms window with 8 ms steps was used for each event. At each window step a Morlet Wavelet decomposition was then performed for integer frequencies of 1–500 Hz.

Current source density analysis

Current source density plots (Figures 2, 3, 11, and 13) were created by finding the second spatial derivative over all electrodes on the probe at each time point around the events. All HIR or HOR triggered CSDs were averaged together for both gRSC and HPC recordings.

HOR theta phase preference

For each session the channel used to detect HFOs and SPW-Rs were selected, bandpass filtered from 6 to 10 Hz, and a Hilbert transform was performed on each. The phase of the signal at each time point was then calculated and theta phase at the peak of each HOR was found. The Rayleigh's test was used to determine significance (Figure 11).

Independent component analysis

Independent component analysis (ICA) was conducted following established methods.36,37,38 Briefly, here we identified independent components corresponding to the Str. Rad and Str. LM gamma source generators. This resulted in independent signals corresponding to these components. We then used these components in combination with the gRSC L2/3 channel used to detect HFOs and conducted power-power comodulation analysis (Figure 13).

Power-power comodulation analysis

Channels used to detect HFOs and the ICRad and ICLM signals derived from ICA were selected and a fast Fourier transform was performed in sliding 2 s windows with 1 s steps. The Spearman correlation for each frequency bin from the gRSC was found for the comparison to every frequency bin in the ICs over the duration of the entire recording. Statistical analyses were then conducted using sub bands of the comodulation output using a one-way ANOVA (Figure 13).

Bibliography

Abadchi, J. K., Rezaei, Z., Knöpfel, T., McNaughton, B. L., & Mohajerani, M. H. (2023). Inhibition is a prevalent mode of activity in the neocortex around awake hippocampal ripples in mice. *ELife*, *12*, 1–22. https://doi.org/10.7554/eLife.79513

Alexander, A. S., Carstensen, L. C., Hinman, J. R., Raudies, F., Chapman, G. W., & Hasselmo, M. E. (2020). Egocentric boundary vector tuning of the retrosplenial cortex. *Science Advances*, *6*(8), 1–18. https://doi.org/10.1126/sciadv.aaz2322

Alexander, A. S., Place, R., Starrett, M. J., Chrastil, E. R., & Nitz, D. A. (2023). Rethinking retrosplenial cortex: Perspectives and predictions. *Neuron*, *111*(2), 150–175. https://doi.org/10.1016/j.neuron.2022.11.006

Alexander, A. S., Rangel, L. M., Tingley, D., & Nitz, D. A. (2018). Neurophysiological signatures of temporal coordination between retrosplenial cortex and the hippocampal formation. *Behavioral Neuroscience*, *132*(5), 453–468. https://doi.org/10.1037/bne0000254

Alexander, A. S., Robinson, J. C., Dannenberg, H., Kinsky, N. R., Levy, S. J., Mau, W., Chapman, G. W., Sullivan, D. W., & Hasselmo, M. E. (2020). Neurophysiological coding of space and time in the hippocampus, entorhinal cortex, and retrosplenial cortex. *Brain and Neuroscience Advances*, *4*, 1–18. https://doi.org/10.1177/2398212820972871

Amaral, D. G., & Witter, M. P. (1989). The three-dimensional organization of the hippocampal formation: A review of anatomical data. *Neuroscience*, *31*(3), 571–591.

https://doi.org/10.1016/0306-4522(89)90424-7

Anzalone, S., Roland, J., Vogt, B., & Savage, L. (2009). Acetylcholine efflux from retrosplenial areas and hippocampal sectors during maze exploration. *Behavioural Brain Research*, *201*(2), 272–278. https://doi.org/10.1016/j.bbr.2009.02.023

Arndt, K. C., Gilbert, E. T., Klaver, L. M. F., Kim, J., Buhler, C. M., Basso, J. C., McKenzie, S., & English, D. F. (2024). Granular retrosplenial cortex layer 2/3 generates high-frequency oscillations dynamically coupled with hippocampal rhythms across brain states. *Cell Reports*, *43*(3), 113910. https://doi.org/10.1016/j.celrep.2024.113910

Averkin, R. G., Szemenyei, V., Bordé, S., & Tamás, G. (2016). Identified Cellular Correlates of Neocortical Ripple and High-Gamma Oscillations during Spindles of Natural Sleep. *Neuron*, *92*(4), 916–928. https://doi.org/10.1016/j.neuron.2016.09.032

Bailey, D. J., Wade, J., & Saldanha, C. J. (2009). Hippocampal lesions impair spatial memory performance, but not song—A developmental study of independent memory systems in the zebra finch. *Developmental Neurobiology*, *69*(8), 491–504. https://doi.org/10.1002/dneu.20713

Barthó, P., Hirase, H., Monconduit, L., Zugaro, M., Harris, K. D., & Buzsáki, G. (2004). Characterization of Neocortical Principal Cells and Interneurons by Network Interactions and Extracellular Features. *Journal of Neurophysiology*, *92*(1), 600–608. https://doi.org/10.1152/jn.01170.2003

Ben-Yakov, A., & Dudai, Y. (2011). Constructing Realistic Engrams: Poststimulus Activity of Hippocampus and Dorsal Striatum Predicts Subsequent Episodic Memory. *Journal of Neuroscience*, *31*(24), 9032–9042. https://doi.org/10.1523/JNEUROSCI.0702-11.2011

Ben-Yakov, A., Eshel, N., & Dudai, Y. (2013). Hippocampal immediate poststimulus activity in the encoding of consecutive naturalistic episodes. *Journal of Experimental Psychology: General*, *142*(4), 1255–1263. https://doi.org/10.1037/a0033558

Blanco, I., Caccavano, A., Wu, J.-Y., Vicini, S., Glasgow, E., & Conant, K. (2024). Coupling of Sharp Wave Events between Zebrafish Hippocampal and Amygdala Homologues. *The Journal of Neuroscience*, *August 2023*, e1467232024. https://doi.org/10.1523/JNEUROSCI.1467-23.2024

Bragin, A., Engel, J., Wilson, C. L., Fried, I., & Buzski, G. (1999). High-frequency oscillations in human brain. *Hippocampus*, *9*(2), 137–142. https://doi.org/10.1002/(SICI)1098-1063(1999)9:2<137::AID-HIPO5>3.0.CO;2-0

Bragin, A., Jando, G., Nadasdy, Z., Hetke, J., Wise, K., & Buzsaki, G. (1995). Gamma (40-100 Hz) oscillation in the hippocampus of the behaving rat. *The Journal of Neuroscience*, *15*(1), 47–60. https://doi.org/10.1523/JNEUROSCI.15-01-00047.1995

Brankačk, J., Stewart, M., & E. Fox, S. (1993). Current source density analysis of the hippocampal theta rhythm: associated sustained potentials and candidate synaptic generators. *Brain Research*, *615*(2), 310–327. https://doi.org/10.1016/0006-8993(93)90043-M

Brennan, E. K. W., Jedrasiak-Cape, I., Kailasa, S., Rice, S. P., Sudhakar, S. K., & Ahmed, O. J. (2021). Thalamus and claustrum control parallel layer 1 circuits in retrosplenial cortex. *ELife*, *10*, 1–42. https://doi.org/10.7554/eLife.62207

Brennan, E. K. W., Sudhakar, S. K., Jedrasiak-Cape, I., John, T. T., & Ahmed, O. J. (2020). Hyperexcitable Neurons Enable Precise and Persistent Information Encoding in the Superficial Retrosplenial Cortex. *Cell Reports*, *30*(5), 1598-1612.e8. https://doi.org/10.1016/j.celrep.2019.12.093

Brunel, N., & Wang, X.-J. (2003). What Determines the Frequency of Fast Network Oscillations With Irregular Neural Discharges? I. Synaptic Dynamics and Excitation-Inhibition Balance. *Journal of Neurophysiology*, *90*(1), 415–430. https://doi.org/10.1152/jn.01095.2002

Buzsáki, G. (1986). Hippocampal sharp waves: Their origin and significance. *Brain Research*, *398*(2), 242–252. https://doi.org/10.1016/0006-8993(86)91483-6

Buzsáki, G. (2002). Theta Oscillations in the Hippocampus. *Neuron*, *33*(3), 325–340. https://doi.org/10.1016/S0896-6273(02)00586-X

Buzsáki, G. (2010). Neural Syntax: Cell Assemblies, Synapsembles, and Readers. *Neuron*, *68*(3), 362–385. https://doi.org/10.1016/j.neuron.2010.09.023

Buzsáki, G. (2015). Hippocampal sharp wave-ripple: A cognitive biomarker for episodic memory and planning. *Hippocampus*, *25*(10), 1073–1188.

https://doi.org/10.1002/hipo.22488

Buzsáki, G., Lai-Wo S., L., & Vanderwolf, C. H. (1983). Cellular bases of hippocampal EEG in the behaving rat. *Brain Research Reviews*, *6*(2), 139–171. https://doi.org/10.1016/0165-0173(83)90037-1

Buzsáki, G., Logothetis, N., & Singer, W. (2013). Scaling Brain Size, Keeping Timing: Evolutionary Preservation of Brain Rhythms. *Neuron*, *80*(3), 751–764. https://doi.org/10.1016/j.neuron.2013.10.002

Buzsáki, G., & Schomburg, E. W. (2015). What does gamma coherence tell us about inter-regional neural communication? *Nature Neuroscience*, *18*(4), 484–489. https://doi.org/10.1038/nn.3952

Buzśaki, G., & Wang, X. J. (2012). Mechanisms of gamma oscillations. *Annual Review of Neuroscience*, *35*, 203–225. https://doi.org/10.1146/annurev-neuro-062111-150444

Cardenas, A., Ramirez-Villegas, J., Kovach, C., Gander, P., Cole, R., Grossback, A., Kawasaki, H., Greenlee, J., Howard, M., Nourski, K., Banks, M., & Voss, M. (2023). Exercise modulates human hippocampal-cortical ripple dynamics. *BioRxiv*, 1–28. https://doi.org/https://doi.org/10.1101/2024.01.26.577338

Carroll, R. C., Lissin, D. V., Zastrow, M. von, Nicoll, R. A., & Malenka, R. C. (1999). Rapid redistribution of glutamate receptors contributes to long-term depression in hippocampal cultures. *Nature Neuroscience*, *2*(5), 454–460. https://doi.org/10.1038/8123

Castiello, S., Zhang, W., & Delamater, A. R. (2021). The retrosplenial cortex as a possible "sensory integration" area: A neural network modeling approach of the differential outcomes effect in negative patterning. *Neurobiology of Learning and Memory*, *185*(2012), 1–25. https://doi.org/10.1016/j.nlm.2021.107527

Chen, G., King, J. A., Burgess, N., & O'Keefe, J. (2013). How vision and movement combine in the hippocampal place code. *Proceedings of the National Academy of Sciences*, *110*(1), 378–383. https://doi.org/10.1073/pnas.1215834110

Colgin, L. L. (2015a). Theta–gamma coupling in the entorhinal–hippocampal system. *Current Opinion in Neurobiology*, *31*, 45–50. https://doi.org/10.1016/j.conb.2014.08.001

Colgin, L. L. (2015b). Do slow and fast gamma rhythms correspond to distinct functional states in the hippocampal network? *Brain Research*, *1621*, 309–315. https://doi.org/10.1016/j.brainres.2015.01.005

Colgin, L. L. (2016). Rhythms of the hippocampal network. *Nature Reviews Neuroscience*, *17*(4), 239–249. https://doi.org/10.1038/nrn.2016.21

Colgin, L. L., Denninger, T., Fyhn, M., Hafting, T., Bonnevie, T., Jensen, O., Moser, M.-B., & Moser, E. I. (2009). Frequency of gamma oscillations routes flow of information in the hippocampus. *Nature*, *462*(7271), 353–357. https://doi.org/10.1038/nature08573

Dahal, P., Rauhala, O. J., Khodagholy, D., & Gelinas, J. N. (2023). Hippocampal–cortical coupling differentiates long-term memory processes. *Proceedings of the National*

Academy of Sciences, *120*(7), 2017. https://doi.org/10.1073/pnas.2207909120

de Almeida-Filho, D. G., Koike, B. D. V., Billwiller, F., Farias, K. S., de Sales, I. R. P., Luppi, P.-H., Ribeiro, S., & Queiroz, C. M. (2021). Hippocampus-retrosplenial cortex interaction is increased during phasic REM and contributes to memory consolidation. *Scientific Reports*, *11*(1), 13078. https://doi.org/10.1038/s41598-021-91659-5

de Sousa, A. F., Cowansage, K. K., Zutshi, I., Cardozo, L. M., Yoo, E. J., Leutgeb, S., & Mayford, M. (2019). Optogenetic reactivation of memory ensembles in the retrosplenial cortex induces systems consolidation. *Proceedings of the National Academy of Sciences*, *116*(17), 8576–8581. https://doi.org/10.1073/pnas.1818432116

Diba, K., & Buzsáki, G. (2007). Forward and reverse hippocampal place-cell sequences during ripples. *Nature Neuroscience*, *10*(10), 1241–1242. https://doi.org/10.1038/nn1961

Dickey, C. W., Verzhbinsky, I. A., Jiang, X., Rosen, B. Q., Kajfez, S., Stedelin, B., Shih, J. J., Ben-Haim, S., Raslan, A. M., Eskandar, E. N., Gonzalez-Martinez, J., Cash, S. S., & Halgren, E. (2022). Widespread ripples synchronize human cortical activity during sleep, waking, and memory recall. *Proceedings of the National Academy of Sciences*, *119*(28), 1–12. https://doi.org/10.1073/pnas.2107797119

Diekelmann, S., & Born, J. (2010). The memory function of sleep. *Nature Reviews Neuroscience*, *11*(2), 114–126. https://doi.org/10.1038/nrn2762

Dragoi, G. (2013). Internal operations in the hippocampus: single cell and ensemble temporal

coding. *Frontiers in Systems Neuroscience*, *7*(August), 1–4. https://doi.org/10.3389/fnsys.2013.00046

Dragoi, G., & Buzsáki, G. (2006). Temporal Encoding of Place Sequences by Hippocampal Cell Assemblies. *Neuron*, *50*(1), 145–157. https://doi.org/10.1016/j.neuron.2006.02.023

Dudai, Y. (2012). The Restless Engram: Consolidations Never End. *Annual Review of Neuroscience*, *35*(1), 227–247. https://doi.org/10.1146/annurev-neuro-062111-150500

Dvorak, D., Radwan, B., Sparks, F. T., Talbot, Z. N., & Fenton, A. A. (2018). Control of recollection by slow gamma dominating mid-frequency gamma in hippocampus CA1. *PLOS Biology*, *16*(1), e2003354. https://doi.org/10.1371/journal.pbio.2003354

Ekstrom, A. D., Kahana, M. J., Caplan, J. B., Fields, T. A., Isham, E. A., Newman, E. L., & Fried, I. (2003). Cellular networks underlying human spatial navigation. *Nature*, *425*(6954), 184–188. https://doi.org/10.1038/nature01964

El-Gaby, M., Reeve, H. M., Lopes-dos-Santos, V., Campo-Urriza, N., Perestenko, P. V., Morley, A., Strickland, L. A. M., Lukács, I. P., Paulsen, O., & Dupret, D. (2021). An emergent neural coactivity code for dynamic memory. *Nature Neuroscience*, *24*(5), 694–704. https://doi.org/10.1038/s41593-021-00820-w

English, D. F., McKenzie, S., Evans, T., Kim, K., Yoon, E., & Buzsáki, G. (2017). Pyramidal Cell-Interneuron Circuit Architecture and Dynamics in Hippocampal Networks. *Neuron*, *96*(2), 505–520. https://doi.org/10.1016/j.neuron.2017.09.033

English, D. F., Peyrache, A., Stark, E., Roux, L., Vallentin, D., Long, M. A., & Buzsáki, G. (2014). Excitation and Inhibition Compete to Control Spiking during Hippocampal Ripples: Intracellular Study in Behaving Mice. *The Journal of Neuroscience*, *34*(49), 16509–16517. https://doi.org/10.1523/JNEUROSCI.2600-14.2014

Eschenko, O., Ramadan, W., Mölle, M., Born, J., & Sara, S. J. (2008). Sustained increase in hippocampal sharp-wave ripple activity during slow-wave sleep after learning. *Learning & Memory*, *15*(4), 222–228. https://doi.org/10.1101/lm.726008

Etter, G., Carmichael, J. E., & Williams, S. (2023). Linking temporal coordination of hippocampal activity to memory function. *Frontiers in Cellular Neuroscience*, *17*. https://doi.org/10.3389/fncel.2023.1233849

Fernández-Ruiz, A., Makarov, V. A., Benito, N., & Herreras, O. (2012). Schaffer-Specific Local Field Potentials Reflect Discrete Excitatory Events at Gamma Frequency That May Fire Postsynaptic Hippocampal CA1 Units. *The Journal of Neuroscience*, *32*(15), 5165–5176. https://doi.org/10.1523/JNEUROSCI.4499-11.2012

Fernández-Ruiz, A., Oliva, A., de Oliveira, E. F., Rocha-Almeida, F., Tingley, D., & Buzsáki, G. (2019). Long-duration hippocampal sharp wave ripples improve memory. *Science*, *364*(6445), 1082–1086. https://doi.org/10.1126/science.aax0758

Fernández-Ruiz, A., Oliva, A., Nagy, G. A., Maurer, A. P., Berényi, A., & Buzsáki, G. (2017). Entorhinal-CA3 Dual-Input Control of Spike Timing in the Hippocampus by Theta-Gamma Coupling. *Neuron*, *93*(5), 1213–1226.

https://doi.org/10.1016/j.neuron.2017.02.017

Fernández-Ruiz, A., Oliva, A., Soula, M., Rocha-Almeida, F., Nagy, G. A., Martin-Vazquez, G., & Buzsáki, G. (2021). Gamma rhythm communication between entorhinal cortex and dentate gyrus neuronal assemblies. *Science*, *372*(6537). https://doi.org/10.1126/science.abf3119

Fernandez-Ruiz, A., Sirota, A., Lopes-dos-Santos, V., & Dupret, D. (2023). Over and above frequency: Gamma oscillations as units of neural circuit operations. *Neuron*, *111*(7), 936–953. https://doi.org/10.1016/j.neuron.2023.02.026

Fischer, L. F., Mojica Soto-Albors, R., Buck, F., & Harnett, M. T. (2020). Representation of visual landmarks in retrosplenial cortex. *ELife*, *9*, 1–25. https://doi.org/10.7554/eLife.51458

Fischler-Ruiz, W., Clark, D. G., Joshi, N. R., Devi-Chou, V., Kitch, L., Schnitzer, M., Abbott, L. F., & Axel, R. (2021). Olfactory landmarks and path integration converge to form a cognitive spatial map. *Neuron*, *109*(24), 4036-4049.e5. https://doi.org/10.1016/j.neuron.2021.09.055

Foster, D. J., & Wilson, M. A. (2006). Reverse replay of behavioural sequences in hippocampal place cells during the awake state. *Nature*, *440*(7084), 680–683. https://doi.org/10.1038/nature04587

Gan, J., Weng, S. ming, Pernía-Andrade, A. J., Csicsvari, J., & Jonas, P. (2017). Phase-Locked

Inhibition, but Not Excitation, Underlies Hippocampal Ripple Oscillations in Awake Mice In Vivo. *Neuron*, *93*(2), 308–314. https://doi.org/10.1016/j.neuron.2016.12.018

Gerstein, G. L., & Clark, W. A. (1964). Simultaneous Studies of Firing Patterns in Several Neurons. *Science*, *143*(3612), 1325–1327. https://doi.org/10.1126/science.143.3612.1325

Ghosh, M., Yang, F.-C., Rice, S. P., Hetrick, V., Gonzalez, A. L., Siu, D., Brennan, E. K. W., John, T. T., Ahrens, A. M., & Ahmed, O. J. (2022). Running speed and REM sleep control two distinct modes of rapid interhemispheric communication. *Cell Reports*, *40*(1), 1–19. https://doi.org/10.1016/j.celrep.2022.111028

Girardeau, G., Benchenane, K., Wiener, S. I., Buzsáki, G., & Zugaro, M. B. (2009). Selective suppression of hippocampal ripples impairs spatial memory. *Nature Neuroscience*, *12*(10), 1222–1223. https://doi.org/10.1038/nn.2384

Gorriz, M. H., Takigawa, M., & Bendor, D. (2023). The role of experience in prioritizing hippocampal replay. *Nature Communications*, *14*(1), 1–15. https://doi.org/10.1038/s41467-023-43939-z

Grenier, F., Timofeev, I., & Steriade, M. (2001). Focal Synchronization of Ripples (80–200 Hz) in Neocortex and Their Neuronal Correlates. *Journal of Neurophysiology*, *86*(4), 1884–1898. https://doi.org/10.1152/jn.2001.86.4.1884

Gridchyn, I., Schoenenberger, P., O'Neill, J., & Csicsvari, J. (2020). Assembly-Specific Disruption of Hippocampal Replay Leads to Selective Memory Deficit. *Neuron*, *106*(2),

291-300.e6. https://doi.org/10.1016/j.neuron.2020.01.021

Haam, J., & Yakel, J. L. (2017). Cholinergic modulation of the hippocampal region and memory function. *Journal of Neurochemistry*, *142*(S2), 111–121. https://doi.org/10.1111/jnc.14052

Harker, K. T., & Whishaw, I. Q. (2002). Impaired Spatial Performance in Rats with Retrosplenial Lesions: Importance of the Spatial Problem and the Rat Strain in Identifying Lesion Effects in a Swimming Pool. *The Journal of Neuroscience*, *22*(3), 1155–1164. https://doi.org/10.1523/JNEUROSCI.22-03-01155.2002

Harvey, C. D., Collman, F., Dombeck, D. A., & Tank, D. W. (2009). Intracellular dynamics of hippocampal place cells during virtual navigation. *Nature*, *461*(7266), 941–946. https://doi.org/10.1038/nature08499

Hasselmo, M. E. (1999). Neuromodulation: acetylcholine and memory consolidation. *Trends in Cognitive Sciences*, *3*(9), 351–359. https://doi.org/10.1016/S1364-6613(99)01365-0

Hasselmo, M. E., Bodelón, C., & Wyble, B. P. (2002). A Proposed Function for Hippocampal Theta Rhythm: Separate Phases of Encoding and Retrieval Enhance Reversal of Prior Learning. *Neural Computation*, *14*(4), 793–817. https://doi.org/10.1162/089976602317318965

Hasselmo, M. E., & Stern, C. E. (2014). Theta rhythm and the encoding and retrieval of space and time. *NeuroImage*, *85*, 656–666. https://doi.org/10.1016/j.neuroimage.2013.06.022

1542 Herreras, O., Solís, J. M., Herranz, A. S., del Río, R. M., & Lerma, J. (1988). Sensory
1543 modulation of hippocampal transmission. II. Evidence for a cholinergic locus of
1544 inhibition in the Schaffer-CA1 synapse. *Brain Research*, *461*(2), 303–313.
1545 https://doi.org/10.1016/0006-8993(88)90260-0

1546 Isomura, Y., Sirota, A., Özen, S., Montgomery, S., Mizuseki, K., Henze, D. A., & Buzsáki, G.
1547 (2006). Integration and Segregation of Activity in Entorhinal-Hippocampal Subregions
1548 by Neocortical Slow Oscillations. *Neuron*, *52*(5), 871–882.
1549 https://doi.org/10.1016/j.neuron.2006.10.023

1550 Kamondi, A., Acsády, L., Wang, X.-J., & Buzsáki, G. (1998). Theta oscillations in somata and
1551 dendrites of hippocampal pyramidal cells in vivo: Activity-dependent phase-precession
1552 of action potentials. *Hippocampus*, *8*(3), 244–261. https://doi.org/10.1002/(SICI)1098-
1553 1063(1998)8:3<244::AID-HIPO7>3.0.CO;2-J

1554 Kanamori, N. (1985). A spindle-like wave in the cat hippocampus: a novel vigilance level-
1555 dependent electrical activity. *Brain Research*, *334*(1), 180–182.
1556 https://doi.org/10.1016/0006-8993(85)90584-0

1557 Karimi Abadchi, J., Nazari-Ahangarkolaee, M., Gattas, S., Bermudez-Contreras, E., Luczak,
1558 A., McNaughton, B. L., & Mohajerani, M. H. (2020). Spatiotemporal patterns of
1559 neocortical activity around hippocampal sharp-wave ripples. *ELife*, *9*, 1–26.
1560 https://doi.org/10.7554/eLife.51972

1561 Khodagholy, D., Gelinas, J. N., & Buzsáki, G. (2017). Learning-enhanced coupling between

ripple oscillations in association cortices and hippocampus. *Science*, *358*(6361), 369–372. https://doi.org/10.1126/science.aan6203

Kim, J., Huang, H., Gilbert, E. T., Arndt, K. C., English, D. F., & Jia, X. (2024). T-DOpE probes reveal sensitivity of hippocampal oscillations to cannabinoids in behaving mice. *Nature Communications*, *15*(1), 1686. https://doi.org/10.1038/s41467-024-46021-4

Kitamura, T., Ogawa, S. K., Roy, D. S., Okuyama, T., Morrissey, M. D., Smith, L. M., Redondo, R. L., & Tonegawa, S. (2017). Engrams and circuits crucial for systems consolidation of a memory. *Science*, *356*(6333), 73–78. https://doi.org/10.1126/science.aam6808

Kocsis, B., Bragin, A., & Buzsáki, G. (1999). Interdependence of Multiple Theta Generators in the Hippocampus: a Partial Coherence Analysis. *The Journal of Neuroscience*, *19*(14), 6200–6212. https://doi.org/10.1523/JNEUROSCI.19-14-06200.1999

Koike, B. D. V., Farias, K. S., Billwiller, F., Almeida-Filho, D., Libourel, P.-A., Tiran-Cappello, A., Parmentier, R., Blanco, W., Ribeiro, S., Luppi, P.-H., & Queiroz, C. M. (2017). Electrophysiological Evidence That the Retrosplenial Cortex Displays a Strong and Specific Activation Phased with Hippocampal Theta during Paradoxical (REM) Sleep. *The Journal of Neuroscience*, *37*(33), 8003–8013. https://doi.org/10.1523/JNEUROSCI.0026-17.2017

Lee, J. S., Briguglio, J. J., Cohen, J. D., Romani, S., & Lee, A. K. (2020). The Statistical Structure of the Hippocampal Code for Space as a Function of Time, Context, and Value.

Cell, *183*(3), 620-635.e22. https://doi.org/10.1016/j.cell.2020.09.024

Lee, M. G., Chrobak, J. J., Sik, A., Wiley, R. G., & Buzsáki, G. (1994). Hippocampal theta activity following selective lesion of the septal cholinergic systeM. *Neuroscience*, *62*(4), 1033–1047. https://doi.org/10.1016/0306-4522(94)90341-7

Lesburguères, E., Gobbo, O. L., Alaux-Cantin, S., Hambucken, A., Trifilieff, P., & Bontempi, B. (2011). Early Tagging of Cortical Networks Is Required for the Formation of Enduring Associative Memory. *Science*, *331*(6019), 924–928. https://doi.org/10.1126/science.1196164

Liu, C., Todorova, R., Tang, W., Oliva, A., & Fernandez-Ruiz, A. (2023). Associative and predictive hippocampal codes support memory-guided behaviors. *Science*, *382*(6668), 1–16. https://doi.org/10.1126/science.adi8237

Liu, X., Ren, C., Lu, Y., Liu, Y., Kim, J.-H., Leutgeb, S., Komiyama, T., & Kuzum, D. (2021). Multimodal neural recordings with Neuro-FITM uncover diverse patterns of cortical–hippocampal interactions. *Nature Neuroscience*, *24*(6), 886–896. https://doi.org/10.1038/s41593-021-00841-5

López-Madrona, V. J., Pérez-Montoyo, E., Álvarez-Salvado, E., Moratal, D., Herreras, O., Pereda, E., Mirasso, C. R., & Canals, S. (2020). Different theta frameworks coexist in the rat hippocampus and are coordinated during memory-guided and novelty tasks. *ELife*, *9*, 1–35. https://doi.org/10.7554/eLife.57313

Lozano, Y. R., Page, H., Jacob, P.-Y., Lomi, E., Street, J., & Jeffery, K. (2017). Retrosplenial and postsubicular head direction cells compared during visual landmark discrimination. *Brain and Neuroscience Advances*, *1*, 1–17. https://doi.org/10.1177/2398212817721859

Lu, W.-Y., Man, H.-Y., Ju, W., Trimble, W. S., MacDonald, J. F., & Wang, Y. T. (2001). Activation of Synaptic NMDA Receptors Induces Membrane Insertion of New AMPA Receptors and LTP in Cultured Hippocampal Neurons. *Neuron*, *29*(1), 243–254. https://doi.org/10.1016/S0896-6273(01)00194-5

Manabe, H., Kusumoto-Yoshida, I., Ota, M., & Mori, K. (2011). Olfactory Cortex Generates Synchronized Top-Down Inputs to the Olfactory Bulb during Slow-Wave Sleep. *The Journal of Neuroscience*, *31*(22), 8123–8133. https://doi.org/10.1523/JNEUROSCI.6578-10.2011

Mao, D., Kandler, S., McNaughton, B. L., & Bonin, V. (2017). Sparse orthogonal population representation of spatial context in the retrosplenial cortex. *Nature Communications*, *8*(1), 243. https://doi.org/10.1038/s41467-017-00180-9

Mao, D., Neumann, A. R., Sun, J., Bonin, V., Mohajerani, M. H., & McNaughton, B. L. (2018). Hippocampus-dependent emergence of spatial sequence coding in retrosplenial cortex. *Proceedings of the National Academy of Sciences*, *115*(31), 8015–8018. https://doi.org/10.1073/pnas.1803224115

Markram, H., Gerstner, W., & Sjöström, P. J. (2012). Spike-Timing-Dependent Plasticity: A Comprehensive Overview. *Frontiers in Synaptic Neuroscience*, *4*(JULY), 2010–2012.

https://doi.org/10.3389/fnsyn.2012.00002

Markram, H., Lübke, J., Frotscher, M., & Sakmann, B. (1997). Regulation of Synaptic Efficacy by Coincidence of Postsynaptic APs and EPSPs. *Science*, *275*(5297), 213–215. https://doi.org/10.1126/science.275.5297.213

McKenzie, S., Nitzan, N., & English, D. F. (2020). Mechanisms of neural organization and rhythmogenesis during hippocampal and cortical ripples. *Philosophical Transactions of the Royal Society B: Biological Sciences*, *375*, 1–12. https://doi.org/10.1098/rstb.2019.0237

Mikulovic, S., Restrepo, C. E., Siwani, S., Bauer, P., Pupe, S., Tort, A. B. L., Kullander, K., & Leão, R. N. (2018). Ventral hippocampal OLM cells control type 2 theta oscillations and response to predator odor. *Nature Communications*, *9*(1), 3638. https://doi.org/10.1038/s41467-018-05907-w

Mitchell, A. S., Czajkowski, R., Zhang, N., Jeffery, K., & Nelson, A. J. D. (2018). Retrosplenial cortex and its role in spatial cognition. *Brain and Neuroscience Advances*, *2*, 1–13. https://doi.org/10.1177/2398212818757098

Mitelman, S. A., Shihabuddin, L., Brickman, A. M., Hazlett, E. A., & Buchsbaum, M. S. (2005). Volume of the cingulate and outcome in schizophrenia. *Schizophrenia Research*, *72*(2–3), 91–108. https://doi.org/10.1016/j.schres.2004.02.011

Mizuseki, K., Sirota, A., Pastalkova, E., & Buzsáki, G. (2009). Theta Oscillations Provide

Temporal Windows for Local Circuit Computation in the Entorhinal-Hippocampal Loop. *Neuron*, *64*(2), 267–280. https://doi.org/10.1016/j.neuron.2009.08.037

Montoya, C. P., Heynen, A. J., Faris, P. D., & Sainsbury, R. S. (1989). Modality specific Type 2 theta production in the immobile rat. *Behavioral Neuroscience*, *103*(1), 106–111. https://doi.org/10.1037/0735-7044.103.1.106

Mou, X., Cheng, J., Yu, Y. S. W., Kee, S. E., & Ji, D. (2018). Comparing Mouse and Rat Hippocampal Place Cell Activities and Firing Sequences in the Same Environments. *Frontiers in Cellular Neuroscience*, *12*(September), 1–13. https://doi.org/10.3389/fncel.2018.00332

Murakami, K., Ishikawa, Y., & Sato, F. (2013). Localization of α7 nicotinic acetylcholine receptor immunoreactivity on GABAergic interneurons in layers I–III of the rat retrosplenial granular cortex. *Neuroscience*, *252*, 443–459. https://doi.org/10.1016/j.neuroscience.2013.08.024

Nestor, P. J., Fryer, T. D., Ikeda, M., & Hodges, J. R. (2003). Retrosplenial cortex (BA 29/30) hypometabolism in mild cognitive impairment (prodromal Alzheimer's disease). *European Journal of Neuroscience*, *18*(9), 2663–2667. https://doi.org/10.1046/j.1460-9568.2003.02999.x

Newman, E. L., Gillet, S. N., Climer, J. R., & Hasselmo, M. E. (2013). Cholinergic Blockade Reduces Theta-Gamma Phase Amplitude Coupling and Speed Modulation of Theta Frequency Consistent with Behavioral Effects on Encoding. *The Journal of*

Neuroscience, *33*(50), 19635–19646. https://doi.org/10.1523/JNEUROSCI.2586-13.2013

Niediek, J., & Bain, J. (2014). Human single-unit recordings reveal a link between place-cells and episodic memory. *Frontiers in Systems Neuroscience*, *8*(6954), 184–188. https://doi.org/10.3389/fnsys.2014.00158

Nitzan, N., McKenzie, S., Beed, P., English, D. F., Oldani, S., Tukker, J. J., Buzsáki, G., & Schmitz, D. (2020). Propagation of hippocampal ripples to the neocortex by way of a subiculum-retrosplenial pathway. *Nature Communications*, *11*(1), 1947. https://doi.org/10.1038/s41467-020-15787-8

Nokia, M. S., Penttonen, M., & Wikgren, J. (2010). Hippocampal Ripple-Contingent Training Accelerates Trace Eyeblink Conditioning and Retards Extinction in Rabbits. *The Journal of Neuroscience*, *30*(34), 11486–11492. https://doi.org/10.1523/JNEUROSCI.2165-10.2010

Nokia, M. S., Waselius, T., Sahramäki, J., & Penttonen, M. (2020). Most hippocampal CA1 pyramidal cells in rabbits increase firing during awake sharp-wave ripples and some do so in response to external stimulation and theta. *Journal of Neurophysiology*, *123*(5), 1671–1681. https://doi.org/10.1152/jn.00056.2020

Norman, Y., Yeagle, E. M., Khuvis, S., Harel, M., Mehta, A. D., & Malach, R. (2019). Hippocampal sharp-wave ripples linked to visual episodic recollection in humans. *Science*, *365*(6454). https://doi.org/10.1126/science.aax1030

Nugent, A. C., Milham, M. P., Bain, E. E., Mah, L., Cannon, D. M., Marrett, S., Zarate, C. A., Pine, D. S., Price, J. L., & Drevets, W. C. (2006). Cortical abnormalities in bipolar disorder investigated with MRI and voxel-based morphometry. *NeuroImage*, *30*(2), 485–497. https://doi.org/10.1016/j.neuroimage.2005.09.029

O'Keefe, J. (1976). Place units in the hippocampus of the freely moving rat. *Experimental Neurology*, *51*(1), 78–109. https://doi.org/10.1016/0014-4886(76)90055-8

O'Keefe, J., & Dostrovsky, J. (1971). The hippocampus as a spatial map. Preliminary evidence from unit activity in the freely-moving rat. *Brain Research*, *34*(1), 171–175. https://doi.org/10.1016/0006-8993(71)90358-1

O'Keefe, J., & Recce, M. L. (1993). Phase relationship between hippocampal place units and the EEG theta rhythm. *Hippocampus*, *3*(3), 317–330. https://doi.org/10.1002/hipo.450030307

Opalka, A. N., Huang, W., Liu, J., Liang, H., & Wang, D. V. (2020). Hippocampal Ripple Coordinates Retrosplenial Inhibitory Neurons during Slow-Wave Sleep. *Cell Reports*, *30*(2), 432-441.e3. https://doi.org/10.1016/j.celrep.2019.12.038

Payne, H. L., Lynch, G. F., & Aronov, D. (2021). Neural representations of space in the hippocampus of a food-caching bird. *Science*, *373*(6552), 343–348. https://doi.org/10.1126/science.abg2009

Pedrosa, R., Song, C., Knöpfel, T., & Battaglia, F. (2022). Combining Cortical Voltage Imaging

and Hippocampal Electrophysiology for Investigating Global, Multi-Timescale Activity Interactions in the Brain. *International Journal of Molecular Sciences*, *23*(12), 6814. https://doi.org/10.3390/ijms23126814

Petersen, P. C., Siegle, J. H., Steinmetz, N. A., Mahallati, S., & Buzsáki, G. (2021). CellExplorer: A framework for visualizing and characterizing single neurons. *Neuron*, *109*(22), 3594–3608. https://doi.org/10.1016/j.neuron.2021.09.002

Powell, A., Connelly, W. M., Vasalauskaite, A., Nelson, A. J. D., Vann, S. D., Aggleton, J. P., Sengpiel, F., & Ranson, A. (2020). Stable Encoding of Visual Cues in the Mouse Retrosplenial Cortex. *Cerebral Cortex*, *30*(8), 4424–4437. https://doi.org/10.1093/cercor/bhaa030

Reiss, D., & McCowan, B. (1993). Spontaneous vocal mimicry and production by bottlenose dolphins (Tursiops truncatus): Evidence for vocal learning. *Journal of Comparative Psychology*, *107*(3), 301–312. https://doi.org/10.1037/0735-7036.107.3.301

Ribot, T. (1882). Diseases of Memory. *American Psychological Association*.

Robertson, R. T., Baratta, J., Yu, J., & LaFerla, F. M. (2009). Amyloid-β expression in retrosplenial cortex of triple transgenic mice: relationship to cholinergic axonal afferents from medial septum. *Neuroscience*, *164*(3), 1334–1346. https://doi.org/10.1016/j.neuroscience.2009.09.024

Robles, R. M., Domínguez-Sala, E., Martínez, S., & Geijo-Barrientos, E. (2020). Layer 2/3

Pyramidal Neurons of the Mouse Granular Retrosplenial Cortex and Their Innervation by Cortico-Cortical Axons. *Frontiers in Neural Circuits*, *14*(November), 1–15. https://doi.org/10.3389/fncir.2020.576504

RUSSELL, W. R., & NATHAN, P. W. (1946). TRAUMATIC AMNESIA. *Brain*, *69*(4), 280–300. https://doi.org/10.1093/brain/69.4.280

Sainsbury, R. S., Heynen, A., & Montoya, C. P. (1987). Behavioral correlates of hippocampal type 2 theta in the rat. *Physiology & Behavior*, *39*(4), 513–519. https://doi.org/10.1016/0031-9384(87)90382-9

Save, E., Cressant, A., Thinus-Blanc, C., & Poucet, B. (1998). Spatial Firing of Hippocampal Place Cells in Blind Rats. *The Journal of Neuroscience*, *18*(5), 1818–1826. https://doi.org/10.1523/JNEUROSCI.18-05-01818.1998

Schlingloff, D., Káli, S., Freund, T. F., Hájos, N., & Gulyás, A. I. (2014). Mechanisms of Sharp Wave Initiation and Ripple Generation. *The Journal of Neuroscience*, *34*(34), 11385–11398. https://doi.org/10.1523/JNEUROSCI.0867-14.2014

Schmidt, R., Diba, K., Leibold, C., Schmitz, D., Buzsáki, G., & Kempter, R. (2009). Single-Trial Phase Precession in the Hippocampus. *The Journal of Neuroscience*, *29*(42), 13232–13241. https://doi.org/10.1523/JNEUROSCI.2270-09.2009

Schomburg, E. W., Fernández-Ruiz, A., Mizuseki, K., Berényi, A., Anastassiou, C. A., Koch, C., & Buzsáki, G. (2014). Theta Phase Segregation of Input-Specific Gamma Patterns in

Entorhinal-Hippocampal Networks. *Neuron*, *84*(2), 470–485. https://doi.org/10.1016/j.neuron.2014.08.051

Shein-Idelson, M., Ondracek, J. M., Liaw, H.-P., Reiter, S., & Laurent, G. (2016). Slow waves, sharp waves, ripples, and REM in sleeping dragons. *Science*, *352*(6285), 590–595. https://doi.org/10.1126/science.aaf3621

Shine, J. P., Valdés-Herrera, J. P., Hegarty, M., & Wolbers, T. (2016). The human retrosplenial cortex and thalamus code head direction in a global reference frame. *Journal of Neuroscience*, *36*(24), 6371–6381. https://doi.org/10.1523/JNEUROSCI.1268-15.2016

Sirota, A., Montgomery, S., Fujisawa, S., Isomura, Y., Zugaro, M., & Buzsáki, G. (2008). Entrainment of Neocortical Neurons and Gamma Oscillations by the Hippocampal Theta Rhythm. *Neuron*, *60*(4), 683–697. https://doi.org/10.1016/j.neuron.2008.09.014

Skaggs, W. E., & McNaughton, B. L. (1996). Replay of Neuronal Firing Sequences in Rat Hippocampus During Sleep Following Spatial Experience. *Science*, *271*(5257), 1870–1873. https://doi.org/10.1126/science.271.5257.1870

Skaggs, W. E., McNaughton, B. L., Permenter, M., Archibeque, M., Vogt, J., Amaral, D. G., & Barnes, C. A. (2007). EEG Sharp Waves and Sparse Ensemble Unit Activity in the Macaque Hippocampus. *Journal of Neurophysiology*, *98*(2), 898–910. https://doi.org/10.1152/jn.00401.2007

Skaggs, W. E., McNaughton, B. L., Wilson, M. A., & Barnes, C. A. (1996). Theta phase precession in hippocampal neuronal populations and the compression of temporal sequences. *Hippocampus*, *6*(2), 149–172. https://doi.org/10.1002/(SICI)1098-1063(1996)6:2<149::AID-HIPO6>3.0.CO;2-K

Sloin, H. E., Bikovski, L., Levi, A., Amber-Vitos, O., Katz, T., Spivak, L., Someck, S., Gattegno, R., Sivroni, S., Sjulson, L., & Stark, E. (2022). Hybrid Offspring of C57BL/6J Mice Exhibit Improved Properties for Neurobehavioral Research. *Eneuro*, *9*(4), 1–16. https://doi.org/10.1523/ENEURO.0221-22.2022

Squire, L. R., Clark, R. E., & Knowlton, B. J. (2001). Retrograde amnesia. *Hippocampus*, *11*(1), 50–55. https://doi.org/10.1002/1098-1063(2001)11:1<50::AID-HIPO1019>3.0.CO;2-G

Squire, L. R., Roesler, R., & McGaugh, J. L. (2015). Memory Consolidation. In *Encyclopedia of Behavioral Neuroscience, 2nd edition* (Vol. 7, pp. 1–21). Elsevier. https://doi.org/10.1016/B978-0-12-809324-5.21493-4

Stacho, M., & Manahan-Vaughan, D. (2022). Mechanistic flexibility of the retrosplenial cortex enables its contribution to spatial cognition. *Trends in Neurosciences*, *45*(4), 284–296. https://doi.org/10.1016/j.tins.2022.01.007

Stackman, R. W., Clark, A. S., & Taube, J. S. (2002). Hippocampal spatial representations require vestibular input. *Hippocampus*, *12*(3), 291–303. https://doi.org/10.1002/hipo.1112

Staresina, B. P., Alink, A., Kriegeskorte, N., & Henson, R. N. (2013). Awake reactivation predicts memory in humans. *Proceedings of the National Academy of Sciences*, *110*(52), 21159–21164. https://doi.org/10.1073/pnas.1311989110

Staresina, B. P., Bergmann, T. O., Bonnefond, M., van der Meij, R., Jensen, O., Deuker, L., Elger, C. E., Axmacher, N., & Fell, J. (2015). Hierarchical nesting of slow oscillations, spindles and ripples in the human hippocampus during sleep. *Nature Neuroscience*, *18*(11), 1679–1686. https://doi.org/10.1038/nn.4119

Stark, E., Roux, L., Eichler, R., Senzai, Y., Royer, S., & Buzsáki, G. (2014). Pyramidal Cell-Interneuron Interactions Underlie Hippocampal Ripple Oscillations. *Neuron*, *83*(2), 467–480. https://doi.org/10.1016/j.neuron.2014.06.023

Sun, W., Choi, I., Stoyanov, S., Senkov, O., Ponimaskin, E., Winter, Y., Pakan, J. M. P., & Dityatev, A. (2021). Context value updating and multidimensional neuronal encoding in the retrosplenial cortex. *Nature Communications*, *12*(1), 6045. https://doi.org/10.1038/s41467-021-26301-z

Takehara-Nishiuchi, K., & McNaughton, B. L. (2008). Spontaneous Changes of Neocortical Code for Associative Memory During Consolidation. *Science*, *322*(5903), 960–963. https://doi.org/10.1126/science.1161299

Tambini, A., Ketz, N., & Davachi, L. (2010). Enhanced Brain Correlations during Rest Are Related to Memory for Recent Experiences. *Neuron*, *65*(2), 280–290. https://doi.org/10.1016/j.neuron.2010.01.001

Tiesinga, P., & Sejnowski, T. J. (2009). Cortical Enlightenment: Are Attentional Gamma Oscillations Driven by ING or PING? *Neuron*, *63*(6), 727–732. https://doi.org/10.1016/j.neuron.2009.09.009

Todd, T. P., Mehlman, M. L., Keene, C. S., DeAngeli, N. E., & Bucci, D. J. (2016). Retrosplenial cortex is required for the retrieval of remote memory for auditory cues. *Learning & Memory*, *23*(6), 278–288. https://doi.org/10.1101/lm.041822.116

Tomé, D. F., Sadeh, S., & Clopath, C. (2022). Coordinated hippocampal-thalamic-cortical communication crucial for engram dynamics underneath systems consolidation. *Nature Communications*, *13*(1), 840. https://doi.org/10.1038/s41467-022-28339-z

Troy Harker, K., & Whishaw, I. Q. (2004). A reaffirmation of the retrosplenial contribution to rodent navigation: Reviewing the influences of lesion, strain, and task. *Neuroscience and Biobehavioral Reviews*, *28*(5), 485–496. https://doi.org/10.1016/j.neubiorev.2004.06.005

Tse, D., Langston, R. F., Kakeyama, M., Bethus, I., Spooner, P. A., Wood, E. R., Witter, M. P., & Morris, R. G. M. (2007). Schemas and memory consolidation. *Science*, *316*(5821), 76–82. https://doi.org/10.1126/science.1135935

Tse, D., Takeuchi, T., Kakeyama, M., Kajii, Y., Okuno, H., Tohyama, C., Bito, H., & Morris, R. G. M. (2011). *Schema-Dependent Gene Activation*. *9596*(August), 891–895.

Ulanovsky, N., & Moss, C. F. (2007). Hippocampal cellular and network activity in freely

moving echolocating bats. *Nature Neuroscience*, *10*(2), 224–233. https://doi.org/10.1038/nn1829

Vaidya, S. P., & Johnston, D. (2013). Temporal synchrony and gamma-to-theta power conversion in the dendrites of CA1 pyramidal neurons. *Nature Neuroscience*, *16*(12), 1812–1820. https://doi.org/10.1038/nn.3562

Valero, M., Navas-Olive, A., de la Prida, L. M., & Buzsáki, G. (2022). Inhibitory conductance controls place field dynamics in the hippocampus. *Cell Reports*, *40*(8), 111232. https://doi.org/10.1016/j.celrep.2022.111232

van Groen, T., & Michael Wyss, J. (1990). Connections of the retrosplenial granular a cortex in the rat. *Journal of Comparative Neurology*, *300*(4), 593–606. https://doi.org/10.1002/cne.903000412

van Groen, T., & Wyss, J. M. (1992). Connections of the retrosplenial dysgranular cortex in the rat. *Journal of Comparative Neurology*, *315*(2), 200–216. https://doi.org/10.1002/cne.903150207

Van Groen, T., & Wyss, J. M. (2003). Connections of the retrosplenial granular b cortex in the rat. *Journal of Comparative Neurology*, *463*(3), 249–263. https://doi.org/10.1002/cne.10757

van Kesteren, M. T. R., Fernández, G., Norris, D. G., & Hermans, E. J. (2010). Persistent schema-dependent hippocampal-neocortical connectivity during memory encoding and

postencoding rest in humans. *Proceedings of the National Academy of Sciences*, *107*(16), 7550–7555. https://doi.org/10.1073/pnas.0914892107

van Wijngaarden, J. B. G., Babl, S. S., & Ito, H. T. (2020). Entorhinal-retrosplenial circuits for allocentric-egocentric transformation of boundary coding. *ELife*, *9*, 1–25. https://doi.org/10.7554/eLife.59816

Vandecasteele, M., Varga, V., Berényi, A., Papp, E., Barthó, P., Venance, L., Freund, T. F., & Buzsáki, G. (2014). Optogenetic activation of septal cholinergic neurons suppresses sharp wave ripples and enhances theta oscillations in the hippocampus. *Proceedings of the National Academy of Sciences*, *111*(37), 13535–13540. https://doi.org/10.1073/pnas.1411233111

Vanderwolf, C. H. (1988). Cerebral Activity and Behavior: Control by Central Cholinergic and Serotonergic Systems. In *International Review of Neurobiology* (Vol. 30, Issue C, pp. 225–340). https://doi.org/10.1016/S0074-7742(08)60050-1

Vann, S. D., & Aggleton, J. P. (2002). Extensive cytotoxic lesions of the rat retrosplenial cortex reveal consistent deficits on tasks that tax allocentric spatial memory. *Behavioral Neuroscience*, *116*(1), 85–94. https://doi.org/10.1037/0735-7044.116.1.85

Vann, S. D., & Aggleton, J. P. (2004). Testing the importance of the retrosplenial guidance system: effects of different sized retrosplenial cortex lesions on heading direction and spatial working memory. *Behavioural Brain Research*, *155*(1), 97–108. https://doi.org/10.1016/j.bbr.2004.04.005

Vann, S. D., Aggleton, J. P., & Maguire, E. A. (2009). What does the retrosplenial cortex do? *Nature Reviews Neuroscience*, *10*(11), 792–802. https://doi.org/10.1038/nrn2733

Vaz, A. P., Inati, S. K., Brunel, N., & Zaghloul, K. A. (2019). Coupled ripple oscillations between the medial temporal lobe and neocortex retrieve human memory. *Science*, *363*(6430), 975–978. https://doi.org/10.1126/science.aau8956

Voglis, G., & Tavernarakis, N. (2006). The role of synaptic ion channels in synaptic plasticity. *EMBO Reports*, *7*(11), 1104–1110. https://doi.org/10.1038/sj.embor.7400830

Vogt, B. A., & Miller, M. W. (1983). Cortical connections between rat cingulate cortex and visual, motor, and postsubicular cortices. *Journal of Comparative Neurology*, *216*(2), 192–210. https://doi.org/10.1002/cne.902160207

Wang, X. J., & Buzsáki, G. (1996). Gamma oscillation by synaptic inhibition in a hippocampal interneuronal network model. *Journal of Neuroscience*, *16*(20), 6402–6413. https://doi.org/10.1523/jneurosci.16-20-06402.1996

Wang, X., Zhang, C., Szabo, G., & Sun, Q.-Q. (2013). Distribution of CaMKIIα expression in the brain in vivo, studied by CaMKIIα-GFP mice. *Brain Research*, *1518*, 9–25. https://doi.org/10.1016/j.brainres.2013.04.042.Distribution

Whittington, M. A., Traub, R. D., & Jefferys, J. G. R. (1995). Synchronized oscillations in interneuron networks driven by metabotropic glutamate receptor activation. *Nature*, *373*(6515), 612–615. https://doi.org/10.1038/373612a0

Wu, F., Stark, E., Ku, P.-C., Wise, K. D., Buzsáki, G., & Yoon, E. (2015). Monolithically Integrated μLEDs on Silicon Neural Probes for High-Resolution Optogenetic Studies in Behaving Animals. *Neuron*, *88*(6), 1136–1148. https://doi.org/10.1016/j.neuron.2015.10.032

Yamawaki, N., Li, X., Lambot, L., Ren, L. Y., Radulovic, J., & Shepherd, G. M. G. (2019). Long-range inhibitory intersection of a retrosplenial thalamocortical circuit by apical tuft-targeting CA1 neurons. *Nature Neuroscience*, *22*(4), 618–626. https://doi.org/10.1038/s41593-019-0355-x

Yamawaki, N., Radulovic, J., & Shepherd, G. M. G. (2016). A corticocortical circuit directly links retrosplenial cortex to M2 in the mouse. *Journal of Neuroscience*, *36*(36), 9365–9374. https://doi.org/10.1523/JNEUROSCI.1099-16.2016

Zhou, Y., Sheremet, A., Kennedy, J. P., Qin, Y., DiCola, N. M., Lovett, S. D., Burke, S. N., & Maurer, A. P. (2022). Theta dominates cross-frequency coupling in hippocampal-medial entorhinal circuit during awake-behavior in rats. *IScience*, *25*(11), 105457. https://doi.org/10.1016/j.isci.2022.105457

Zhou, Y., Sheremet, A., Qin, Y., Kennedy, J. P., DiCola, N. M., Burke, S. N., & Maurer, A. P. (2019). Methodological Considerations on the Use of Different Spectral Decomposition Algorithms to Study Hippocampal Rhythms. *Eneuro*, *6*(4), ENEURO.0142-19.2019. https://doi.org/10.1523/ENEURO.0142-19.2019

Zielinski, M. C., Shin, J. D., & Jadhav, S. P. (2021). Hippocampal theta sequences in REM

sleep during spatial learning. *BioRxiv*, 1–59. https://doi.org/2021.04.15.439854